T.C

(MASTER THESIS)

YAŞAR UNIVERSITY

GRADUATE SCHOOL OF NATURAL AND APPLIED SCIENCE

AUTOMATIC ELECTROCARDIOGRAM (ECG) BEAT CLASSIFICATION SYSTEM USING HYBRID TECHNIQUE

Sani SAMINU

Thesis Advisor: Asst. Prof. Dr. Nalan ÖZKURT

Department of Electrical and Electronics Engineering

Bornova -İZMİR

2014

YAŞAR UNIVERSITY

GRADUATE SCHOOL OF NATURAL AND APPLIED SCIENCE

(MASTER THESIS)

AUTOMATIC ELECTROCARDIOGRAM (ECG) BEAT CLASSIFICATION SYSTEM USING HYBRID TECHNIQUE

Sani SAMINU

Thesis Advisor: Asst. Prof. Dr. Nalan ÖZKURT

Department of Electrical and Electronics Engineering

Bornova -İZMİR

2014

APPROVAL PAGE

This study titled "AUTOMATIC ELECTROCARDIOGRAM (ECG) BEAT CLASSIFICATION SYSTEM USING HYBRID TECHNIQUE" and presented as M.Sc Thesis by **Sani Saminu** has been evaluated in compliance with the relevant provision of Y.U Graduate Education and Training Regulations of Y.U institute of Science Education and Training Directions. The jury members below have decided for the defense of this thesis, and it has been declared by consensus/ majority of votes that the candidate has succeeded in his thesis defense examination dated ……

Jury Members:	**Signature:**
Head: ……..	……
Rapporteur Member: ……..	…….
Member: ……..	……...…….

ABSTRACT

AUTOMATIC ELECTROCARDIOGRAM (ECG) BEAT CLASSIFICATION SYSTEM USING HYBRID TECHNIQUE

Sani SAMINU
MSc in Electrical and Electronics Engineering

Supervisor: Asst. Prof. Dr. Nalan ÖZKURT
June 2014

Heart is one of the critical organs in the human body. Electrocardiography (ECG) signal is a bioelectrical signal which record the electrical activity of the heart, it is a technique used primarily as a diagnostic tool for various cardiac diseases by providing necessary information on the electrophysiology and changes that may occur in the heart. To reduce mortality rate associated with cardiac diseases, early detection of these diseases is of paramount important. In this thesis, automated ECG beat detection system using a hybrid technique has been proposed for classifying four ECG beats as normal, right bundle branch block (Rbbb), paced beat and left bundle branch block (Lbbb) using the signals from Massachusetts Institute of Technology Beth Israel Hospital (MIT-BIH) arrhythmia database and processed using signal processing toolbox, wavelet toolbox and neural network toolbox found in Matlab 2013 environment.

In the preprocessing and QRS detection stage, a well known and acceptable Pan-Tompkins algorithm has been used to remove noise and detect R-peaks. Equivalent R-T interval samples between R-R intervals have been extracted as a time domain features, these features have been decomposed using discrete wavelet transform (DWT) and stationary wavelet transform (SWT) as time-frequency features, statistical parameters have been calculated as mean, median, standard deviation, maximum, minimum, energy and entropy using time-frequency features and classification has been performed using neural network. The hybrid method gives a promising result as equivalent R-T interval features gives average accuracy of 98.22% and 94.18%, the DWT with statistical features gives average accuracy of 99.84% and 97.59% for reduced and large number of samples respectively. However, an improvement was recorded when employing SWT for wavelet decomposition using large number of samples with average accuracy of 98.33%. Also comparative performance has been carried out between different wavelet families in which db4, coif5 and sym8 give higher performance. Wavelet time and frequency entropy using SWT have been calculated as a new feature; based on the classification results wavelet time entropy gives average accuracy of 98.21% against frequency entropy of 97.77%. Based on the comparative analysis among all the proposed methods combined SWT with statistical features gives higher and satisfactory results.

Keywords: ECG, DWT, SWT, Pan-Tompkins, ECG beat classification

ÖZET
KARMA BİR TEKNİK KULLANARAK OTOMATİK ELEKTROKARDİOGRAM VURU SINIFLANDIRMA SİSTEMİ

Sani SAMINU
Elektrik ve Elektronik MühendisliğiYüksek Lisans

Danışman: Yard.Doç. Dr. Nalan ÖZKURT
Haziran 2014

Kalp insan vücudundaki kritik organlardan biridir. Elektrokardiografi (EKG) işareti kalbin elektriksel aktivitesini kaydeden biyoelektrik bir işarettir ve bu teknik kalbin elektrofizyolojisi ve meydana çıkabilecek değişiklikler hakkında gerekli bilgileri toplayarak birçok kalp hastalığı için birincil tanı aracı olarak kullanılmaktadır. Kalp hastalıklarından kaynaklanan ölüm oranını azaltmak için bu hastalıkların erken tanısı büyük önem taşımaktadır. Bu tezde, Massachusetts Teknoloji Enstitüsü Beth Israel Hastanesi (MIT-BIH) ritm bozukluğu veri tabanından alınan işaretler kullanılarak EKG vurularını normal, sağ dal bloğu (Rbbb), kalp pili vurusu, sol dal bloğu (Lbbb) olmak üzere dört sınıfa ayırmak için Matlab 2013 ortamında bulunan işaret işleme, dalgacık dönüşümü ve yapay sinir ağları araç kutularını kullanan karma bir sistem önerilmektedir.

Önişleme ve QRS kompleksinin sezilmesi aşamasında, gürültüyü azaltmak ve R-tepelerini tespit etmek amacıyla Pan-Tompkins algoritması kullanılmıştır. Zaman ortamı öznitelikleri olarak R-R aralıkları arasındaki R-T eşdeğer aralığı örnekleri alınmış ve bu örneklere ayrık dalgacık dönüşümü (ADD) ve durağan dalgacık dönüşümü (DDD) uygulanarak zaman-frekans öznitelikleri elde edilmiş, bu büyüklüklerin ortalama, medyan, standart sapma, en büyük, en küçük, enerji ve entropi gibi istatistiksel parametreleri hesaplanarak yapay sinir ağları ile sınıflandırılmıştır. Sırasıyla azaltılmış ve geniş veri seti için R-T eşdeğer aralığı özniteliklerііçin %98.22 ve %94.18 ortalama doğruluk elde edilirken, ADD öznitelikleri için %99.84 ve%97.59 ortalama doğruluk elde edilmiştir. Geniş veri setinde DDD için %98.33 ortalama doğruluk oranı ile bir iyileştirme sağlanmıştır. Ayrıca, farklı dalgacık aileleri arasında da karşılaştırma yapılmış ve db4, coif5 ve sym8 dalgacıkları için daha yüksek başarım elde edilmiştir. Yeni bir öznitelik olarak DDD zaman ve frekans entropisi önerilmiş, %98.21 ile zaman entropisi %97.77 doğruluk oranı olan frekans entropisinden daha iyi bir sonuç vermiştir. Tüm öznitelikler karşılaştırıldığında, DDD istatistiksel parametreleri daha iyi sonuçlar vermiştir.

Anahtar Kelimeler: EKG, ADD, DDD, Pan-Tompkins, EKG vuru sınıflandırma

ACKNOWLEDGEMENTS

All praises and thanks be to Almighty ALLAH for giving me the grace and opportunity to carry out this thesis work. I would like to sincerely express my appreciation and gratitude to the kind gesture of my wonderful supervisor Dr. Nalan Özkurt for her constant and continuous support, guidance, encouragement, corrections and nice suggestions which have been the essential keys in the completion of this work.

Special thanks to my fellow research colleague and closed friend Ibrahim Abdullahi Karaye, Hikmet Gumuş of faculty of medicine Dokuz Eylul University Izmir and my course mates for their friendship, support and thoughtful and motivating discussions we had, throughout my programme.

I would like to acknowledge the academic and technical support of Electrical and Electronic Engineering Department staffs for their support and assistance since the start of my postgraduate work in 2012, especially the head of department, Prof. Dr. Mustafa GÜNDÜZALP.

Thanks to Kano State Government of Nigeria under the leadership of His Excellency Dr. Rabi'u Musa Kwankwaso for awarding me scholarship grant for this masters program.

Last but not least, my sincere gratitude goes to my family for their patience, encouragement and parental care right from the genesis of my life.

TEXT OF OATH

I declare and honestly confirm that my study titled "AUTOMATIC ELECTROCARDIOGRAM (ECG) BEAT CLASSIFICATION SYSTEM USING HYBRID TECHNIQUE", and presented as Master's Thesis has been written without applying to any assistance inconsistent with scientific ethics and traditions, that all sources from which I have benefited listed in bibliography, and that I have benefited from these sources by means of making references.

12/6/2014 …….

Student Name & Signature

DEDICATION

This thesis work is dedicated to Engr. Dr. Rabi'u Musa Kwankwaso, the executive governor of Kano state-Nigeria and the entire people of the state.

TABLE OF CONTENTS

TABLE OF CONTENTS (cont'd)

TABLE OF CONTENTS (cont'd)

INDEX OF FIGURES

INDEX OF FIGURES (cont'd)

INDEX OF FIGURES (cont'd)

INDEX OF TABLES

INDEX OF TABLES (cont'd)

INDEX OF ABBREVIATIONS

A/D	Analog to digital
ANN	Artificial Neural network
AV	Atrio Ventricular
BP	Back propagation
CDV	Cardiovascular disease
CWT	Continuous wavelet transform
DBNN	Decision based neural network
DSP	Digital signal processing
DCT	Discrete cosine transform
DWT	Discrete wavelet transform
ECG	Electrocardiogram
EMG	Electromyogram
FFT	Fast Fourier transform
FIR	Finite impulse response
GUI	Graphical user interface
HBR	Heart beat rate
I/O	Input/Output
ICA	Independent component analysis
IIR	Infinite impulse response
ISO	Isoelectric line
LA	Left arm
Lbbb	Left bundle branch block
LL	Left leg
LMS	Least Mean Square
LVQ	Linear vector quantization
MIT-BIH	Massachusetts Institute of Technology Beth Israel Hospital database
MSE	Mean Squared Error
N	Normal
NLMS	Normalised LMS algorithms

INDEX OF ABBREVIATIONS (cont'd)

NPV	Negative predictive value
P	Paced beats
PAD	Peripheral atrial disease
PCA	Principal component analysis
PLI	Power line interference
PPV	Positive predictive value
PSD	Power spectral density
R	Right bundle branch block
RA	Right arm
Rbbb	Right bundle branch block
RL	Right leg
SA	Sino Atrial
SNR	Signal to noise ratio
STD	Standard deviation
SWT	stationary wavelet transform
TN	True negative
TP	True positive
WE	Wavelet entropy
WHO	World Health Organization
WTFE	Wavelet time frequency entropy

CHAPTER ONE

INTRODUCTION

This chapter discusses the general background information about the principles, benefits and challenges associated with electrocardiogram (ECG) acquisition, processing and classification. Also this part discusses the general health issues in ECG analysis especially in terms of wireless acquisition, ECG features extraction techniques and automatic beats detection system which encourages the present research. Then a brief review and problem definition from the previous studies, the research significance, its aim and objectives, scopes of the present works and thesis outlines are presented.

1.1 Background

Human body consists of different organs that are interconnected together for proper and efficient body function. Heart is one of the most critical organs in the human body because it supply blood to different part of the body organs, therefore there is highly need in the development of methods and systems for monitoring its functionality. One of the most powerful diagnostic tools in medical application that is commonly used for the assessment of the functionality of the heart is Electrocardiography. The ECG is a real-time non-invasive and conventional method for interpretation of the electrical activity of the heart. By attaching electrodes at different outer surface of the human skin, electrical cardiac signals can be recorded by an external device. These currents cause the contractions and relaxations of heart by stimulating cardiac muscle (Guyton and Hall, 2006) and travel as electrical signals through the electrodes to the ECG device, which records them as characteristic waves. Different waves and fiducial points of ECG reflect the activity of different parts of the heart which generate the respective flow of electrical currents. Figure 1 shows a schematic representation of a normal ECG and its various waves.

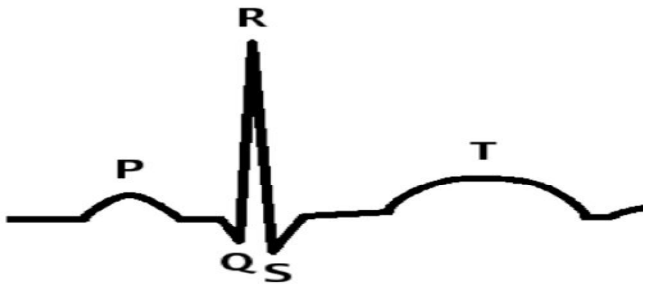

Figure 1.1: Normal ECG wave (Murugavel, 2005)

Generally, healthcare is one of the emerging areas of research in this century and in hospital and health care community, there are considerable commercial interests in the wireless and automatic classification of the ECG signals. Because cardiovascular diseases (CDV) remains as the dominant causes of death all over the world with an estimated of 17.3 million people died from CDV in 2008 which account to 30% of all global death and 23.6 million people will die from these diseases by the year 2030 based on the prediction and statistics from World Health Organization (WHO). Also, according to a recently published (2014) report by Heart failure Working Group of the Turkish Society of Cardiology (TDK), there are 15 million heart-failure patients in Europe and 6 million in the United States (US), in Turkey there are 1 million patients suffering from heart failure. With another 2 million people who are at serious risk of this disease and those figures will increase about two fold within 10 years (Yuksel, 2014). It is very important to detect and diagnose as early as possible and accurately these cardiac arrhythmias since they usually cause sudden cardiac death. It is tedious and time consuming to used visual inspection in ECG analysis even for an expert cardiologist. Therefore, the usage of computer software to automatically detect the ECG beats and diagnose the ECG classes as well as simple and low cost acquisition system is cost effective and significantly improves diagnostic accuracy and patient healing outcomes (Bruce, 1996;Krummen et al., 2010).

In order to address some of the challenges mentioned above, This thesis has focused on developing cost effective, intelligent and easy-to-use ECG wireless acquisition and automatic diagnostic system based on a hardware and software that

uses signal processing and search for effective ECG features extraction techniques to obtain the critical characteristics and useful clinical signatures of ECG waves which can represents different cardiac conditions and classifying these conditions by using application of pattern recognition in artificial neural networks. Unification and implementing of this system in the future will be able to provide patients and doctors with self diagnosis systems that can be used to minimize mortality rates associated with CDVs especially in developing and underdeveloped countries where there is poor doctor to patient ratio, improper health care policies, inadequate of qualified medical experts and lack of health care equipments.

Figure 1.2 below shows a block diagram of a general process of ECG signal processing and analysis.

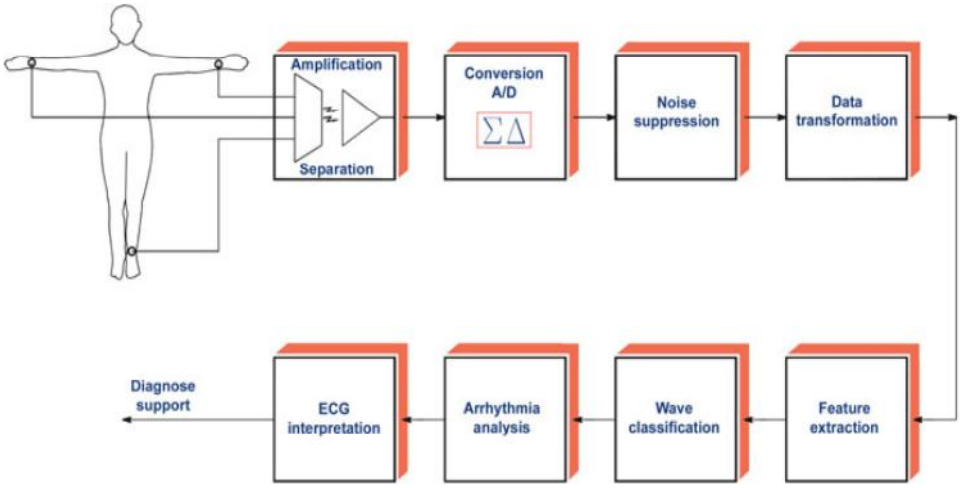

Figure1.2: Main phases of ECG signal processing and analysis (Adam and Witold, 2012)

ECG signal processing and analysis comprises a sequence of steps among which the most essential include

- Amplification of signal and its Analog to digital (A/D) conversion
- Noise elimination
- Feature extraction and selection
- Arrhythmia classification.

The quality of the overall process of acquisition, classification and interpretation of ECG signals depends on the quality and effectiveness of the methods used at these steps. Both signal amplification and A/D conversion are realized in hardware while all filtering and noise elimination are realized through the use of advanced technologies of information processing.

Different unwanted signals called artifacts heavily affect the recording process. In addition, the ECG signals collected from different people are heterogeneous, generally reflected by the variations in the different clinical signatures of the beats. Hence, computationally intensive preprocessing is required for beat detection and feature extraction. The most important features include the information lying in the P, Q, R, S, and T waves of the ECG signal (Wolter, 2011). ECG beats should be classified based on these features in order to detect different types of CVD. Different kinds of noises interfere with ECG signals are

- Baseline wandering,
- Electromyogram (EMG) noise,
- Motion artifact,
- Power-line interference (PLI), and
- Electrode pop or contact noise etc.

After ECG acquisition by suitable electrode, instrumentation amplifiers and filters, the next step is preprocessing which generally takes care of eliminating or minimizing the unwanted signal; a process called denoising. Several works have been reported in the area of ECG denoising. Prior to 1980s noise filtering was based on digital filters (Hirano et al., 1974), to reduce PLI (Hamilton, 1996) makes a comparative analysis between adaptive and non-adaptive notch filters. (Tompkins and Ahlstrom, 1985) implemented an adaptive filtering which was found to be more effective than non-adaptive counterpart. Long computation time as a result of large number of multiplication is a common problem in linear phase filtering. (Mneimneh et al., 2006) proposed a method for baseline removal using adaptive Kalman technique. Other ECG denoising techniques includes using Principal component analysis (PCA) and Independent component analysis (ICA) (Chawla, 2011), Neural

network method (Farahabadi et al., 2009) and multi resolution wavelet based analysis (Pal and Mitra, 2010).

The studies in computerized interpretation of ECG was started with the introduction of digital computer by Caseres and others (Milliken et al., 1969) was able to acquire ECG data from a patient using portable machine. Microprocessor standalone units for automated interpretation were in used in 1970s (Murray, 1982). Gradient –based algorithm and time domain morphology was presented (Mazomenos et al., 2012). Also, (Chatterjee et al., 2011) described statistical method of comparison between relative magnitudes of ECG samples and their time domain slope. Another classifier based on ECG morphological features was reported in (Chazal et al., 2004) and (Chazal and Reilly, 2006). Wavelet transform finds application in ECG beats detection and feature extraction as reported in (Li et al., 1995), (Saxena et al., 2003) and (Martinez et al., 2004). Also, (Mahesh, 2010) used wavelet and Pan-Tompkins to extract time-frequency features for ECG beat detection system. In (Marlar and Aung, 2014), they presented classification of normal and abnormal signal using R-R interval features of ECG waveform. Wavelet entropy analysis of high resolution ECG signal using continuous wavelet transform (CWT) and discrete wavelet transform was presented (Natwong et al., 2006).

So far, several techniques such as support vector machines (Martis et al., 2012), neural networks (Inan et al., 2006), self organizing map (Lagorholm et al., 2000), hybrid fuzzy neural network (Osowski and Linh, 2001) and probabilistic neural network (Martis et al., 2013) have been introduced for the ECG beat classification. The area of automated arrhythmia detection system is still an active area of research in order to provide high classification accuracy for inter and intra patient variation cases due to the fact that these machine learning techniques map new data instances based on the information extracted from the annotated training data in the learning phase and provide a global classifier that may not be always accurate for patient-specific cardiac variations.

1.2 Significance of the Study

Information about the behavior of the heart can be extracted from P, QRS, and T peaks, time domain amplitude and ECG clinical features. Subtle changes in these peaks and their positions however cannot be clearly deciphered by the naked eye. The time domain features cannot provide high discrimination among different normal and abnormal beats. In order to increase the discrimination among classes, various transform domains need to be used .Various contributions have been made in literature regarding beat detection and classification of ECG signal. Most of them use either time or frequency domain representation of the ECG waveforms, on the basis of which many specific features are defined, allowing the recognition between the beats belonging to different classes. The most difficult problem faced by today's automatic ECG analysis is the large variation in the morphologies of ECG waveforms. Moreover, we have to consider the time constraints as well. Thus our basic objective is to come up with a simple method having less computational time without compromising with the efficiency. With this objective in mind, various techniques of ECG preprocessing, R-peak detection, future extraction, feature enhancement and classification has been searched and experimented. In this thesis, R-peak detection of ECG signal is implemented using Pan-Tompkins algorithm and the features were extracted from time, frequency and statistical domain for a precise and robust feature extraction and classification. The classification has been done using neural network back propagation algorithm, taking the features as temporal features, heart beat interval features and ECG statistical features.

1.3 Aim and Objectives

The main aim of this thesis is to develop a simple and reliable automatic ECG beat detection and classification system using a hybrid algorithm by combining a well known Pan Tompkins algorithm with discrete wavelet and stationary wavelet decomposition combined with statistical parameters in order to increase the accuracy of detection and classification, the ECG diagnostic system can recognized four ECG waveforms (Normal, Paced, Rbbb and Lbbb) and classify them accordingly. The above aim would be achieved through the following objectives

1. To review the literature on ECG preprocessing, feature extraction, and classification techniques
2. To extract morphological features from Pan-Tompkins algorithm as R-T interval after QRS detection
3. To apply wavelet transform for extraction of the transform coefficients using DWT and SWT as well as to search for a suitable wavelet.
4. To calculate statistical parameters from the DWT and SWT coefficients as a new feature for classification
5. To search for other feature extraction methods by looking at other ECG characteristics like R-R time intervals and R-peak amplitude
6. To use artificial neural networks for ECG waveform classification
7. To carry out comparative performance analysis with different methods developed in order to find a robust and efficient feature extraction and classification technique
8. To explore the features of eZ430-RF2500 wireless development tool by designing simple low cost wireless ECG acquisition system
9. To make suggestions on the feature improvement of the system and the development of the system into a real time diagnostic system.

1.4 Organization of the Report

In order to provide a continuous and smooth flow of information about the whole work, this thesis consists of seven chapters and organized as follows:

Chapter one is an introduction of the project. This chapter discusses the general research background information, challenges and problems associated with the study and proposed solution. Thesis significance, aim and objectives were presented. Chapter two presents the anatomy of human heart, its physiology, ECG leads and theories of arrhythmias used in the thesis. Chapter three gives a theoretical background information about wavelet transform including discrete wavelet transform and stationary wavelet transform, it also discuss a literature of wavelet entropy and artificial neural networks. Chapter four presents all the methods developed in realizing the feature sets. Also, it explains the tools used in this thesis

including Matlab toolboxes. Chapter five presents the results of the proposed system, discussion and comparative analysis. Chapter six gives information on hardware implementation of wireless ECG acquisition circuit, including background information, features of the components used, design and the result of the system. Lastly, chapter seven concludes the research and gives further suggestions and recommendations for future development and improvement.

CHAPTER TWO

ANATOMY OF THE HEART AND ELECTROCARDIOGRAPHY

2.0 Overview

A main study of this research is to detect abnormal signals generated by the human heart; hence, a substantial understanding of the source of this signal is essential. The human heart is at the center of the cardiovascular system, which is responsible for oxygenating blood and delivering it to different parts of the human body. Electrodes placed on the body's surface can detect electrical activity, which occurs in the heart. The recording of these electrical events comprises an electrocardiogram. Comparison of the information obtained from electrodes, placed in different positions on the body, enables electrical activity to be monitored and so the performance of different areas of cardiac tissue. This chapter commences with a review of the cardiovascular system and electrophysiology. This is followed by an examination of the conduction system of the heart, electrocardiogram, ECG leads, heart problems, and the brief information about the arrhythmias used in this study with their related literature.

2.1 The Heart Anatomy

The heart contains four chambers that is right atrium, left atrium, right ventricle, left ventricle and several atrioventricular and sinoatrial node as shown in Figure 2.1. The two upper chambers are called the left and right atria, while the lower two chambers are called the left and right ventricles. The atria are attached to the ventricles by fibrous, non-conductive tissue that keeps the ventricles electrically isolated from the atria. The right atrium and the right ventricle together form a pump to circulate blood to the lungs. Oxygen-poor blood is received through large veins called the superior and inferior vena cava and flows into the right atrium. The right atrium contracts and forces blood into the right ventricle, stretching the ventricle and maximizing its pumping (contraction) efficiency. The right ventricle then pumps the blood to the lungs where the blood is oxygenated. Similarly, the left atrium and the

left ventricle together form a pump to circulate oxygen-enriched blood received from the lungs (via the pulmonary veins) to the rest of the body (Acharya re al., 2012).

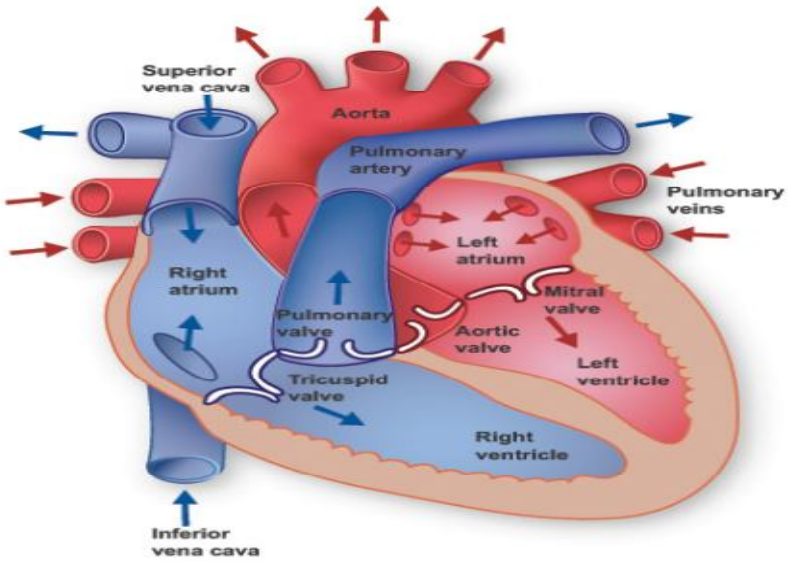

Figure 2.1: A full view of Human Heart, with chambers and valves (T.H, 2012)

2.1.1 Heart valves

There are 4 heart valves that dictate the blood flow through the human heart. The valves are unidirectional to prevent back flow of blood into the atria or ventricles. The valves open when there is a change of pressure in the chambers. The valves can be distinguished as two groups, the atrioventricular (AV) and the semilunar (SL) valves. Atrioventricular (AV) valves are relatively small compared to the semilunar valves. Their function is to ensure that blood does not flow back into the atrium from the ventricles during systole, the contraction of the heart. The mitral valve, in the left chamber, and the tricuspid valve, in the right chamber are considered as atrioventricular (AV) valves. The Aortic and Pulmonary valve are considered to be the Semilunar (SL) valves, which prevents blood flowing back from the arteries into the ventricles during systole. The Aortic valve is located between the left ventricle and the aorta, as the pulmonary valve is between the right ventricle and the pulmonary artery (Texas, 2014).

2.1.2 Circulatory system

A single cardiac cycle is the time between the start of one heartbeat and the beginning of the next. It, therefore, includes alternating periods of contraction and relaxation. For each of the heart chambers the cardiac cycle can be divided into two phases. During contraction, or systole, the chamber contracts and blood is pushed into an adjacent chamber or arterial trunk. Diastole follows systole. During diastole, the chamber fills with blood and prepares for the next cardiac cycle. The pressure within each chamber rises during systole and falls during diastole. The valves help to ensure that the blood flows in the correct direction. However, blood will only flow from the first to the second chamber, if the pressure in the first chamber is greater than that of the second. The correct pressure relationship is dependent on the timing of contractions. Blood movement would not occur if the atria and ventricle contacted together.

The heart, like other organs, also requires an adequate supply of oxygen and nutrients. These are supplied from arterial branches that arise from the ascending aorta. The flow of blood that supplies the heart tissue itself is called the **coronary circulation.** The heart pumps about 380 litres of blood to its own muscle tissue every day (Molly, 2000).

2.1.3 The Electrical Conduction System of the Heart

During a single heartbeat, the entire heart contracts in a coordinated manner. Thus blood flows in the right direction at the proper time. Contractile cells, and the conducting system, are the cardiac muscle cells involved in a normal heartbeat. Gap junctions connect all heart muscle cells, including the cells of the conduction system, to each other. These gap junctions make it easier for impulses to spread between adjacent cells. So, immediately after a heart cell depolarizes, the cells around it depolarize. In this way, a wave of excitation and contraction spreads over the entire heart (Wolters, 2011).

The conduction system of the heart shown in Figure 2.2 consists of the sinoatrial (SA) node, bundle of His, atrioventricular (AV) node, the bundle branches, and Purkinje fibers.

The SA node serves as a pacemaker for the heart, and it provides the trigger signal. It is a small bundle of cells located on the rear wall of the right atrium, just below the point where superior vena cava is attached. The SA node fires electrical impulses through the bioelectric mechanism. It is capable of *self-excitation* (firing on its own).

When the SA node discharges a pulse, the electrical current spreads across the atria, causing them to contract. Blood in the atria is forced by the contraction through the valves to the ventricles. There is a band of specialized tissue between the SA node and the AV node, however, in which the velocity of propagation is faster than it is in atrial tissue. This internal conduction pathway carries the signal to the ventricles.

It would not be desirable for the ventricles to contract in response to an action potential before the atria are empty of their contents. A delay is needed, therefore, to prevent such an occurrence; this is the function of the AV node. The action potential will reach the AV node 30 to 50 ms after the SA node discharges, but another 110 ms will pass before the pulse is transmitted from the AV node. The AV node operates like a delay line to retard the advance of the action potential along the internal electroconduction system toward the ventricles. Conduction into the bundle branches is rapid, consuming only another 60 ms to reach the furthest Purkinje fibers. The muscle cells of the ventricles are actually excited by the Purkinje fibers. The action potential travels along these fibers at a much faster rate, on the order of 2 to 4 m/s. The fibers are arranged in two bundles, one branch to the left and one to the right.

The normal rhythm of the heart is disturbed if the conducting pathways are damaged. If the SA or internodal pathways are damaged, the AV node will take over. The heart will beat at a slower rate. If a conducting cell or ventricular muscle cell generates an action potential more rapidly than the SA or AV node, then this is called

an ectopic pacemaker. This will bypass the conducting system and disrupt the timing of ventricular contraction. This will result in a reduction of the efficiency of the heart, and may be diagnosed with an electrocardiogram (Molly, 2000).

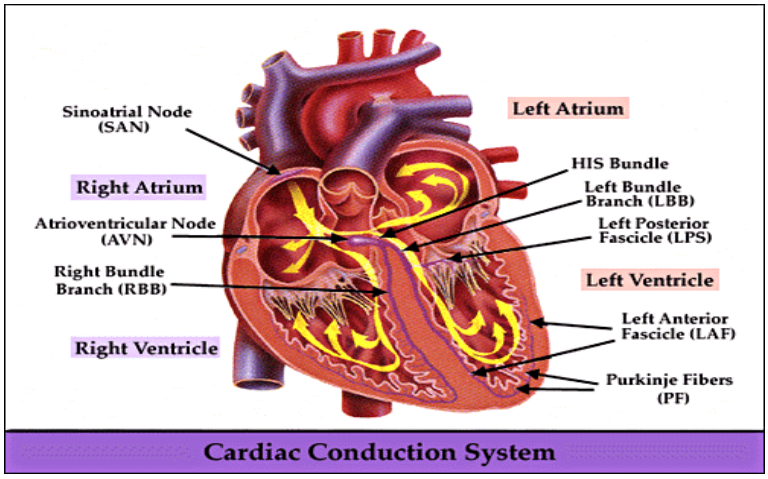

Figure 2.2: Conduction system of the heart (T.H., 2012)

2.2 Electrocardiogram

Electrocardiogram (ECG) is a diagnosis tool that reported the electrical activity of heart recorded by skin electrode. The morphology and heart rate reflects the cardiac health of human heart beat (Acharya, 2012). It is a noninvasive technique that means this signal is measured on the surface of human body, which is used in identification of the heart diseases (Germann, 2002). Any disorder of heart rate or rhythm, or change in the morphological pattern, is an indication of cardiac arrhythmia, which could be detected by analysis of the recorded ECG waveform. The amplitude and duration of the P-QRS-T wave contains useful information about the nature of disease afflicting the heart. The electrical wave is due to depolarization and repolarization of Na+ and k ions in the blood. The ECG signal provides the following information of a human heart (Moss, 1996):

- heart position and its relative chamber size
- impulse origin and propagation
- heart rhythm and conduction disturbances

- extent and location of myocardial ischemia
- changes in electrolyte concentrations
- drug effects on the heart.

2.3 Leads in ECG

There are 3 general types of ECG, the 3-Lead, 5-Lead and 12-Lead, each type differs in the number of electrodes used and the positioning of the electrodes.

The 3-lead ECG is the most basic type of monitoring, adopting the Einthoven's triangle arrangement where 3 electrodes are required. This group of electrodes is known as limb lead. According to the American Heart Association (AHA), the 3 electrodes are colored: white, black and red, and is labeled as the right-arm (RA), the left-arm (LA) and the left-limb (LL), respectively. Each electrode has different electrical polarity; hence, the direction of the current flow has to be addressed for each lead. The RA electrode has negative polarity and it is physically placed at the right collarbone area of the subject. The LL electrode has positive polarity and it is placed at the bottom left area of the ribcage. The LA electrode is negative polarity when paired with LL and positive polarity when paired with RA; it is physically placed at the right collarbone area of the subject. RA-LA (lead 1), RA-LL (lead 2) and LA-LL (lead 3) denotes the 3 lead pairings, each monitors different parts of the heart, as shown in Figure 2.3.

Table 2.1: types of leads used in ECG monitoring

Standard leads	Limb leads	Chest leads
Bipolar leads	Unipolar leads	Unipolar leads
Lead I	AVR	V1
Lead II	AVF	V2
Lead III	AVL	V3
		V4
		V5
		V6

Einthoven leads:

Lead I: records potentials between the left and right arm,

Lead II: between the right arm and left leg, and

Lead III: those between the left arm and left leg

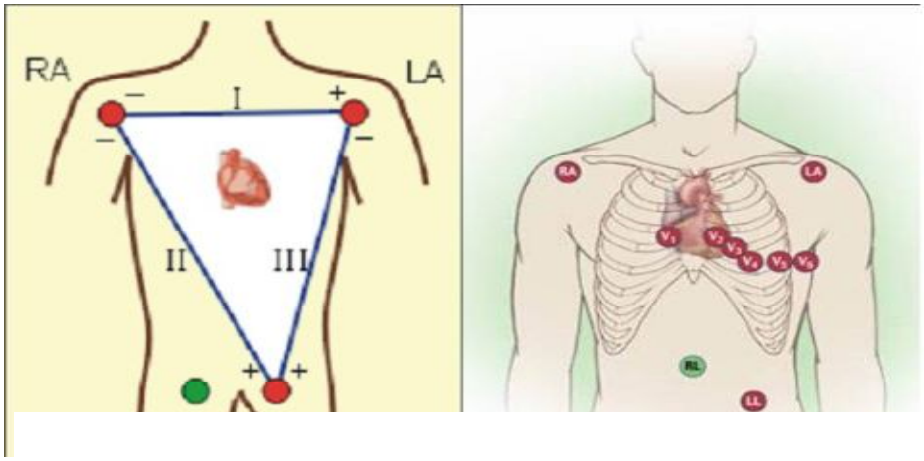

Figure 2.3: (a)The Einthoven Triangle for 3-lead ECG configuration(Klabunde, 2008)
(b)12-lead ECG configuration(Tompkins, 2008)

Another ECG monitoring type is the 5-lead ECG. This method uses the limb leads (RA, LA and LL) with two additional electrodes lead pairings. The additional electrodes are the chest lead (V1) and the right-limb (RL). The chest lead (V1) electrode is colored brown and has negative polarity; it is physically placed at the 4th interscostal space on right sternal border. Lead V1 captures the best waveform that can be used reliably to determine between SVT and VT. The right-limb (RL) electrode is colored green and has positive polarity; it is physically placed on the opposite side of the left-limb (LL) electrode. Lead RL is used as a complement to lead V1, to provide positive polarity. The advantages of the 5-lead ECG are that it provides a more comprehensive electrical view of the heart with additional leads; another advantage is that it helps to increase detection of an episode in ischemic monitoring.

The 12-lead ECG monitoring of the heart is the most comprehensive technique, it allows the electrical activity of the heart to be observed from three areas, anterior, interior and lateral. It uses the 3 limb leads (RA, LA, LL) and the 6 chest leads (V1-6) to acquire the ECG signal. The limb leads are used as bipolar and unipolar leads to complete 6 orientation of the frontal plane. The chest leads are unipolar and are placed across the patient mid-chest area; this lead placement captures the horizontal plane electrical activity of the heart. The placement for 12-lead ECG is shown in Figure 2.3b. The advantage of the 12-lead ECG is that medical experts can diagnose more specific arrhythmias with the full observation of the heart from three areas. Another advantage is that changes in the ECG segments from different lead can help to locate the cause of the arrhythmia (Fook, 2012).

2.4 ECG waves and interval

Figure 2.4 shows useful clinical signatures of ECG, durations and intervals commonly used for clinical diagnosis.

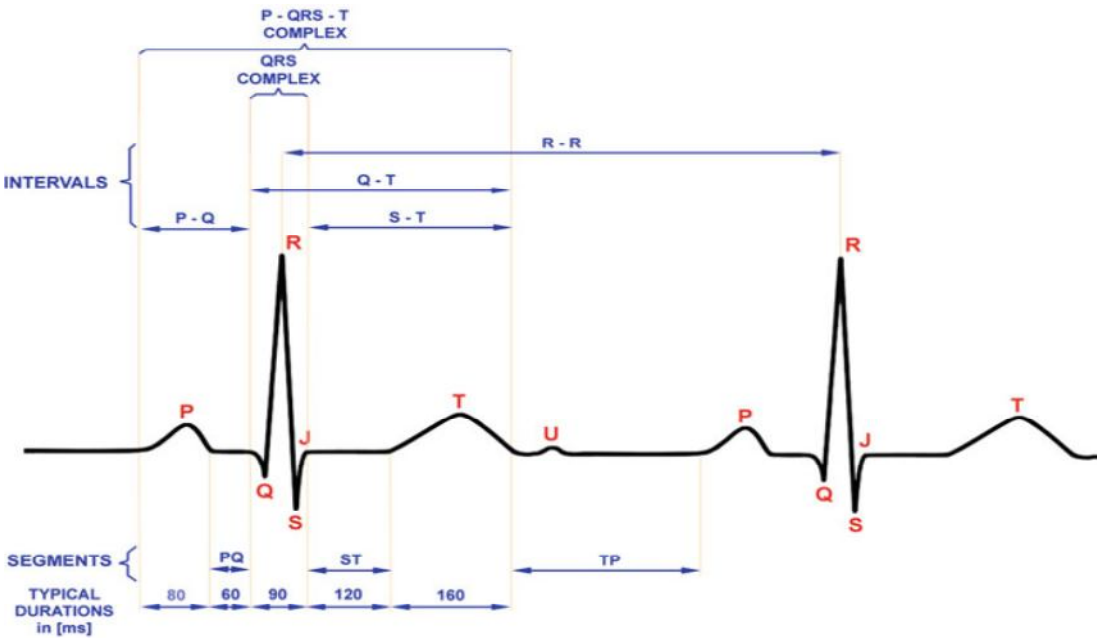

Figure 2.4: Typical shape of ECG signal and its essential waves and characteristic points (Adam and Witold 2012)

2.4.1 The P wave

The propagation of the SA action potential through the atria results in contraction of the atria, producing the P wave. The magnitude of the P wave is normally low (50-100uV) and 100msec in duration.

2.4.2 The PR interval

The PR interval begins with the onset of the P wave and ends at the onset of the Q wave. It represents the duration of the conduction through the atria to the ventricles. Normal measurement for PR interval is 120ms-200ms.

The PR segment begins with the endpoint of the P wave and ends at the onset of the Q wave. It represents the duration of the conduction from the atrioventricular node, down the bundle of its end through the bundle branches to the muscle.

2.4.3 The QRS complex

The QRS complex corresponds to the period of ventricular contraction or depolarization. The atrial repolarization signal is swamped by the much larger ventricular signal. It is the result of ventricular depolarization through the Bundle Branches and Purkinje fibre.

The QRS complex is much larger signal than the P wave due to the volume of ventricular tissue involved. If either side of the heart is not functioning properly, the size of the QRS complex may increase.QRS can be measured from the beginning of the first wave in the QRS to where the last wave in the QRS returns to the baseline. Normal measurement for QRS is 60ms-100ms.

2.4.4 The ST segment

The ST segment represents the time between the ventricular depolarization and the repolarization. The ST segment begins at the end of the QRS complex (called J point) and ends at the beginning of the T wave. Normally, the ST segment measures 0.12 second or less. The precise end of the depolarization (S) is difficult to determine as some of the ventricular cells are beginning to repolarise.

2.4.5 The T wave

The T wave results from the repolarization of the ventricles and is of a longer duration than the QRS complex because the ventricular repolarization happens more slowly than depolarization. Normally, the T wave has a positive deflection about 0.5mv, although it may have a negative deflection. It may, however, be of such low amplitude that it is difficult to read. The duration of the T wave normally measures 0.20 sec or less.

2.4.6 The QT interval

The QT interval begins at the onset of the Q wave and ends at the endpoint of the T wave, representing the duration of the ventricular depolarization/repolarization cycle.

Table 2.2 Amplitude and duration of waves, intervals and segments (Frank, 2014)

s/n	Features	Amplitude(mV)	Duration(ms)
1	P wave	0.1-0.2	60-80
2	PR-segment	-	50-120
3	PR-interval	-	102-200
4	QRS complex	1	80-120
5	ST-segment	-	100-120
6	T-wave	0.1-0.3	120-160
7	ST-interval	-	320
8	RR-interval	-	(0.4-1.2)s

The normal QT interval measures about 0.38 second, and varies in males and females and with age. As a general rule, the QT interval should be about 40 percent of the measured R-R interval (Dubowik, 1999).

2.5 Heart Diseases

In the early 1980, according to the Centers for Disease Control and Prevention, United States (2007), heart disease is the leading cause of death for both women and men almost in the world and it is also a major cause of disability. In the worldwide, coronary heart disease kills more than 7 million people each year. Heart disease is a broad term that includes several more specific heart conditions which are coronary heart disease, heart attack, ischemia, arrhythmias, cardiomyopathy, congenital heart disease, peripheral arterial disease (PAD). The most common heart condition is coronary heart disease, which can lead to heart attack and other serious conditions and the research from PubMed Central Journals (2007) shows that the Ischemia is the most common cause of death in the industrialized countries. So the earliest diagnosis and treatment using electrocardiography (ECG) has been developed to observe the disease signal. (Papaloukas et al. 2003) has indicated that the development of suitable automated analysis techniques can make this method very effective in supporting the physician's diagnosis and in guiding clinical management.

2.5.1 Heart Problems in This Thesis

Changes from the normal morphology of the ECG can be used to diagnose many different types of arrhythmia or conduction problems. ECG can be split into different segments and intervals, which relate directly to phases of cardiac conduction. Limits can be set on these to diagnose abnormality.

There are lots of heart problems which can be diagnosed from different ECG waveforms. This thesis aims at classifying 4 different waveforms. They are: Normal (N), Right Bundle Branch Block (R or RBBB) Paced Beats (P) and Left Bundle Branch Block (L or LBBB). They will be explained as follows (Wartak J., 1978).

2.5.2 Normal Waveform

This is the normal adult human waveform with features described as in previous section.

2.5.3 Right Bundle Branch Block

Right Bundle Branch Block (RBBB) shown in Figure 2.5 has the following ECG characters (KCUMB, 2006):

- The QRS duration between 0.10 and 0.11 sec (incomplete RBBB) or 0.12sec or more (complete RBBB) as shown in Figure 2.6 and 2.7.
- Prolonged ventricular activation time or QR interval (0.03sec or more in V1-V2)
- Right axis deviation (Figure 2.8).

Incomplete RBBB often produce patterns similar to those of right ventricular hypertrophy.

The ECG pattern of RBBB is frequently associated with ischemic, hypertensive, rheumatic and pulmonary heart disease, right ventricular hypertrophy and some drug intoxication; occasionally it may be found in healthy individuals.

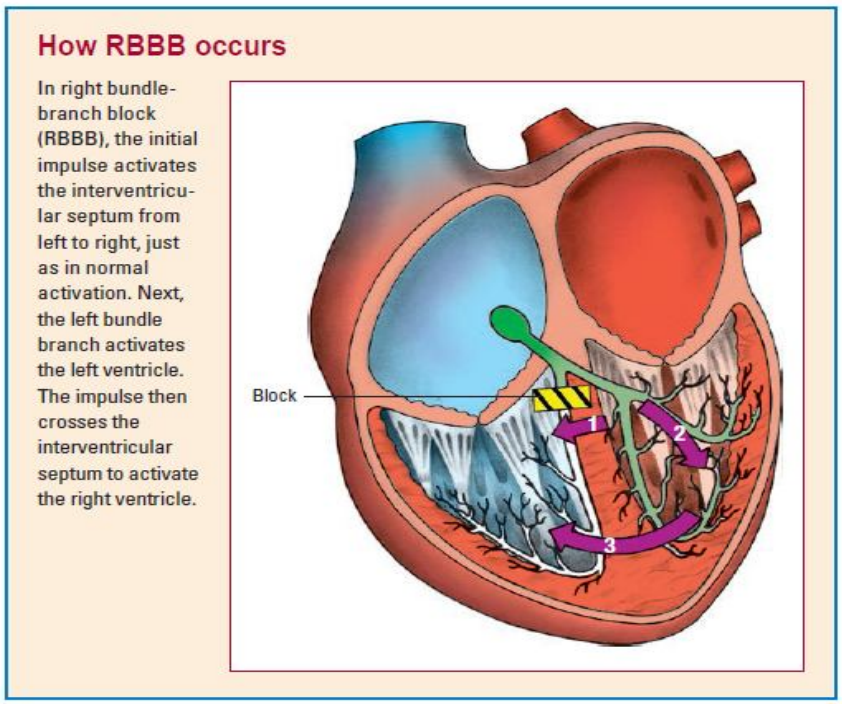

Figure 2.5: Right bundle branch block (Wolters, 2011)

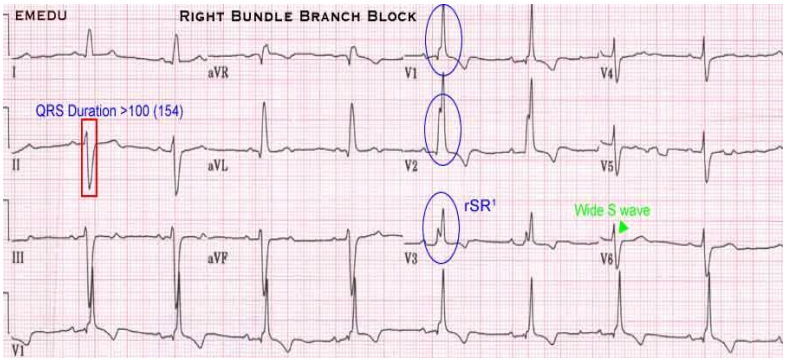

Figure 2.6: Right bundle branch block with markup (Emedu, 2012)

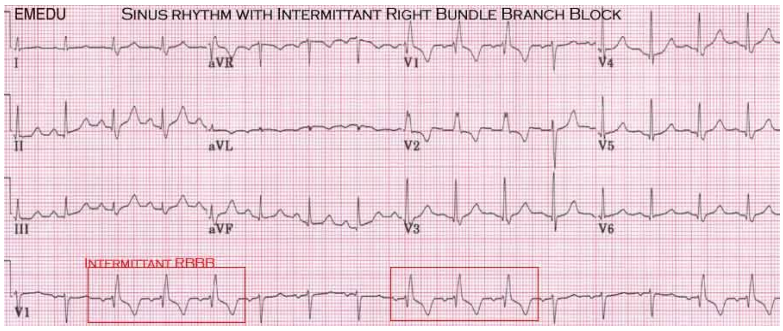

Figure 2.7: Sinus rhythm with intermittent Right bundle branch block (Emedu, 2012)

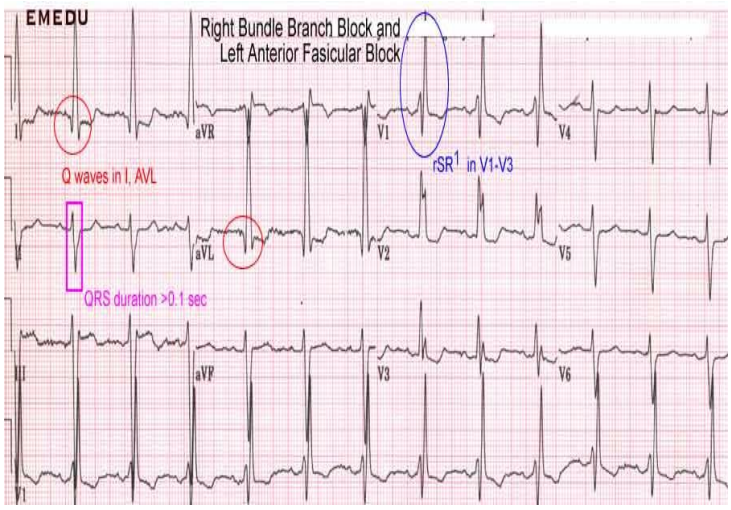

Figure 2.8: Right bundle branch block and left anterior fasicular block (Emedu, 2012)

2.5.4 Paced Beats

This is the artificial beat form from the device called pacemaker. A pacemaker is a treatment for dangerously slow heart beats. Without treatment, a slow heart beat can lead to weakness, confusion, dizziness, fainting, shortness of breath and death. Slow heart beats can be the result of metabolic abnormalities or occur as a result of blocked arteries to the heart's conduction system. These conditions can often be treated and a normal heart beat will resume. Slow heart beats can also be a side effect of certain medications in which case discontinuation of the medicine or a reduction in dose may correct the problem. It can be characterized in ECG by a large peak after QRS complex.(intelligent recognition)

2.5.5 Left bundle branch block

In this condition, activation of the left ventricle is delayed, which causes the left ventricle to contract later than the right ventricle as shown in Figure 2.9. It has the following characteristics (KCUMB, 2006):

- A complete LBBB has a QRS of greater than 0.12sec (Figure 2.10)
- Normally the septum is activated from left to right, producing small Q waves in the lateral leads.
- As the ventricles are activated sequentially (right, then left) rather than simultaneously, this produces a broad or notched ('M'-shaped) R wave in the lateral leads as shown in Figure 2.11.
- Normally the septum is activated from left to right, producing small Q waves in the lateral leads.

Amongst the causes of LBBB are:

- Aortic stenosis
- Dilated cardiomyopath
- Acute myocardial infarction

- Extensive coronary artery disease
- Primary disease of the cardiac electrical conduction system
- Long standing hypertension leading to aortic root dilatation and subsequent aortic regurgitation
- Lyme disease

Treatment

- Patients with LBBB require complete cardiac evaluation, and those with LBBB and syncope or near-syncope may require a pacemaker.
- Some patients with LBBB, a markedly prolonged QRS (usually > 150 ms), and systolic heart failure may benefit from a biventricular pacemaker, which allows for better synchrony of heart contractions (Stevenson et al., 2011).

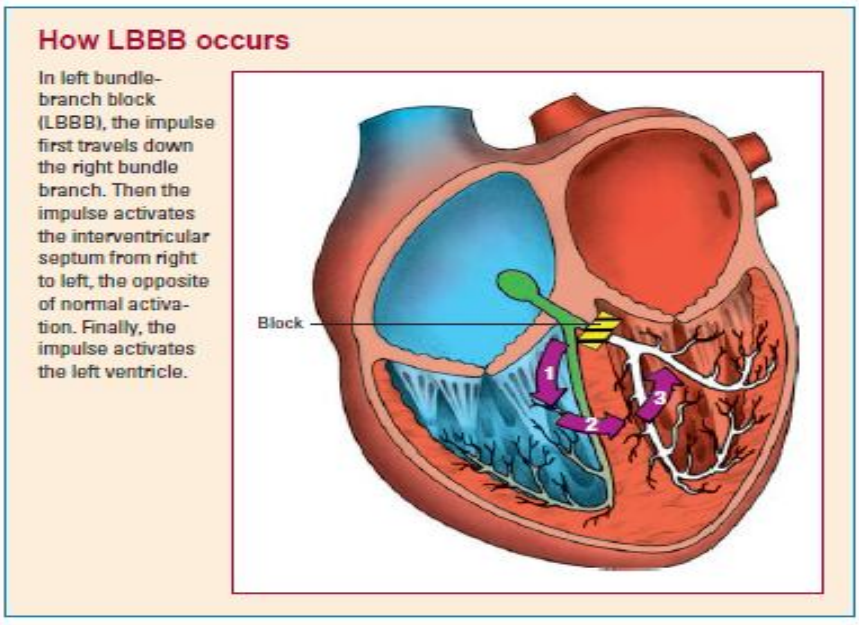

Figure 2.9: Left bundle branch block (Wolters, 2011)

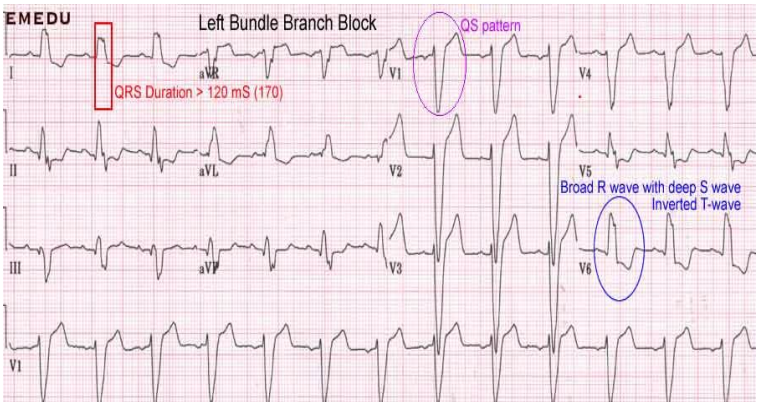

Figure 2.10: Left bundle branch block with markup (Emedu, 2012)

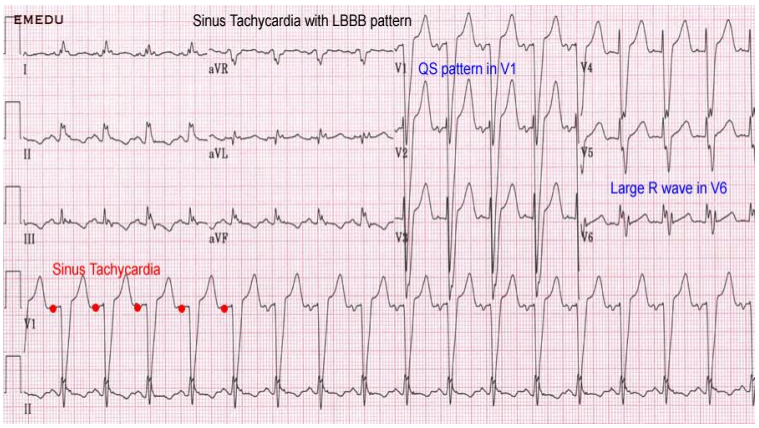

Figure 2.11: Sinus tachycardia with Left bundle branch block (Emedu, 2012)

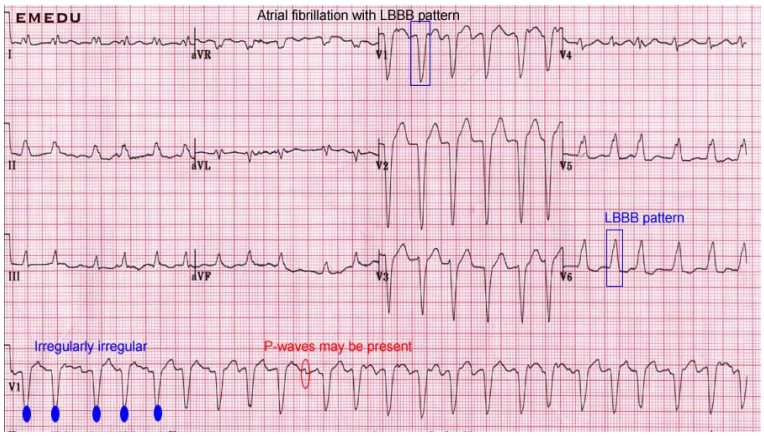

Figure 2.12: Atrial fibrillation with Left bundle branch block(Emedu, 2012

CHAPTER THREE

WAVELET TRANSFORM AND NEURAL NETWORK

3.0 Overview

Wavelet Transform has been proposed as an alternative way to analyze the non-stationary biomedical signals, which expands the signal onto the basis functions. The wavelet method act as a mathematical microscope in which we can observe different parts of signal by just adjusting the focus. A conventional application of wavelet methods to processing of a medical waveform uses a wavelet transform based on the application of a single wavelet, rather than a basis set constructed from a family of mathematically related wavelets. Again, the choice of a wavelet with appropriate morphological characteristics relative to the physiological signal under consideration is crucial to the success of the application. Therefore this chapter gives a brief review of wavelet transforms and its application to biomedical signals. Also, the chapter discusses the theory of wavelet entropy and artificial neural network.

3.1 Mathematical Transformation

Mathematical transformations are applied to signals to obtain further information from that signal that is not readily available in the raw signal. There are a number of transformations that can be applied, among which the Fourier transforms are probably by far the most popular. When we plot time-domain signals, we obtain a time-amplitude representation of the signal. This representation is not always the best representation of the signal for most signal processing related applications. In many cases, the most distinguished information is hidden in the frequency content of the signal. The frequency spectrum of a signal is basically the frequency components (spectral components) of that signal. The frequency spectrum of a signal shows what frequencies exist in the signal.

The Fourier transform is defined mathematically as:

$$F(\omega) = \int f(t) e^{-j\omega t}\, dt \qquad (3.1)$$

$$F(t) = \frac{1}{2\pi} \int f(\omega) e^{j\omega t}\, d\omega \qquad (3.2)$$

3.1.1 Why do we need the frequency information?

Often times, the information that cannot be readily seen in the time-domain can be seen in the frequency domain. Let's give an example from biological signals. Suppose we are looking at an ECG signal (ElectroCardioGraphy, graphical recording of heart's electrical activity). The typical shape of a healthy ECG signal is well known to cardiologists. Any significant deviation from that shape is usually considered to be a symptom of a pathological condition.

This pathological condition, however, may not always be quite obvious in the original time-domain signal. Cardiologists usually use the time-domain ECG signals which are recorded on strip-charts to analyze ECG signals. Recently, the new computerized ECG recorders/analyzers also utilize the frequency information to decide whether a pathological condition exists. A pathological condition can sometimes be diagnosed more easily when the frequency content of the signal is analyzed.

The big disadvantage of a Fourier expansion however is that it has only frequency resolution and no time resolution. This means that although we might be able to determine all the frequencies present in a signal, we do not know when they are present. To overcome this problem in the past decades several solutions have been developed which are more or less able to represent a signal in the time and frequency domain at the same time.

Although FT is probably the most popular transform being used (especially in electrical engineering), it is not the only one. There are many other transforms that are used quite often by engineers and mathematicians. Hilbert transform, short-time Fourier transform, Wigner distributions, the Radon Transform, and of course our featured transformation, the wavelet transform, constitute only a small portion of a huge list of transforms that are available at engineer's and mathematician's disposal. Every transformation technique has its own area of application, with advantages and disadvantages, and the wavelet transform (WT) is no exception.

3.2 Stationarity of a Signal

Signals whose frequency content does not change in time are called stationary signals. In other words, the frequency content of stationary signals does not change in time. In this case, one does not need to know at what times frequency components exist, since all frequency components exist at all times.

For example, consider the following signal

$$x(t) = \cos(2\pi 10t) + \cos(2\pi 25t) + \cos(2\pi 50t) + \cos(2\pi 100t) \qquad (3.3)$$

is a stationary signal, because it has frequencies of 10, 25, 50, and 100 Hz at any given time instant. This signal is plotted below:

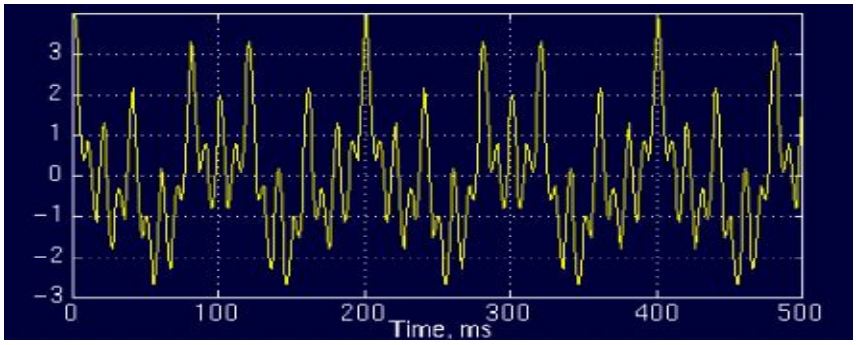

Figure 3.1: Time domain plot of signal in equation 3.1 (Robi, 2006)

And the following is its FT:

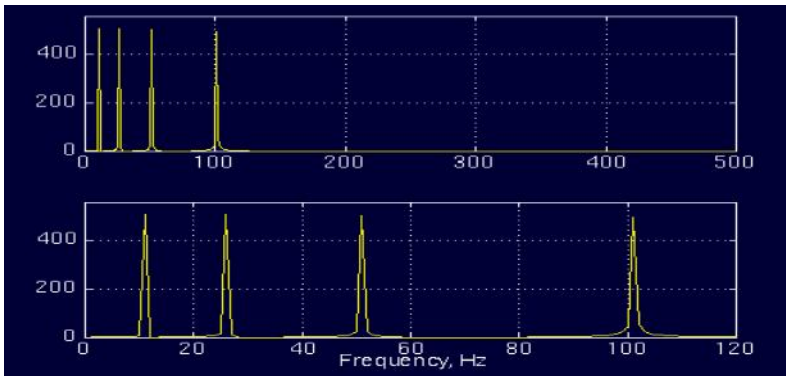

Figure 3.2: Fourier transform plot of signal in equation 3.1(Robi, 2006)

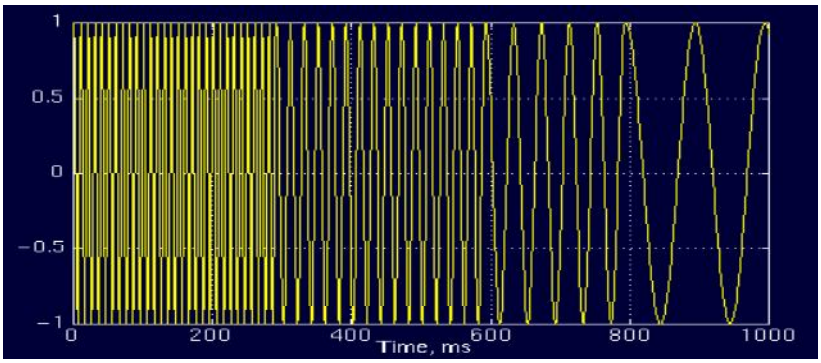

Figure 3.3: Time domain plot of non-stationary signal (Robi, 2006)

Contrary to the signal in the Figure above, Figure below plots a signal with four different frequency components at four different time intervals, hence a non-stationary signal. The interval 0 to 300 ms has a 100 Hz sinusoid, the interval 300 to 600 ms has a 50 Hz sinusoid, the interval 600 to 800 ms has a 25 Hz sinusoid, and finally the interval 800 to 1000 ms has a 10 Hz sinusoid.

And the following is its FT:

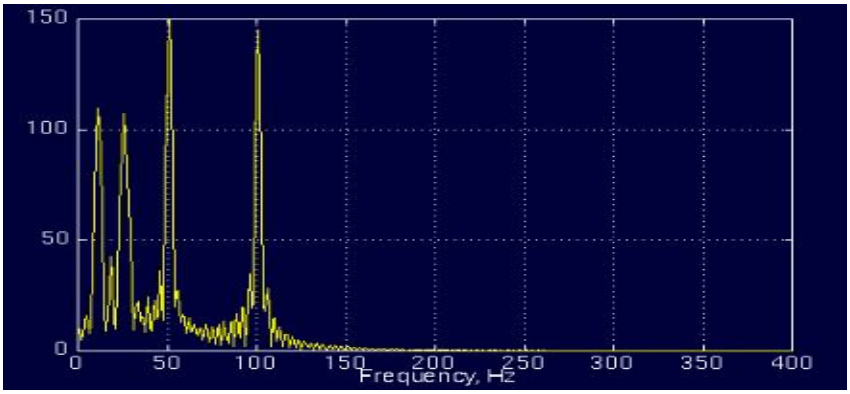

Figure 3.4: Fourier transform of figure 3.3 (Robi, 2006)

FT gives the spectral content of the signal, but it gives no information regarding where in time those spectral components appear. Therefore, FT is not a suitable technique for non-stationary signal, with one exception: FT can be used for non-stationary signals, if we are only interested in what spectral components exist in the signal, but not interested where these occur. However, if this information is

needed, i.e., if we want to know, what spectral component occur at what time (interval), then Fourier transform is not the right transform to use (Robi, 2006).

For practical purposes it is difficult to make the separation, since there are a lot of practical stationary signals, as well as non-stationary ones. Almost all biological signals, for example, are non-stationary. Some of the most famous ones are ECG (electrical activity of the heart, electrocardiograph), EEG (electrical activity of the brain, electroencephalograph), and EMG (electrical activity of the muscles, electromyogram).

3.3 The Short Term Fourier Transforms (STFF)

The STFT is obtained by calculating the Fourier transform of a sliding windowed version of the time signal s(t). The location of the sliding window adds a time dimension and one gets a time-varying frequency analysis.

The mathematical representation of STFT is:

$$S(t,f) = \int_{-\infty}^{+\infty} s(\tau) w(\tau - t) e^{-j2\pi f t}\, d\tau \qquad (3.2)$$

Where $w(\tau - t)$ it is the sliding window applied to the signal $s(t)$, f is the frequency and t is the time.

The length of the window is chosen so that to maintain signal stationary in order to calculate the Fourier transform. To reduce the effect of leakage (the effect of having finite duration), each sub-record is then multiplied by an appropriate window and then the Fourier transform is applied to each sub-record. As long as each sub-record does not contain rapid changes the spectrogram will give an excellent idea of how the spectral composition of the signal has changed during the whole time record. However, there exist many physical signals whose spectral content is so rapidly changing that finding an appropriate short-time window is problematic, since there may not be any time interval for which the signal is stationary. To deal with these time changes properly it is necessary to keep the length of the time window as short

as possible. This, however, will reduce the frequency resolution in the time-frequency plane. Hence, there is a trade-off between time and frequency resolutions.

3.4 Wavelet Theory

Wavelet theory is the mathematics associated with building a model for a signal, system, or process. A wavelet is a wave which has its energy concentrated in time. It has an oscillating wavelike characteristic but also has the ability to allow simultaneous time and frequency analysis and it is a suitable tool for transient, non-stationary or time-varying phenomena. WT has a varying window size, being broad at low frequencies and narrow at high frequencies, thus leading to an optimal time-frequency resolution in all frequency ranges.

Figure 3.5: Sinusoidal signal and Deubecheis wavelet (Michel et al. 1996)

From the figure above, the signals with sharp changes might be better analyzed with an irregular wavelet than with a smooth sinusoid, as quoted in (Mahmoodabadi et al. 2005). Also, local features can be described better with wavelets that have local extent.

3.4.1 Continuous Wavelet Transform (CWT)

The continuous wavelet transform was developed as a method to obtain simultaneous, high resolution time and frequency information about a signal. The CWT rather than the STFT uses a variable sized window region .Because the wavelet may be dilated or compressed; different features of the signal are extracted. While a narrow wavelet extracts high frequency components, a stretched wavelet picks up on the lower frequency components of the signal.

The CWT is computed by correlating the signal s(t) with families of time-frequency atoms Ψ (t), it produce a set of coefficients C(τ,s) given by :

$$C(\tau, s) = \frac{1}{\sqrt{\tau}} \int_{-\infty}^{+\infty} s(t) \Psi * \left(\frac{t-s}{\tau}\right) dt \qquad (3.3)$$

Where

- τ is the time location(translation parameter)
- s is called scale factor and it is inversely proportional to the frequency (s > 0)
- *dénotes a complexe conjugate.
- Ψ (t) is the analysing wavelet (mother wavelet).

The term mother implies that the functions with different region of support that are used in the transformation process are derived from one main function, or the mother wavelet. In other words, the mother wavelet is a prototype for generating the other window functions.

The analyzing wavelet function Ψ(t) should satisfy some properties. The most important ones are continuity, integrability, square integrability, progressivity and it has no d.c component (Hannu, 2011).

3.4.2 Discrete Wavelet Transform

The Discrete Wavelet Transform (DWT), which is a time-scale representation of the digital signal is obtained using digital filtering techniques, is found to yield a fast computation of wavelet transform. It is easy to implement and adopts dyadic scales and translations in order to reduce the amount of computation time, which results in better efficiency of calculation.

The DWT which also referred to as decomposition by wavelet filter banks is computed by successive low pass filter (LPF) and high pass filtering (HPF) of the discrete time-domain signal as the process shown graphically in figure below

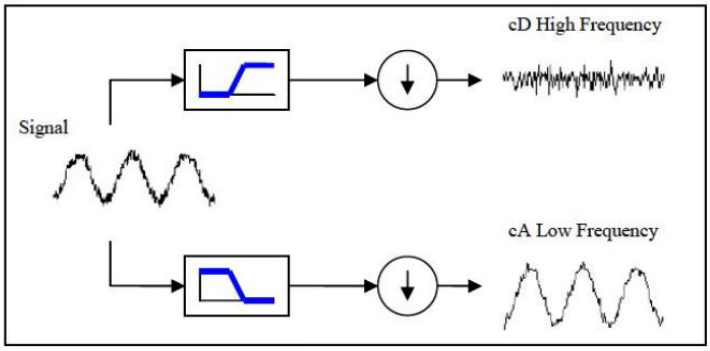

Figure 3.6: Filter banks signal decomposition (Nor, 2010)

The different cutoff frequencies are used for the analysis of the signal at different scales to measure the amount of detail information in the signal and the scale is determined by upsampling and downsampling process where D and A denoting for details and approximations, while c representing coefficients. The approximations of the signal are what define its identity while the details only imparts nuance.

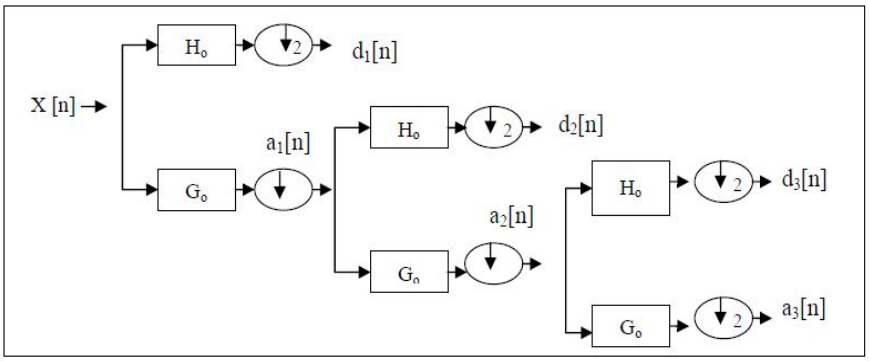

Figure 3.7: Three level Wavelet decomposition tree (Nor and Binti, 2010)

Figure 3.7 show the decomposition process is iterative. It connects the continous-time multiresolution to the discrete-time filters. The signal is denoted by the sequence input signals $x[n]$, where n is an integer passed through a series of high-pass filters to analyze the high frequencies, and through a series of low-pass filters to analyze the low frequencies. Each stage consists of two digital filters and

two downsamplers by 2 to produce the digitized signal. The low pass filter is denoted by G_o while the high pass filter is denoted by H_o. At each level, the high pass filter produces detail information; $d[n]$, while the low pass filter associated with scaling function produces coarse approximations, $a[n]$. The downsampled outputs of first high pass filters and low-pass filters provide the detail, D_1 and the approximation, A. the first approximation, A_1 is decomposed again and this process is continued. The filtering and decimation process is continued until the desired level is reached. The maximum number of levels depends on the length of the signal. Only the last level of approximation is save among all levels of details, which provides sufficient data. The DWT of the original signal is then obtained by concatenating all the coefficients, $a[n]$, and $d[n]$, starting from the last level of decomposition. The signal decomposition can mathematically be expressed in equation 3.4 and 3.5:

$$y_{hi}[k] = \sum x[n].\, g[2k - n] \qquad (3.4)$$

$$y_{lo}[k] = \sum x[n].\, h[2k - n] \qquad (3.5)$$

With this approach, the time resolution becomes arbitrarily good at high frequencies, while the frequency resolution becomes arbitrarily good at low frequencies.

In DWT the signals can be represented by approximations and details. The detail at level j is defined as equation 3.6:

$$D_j = \sum_{k \subset z} a_{j.k}\, \Psi_{j.k}(t) \qquad (3.6)$$

Where, Z is the set of positive integers.

Then, the approximation at level J is defined as Equation 3.7:

$$A_i = \sum_{j>J} D_i \qquad (3.7)$$

Finally, the signal f(t) can be represented by Equation 3.8:

$$f(t) = A_i = \sum_{j>J} D_i \qquad (3.8)$$

In DWT where a scaling function is used, which are related to low-pass and high-pass filters, respectively. The scaling function can be represented as Equation 3.9 and Equation 3.10:

$$\Phi(n) = \sum_{j=0}^{N-1} c_j\, \Phi(2n - j) \qquad (3.9)$$

$$\Phi_{j.k}(t) = 2^{\frac{j}{2}} \Phi\left(2^j t - k\right) \qquad (3.10)$$

Discrete Wavelet analysis corresponds to windowing in a new coordinate system, in which space and frequency are simultaneously localized; this property can be helpful in pattern extraction. Wavelets as an alternative tool to analyze non-stationary signal have been applied to ECG delination, to detect accurately the different waves forming the entire cardiac cycle, especially in areas of limited performance current techniques like QT and ST intervals, P and T-wave recognition, and to classify ECG waves in different cardiopatologies, identifying ECG waveforms from different arrhythmias, or discriminating between normal and abnormal cardiac pattern. In addition, DWT is able to detect specific detailed time-frequency components of ECG signal, for instance, the registers which are sensitive to transient ischemia and eventual restoration of electrophysiological function of the myocardial tissue. Moreover, methods for analyzing heart rate variability using wavelet transform can be used to detect transient changes without losing frequency information. The most common wavelets providing the orthogonality properties are daubechies, symlets, coiflets and discrete meyer in order to provide reconstruction using the fast algorithms.

3.4.3 Stationary wavelet transform

The Stationary wavelet transform (SWT) is a wavelet transform algorithm designed to overcome the lack of translation-invariance of the discrete wavelet transform (DWT). Translation-invariance is achieved by removing the downsamplers and upsamplers in the DWT and upsampling the filter coefficients by a factor of $2^{(j-1)}$ in the jth level of the algorithm (Akansu, 1991; Tazebay, 1995). The SWT is an inherently redundant scheme as the output of each level of SWT contains the same number of samples as the input – so for a decomposition of N levels there is a redundancy of N in the wavelet coefficients. The major advantage of SWT is the preservation of time information of the original signal sequence at each level. This algorithm is more famously known as "*algorithme à trous*" in French (word *trous* means holes in English) which refers to inserting zeros in the filters. It was introduced by (Holdschneider et al, 1989).

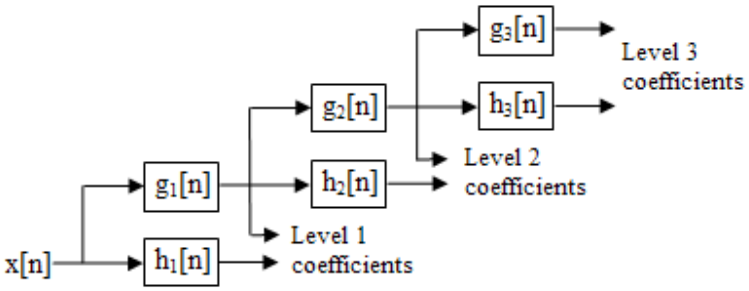

Figure 3.8: A 3 level SWT filter bank (James, 2014)

In the above diagram, filters in each level are up-sampled versions of the previous (see figure below).

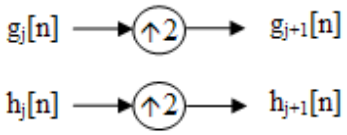

Figure 3.9: SWT filters (James, 2014)

3.5 Wavelet Entropy (WE)

The Shannon entropy (Shannon, 1948) gives a useful criterion for analyzing and comparing probability distribution, it provides a measure of the information of any distribution. We define the total WE (Blanco et al., 1998) as

$$S_{wt} \equiv S_{wt}(p) = -\sum_{j<0} p_j \,.\ln [p_j] \qquad (3.11)$$

The WE appears as a measure of the degree of order/disorder of the signal, so it can provide useful information about the underlying dynamical process associated with the signal. In fact, a very ordered process could be thought of as a periodic mono-frequency signal (signal with a narrow band spectrum). A wavelet representation of such a signal will be greatly resolved in one unique wavelet resolution level, i.e. all relative wavelet energies will be almost zero except for the wavelet resolution level which includes the representative signal frequency. For this

special level the relative wavelet energy will be almost one and in consequence the total WE will be near zero or of a very low value.

A signal generated by a totally random process can be taken as representing a very disordered behavior. This kind of a signal will have a wavelet representation with significant contributions from all frequency bands. Moreover, one could expect that all the contributions will be of the same order. Consequently, the relative wavelet energy will be almost equal for all resolution levels and the WE will take their maximum values.

3.5.1 Wavelet average entropy

Transient signals have some characteristics such as high frequency and instant break, so wavelet transform is strong tool for them in feature picking-up, and it satisfies the analysis need of electric power transient signals. Usually wavelet transform of transient signal is expressed by multi-revolution decomposition fast algorithm which utilizes the orthogonal wavelet bases to decompose the signal to components under different scales. It is equal to recursively filtering the signal with a high-pass and low-pass filter pair. Filtering by high pass filter produces details and filtering by low-pass produces approximations. The band width of these two filters is equal. After each circle of decomposition, the sampling frequency is reduced by half. Then recursively decompose the low-pass filter outputs, both components of the next stage are produced.

Given discrete signal x(n) being fast transformed, at instant k and scale j it has high-frequency component coefficient $d_j(k)$ and low-frequency component coefficient $a_j(k)$. The frequency band of the information contains in signal components $D_j(k)$, $A_j(k)$ obtained by reconstruction is (Daubechies, 1990; Mallat, 1989),

$$\begin{cases} D_j(k): \left[2^{-(j+1)}F_s, 2^{-j}F_s\right] \\ A_j(k): \left[0, 2^{-(j+1)}F_s\right] \end{cases} (j = 1,2,\dots,m) \qquad (3.12)$$

Where f_s is the sampling frequency. The original signal sequence $x(n)$ can be represented by the sum of all components, namely

$$x(n) = D_1(n) + A_1(n) = D_1(n) + D_2(n) + A_2(n) = \sum_{j=1}^{J} D_j(n) + A_J(n) \quad (3.13)$$

For the purpose of unification, denote $A_J(n)$ by $D_{J+1}(n)$ and we get

$$x(n) = \sum_{j=1}^{J} D_j(n) \quad (3.14)$$

$D_j(n)$ represents the component of transient signal $x(n)$ at each scale (frequency band), it is also the multi-resolution representation of the signal which can act as feature subset of classification.

For continuous wavelet transform, series of discrete wavelet coefficients Di under the different scales $j(j = 1, \dots, m)$ are obtained, which can reflect time-frequency distribution to some extent.

3.5.2 Information entropy

The uncertainty of any event is associated with its states and probabilities. The aggregation of all possible states is called sample space $\{x_1, x_2, \dots, x_n\}$ Each piece of information has a probability $P(x_i) = P_i, 0 \leq P_i \leq 1, \ \sum P_i = 1.$ The self information quantity of the event x_i is,

$$I(x_i) = -\log_a P(x_i) = -\log_a P_i \quad (3.15)$$

$I(\mathrm{x_i})$ is a random variable changing with different information, so it is not suitable for measuring the whole information source. Therefore, we define the mathematical expectation of the self-information as the mean self-information of the information source, which is entropy denoted by $H(X)$.

$$H(X) = E[I(x_i)] = E[-\log_a p_i] = -\sum_i P_i \log_a p_i \quad (3.16)$$

The base *a* of the logarithm defines the unit of the entropy.

When a is 2, e and 10, the unit of the entropy is bit, nat and Hartely respectively. Customarily, we choose a=e. The information entropy above is used to measure the

mean information quantity of the information source. When all events have the same probabilities, the uncertainty of a certain event reaches its maximum, so does the entropy. The entropy of any certain event is zero. Therefore, entropy is the measure of the uncertainty.

3.5.3 Spectrum entropy

Based on conception of information entropy and power spectrum, the spectrum entropy is defined in the frequency domain [5].Given $X(\omega)$ as the DTF of signal x(n), the power spectrum is $S(\omega) = \frac{1}{2\pi n}|X(\omega)|^2$ Because of the conversion of energy in time and frequency domain, namely

$\sum x^2(t)\Delta t = \sum|X(\omega)|^2\Delta\omega$, $S = \{S_1, S_2, \dots, S_n\}$ is a partition of original signal, so the proportion of i-th power spectrum occupied in whole is $P_i = \frac{S_i}{\sum_{i=1}^{n} S_i}$ The corresponding information entropy namely power spectrum entropy is the following,

$$H = -\sum_{i=1}^{n} p_i \log p_i \qquad (3.17)$$

Spectrum entropy is a measure of the signal complexity. Narrower the peak of the signal power spectrum is, smaller the spectrum entropy is. Which means the signal is more regular and less complex. Flatter the power spectrum is, larger the spectrum entropy is. For example, the white noise is irregular random signal, it has flat power spectrum and large spectrum entropy, which means the signal has high complexity (Zheng-You, et al. 2006).

3.5.4 Wavelet time-frequency entropy

There are various wavelet entropy measures such as wavelet energy entropy, wavelet time entropy, wavelet singular entropy, wavelet time-frequency entropy, wavelet average entropy and wavelet distance entropy. in each of the above, $E_{jk} = |D_j(k)|^2$ is the wavelet energy spectrum at scale j and instant k, $E_j = \sum_k E_{jk}$ is the wavelet spectrum at scale j.

In this thesis we used wavelet time-frequency entropy as a measure of entropy for ECG signal feature extraction and classification.

The discrete wavelet presentation $D_j(k)$ is in fact a two dimension matrix. Along with variable k and j two vector sequences can be get. Therefore we define wavelet time frequenct entopy (WTFE) as,

$$WTFE(k,j) = [WTFEt(t = kT), WTFEf(a = 2^j)] \quad (3.18)$$

Where

$$WTFEt(t = kT) = -\sum_j P_{D(a=2^j)} \ln P_{D(a=2^j)} \quad (3.19)$$

$$WTFEf(a = 2^j) = -\sum_k P_{D(t=kT)} \ln P_{D(t=kT)} \quad (3.20)$$

Where $P_{D(a=2^j)} = |D_j(k)|^2 / \sum_j |D_j(k)|^2$

$$P_{D(t=kT)} = |D_j(k)|^2 / \sum_k |D_j(k)|^2 \quad (3.21)$$

The result of WTFE measure consists of two vectors or sequences. The first vector stretches on the whole time space and the second vector stretches on the whole frequency space. A large entropy value at instant kT indicates there are widely distributed wavelet coefficients extend all over the frequency space. On the other hand, a small entropy value indicates wavelet coefficients congregate at a few frequency points or segments. WTFE is able to measure the signal information feature at any given instant and frequency. Therefore it can be used to classify different signals and has potential in the fault detection and diagnosis field.

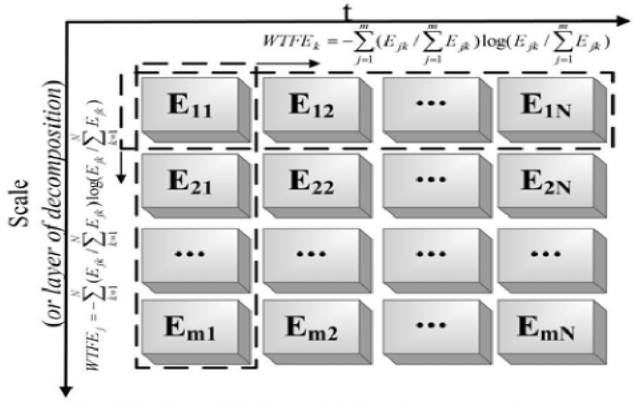

Figure 3.10: Fundamental of wavelet time-frequency entropy (Zheng-You, et al. 2006).

3.6 Artificial Neural network

Artificial neural networks (ANN) have been trained to perform complex function in various fields of application including pattern recognition, identification, classification, speech, vision and control system. A neural network is a massively parallel-distributed processor that has a natural propensity for storing experiential knowledge and making it available for use. It resembles the brain in two aspects (Chazal D.P., 1998):

- Knowledge is acquired by the network through a learning process,
- Inter-neuron connection strengths known as synaptic weights are used to store the knowledge.

In theory, neural networks can do anything a normal digital computer can do. We can train a neural network to perform a particular input leads to a specific target output. Such a situation is shown in Figure 3.11 (Demuth H. and Beale M., 2001). There, the network is adjusted, based on a comparison of the output and the target, until the network output matches the target.

Typically many such input/target pairs are used, in this supervised learning to train a network.

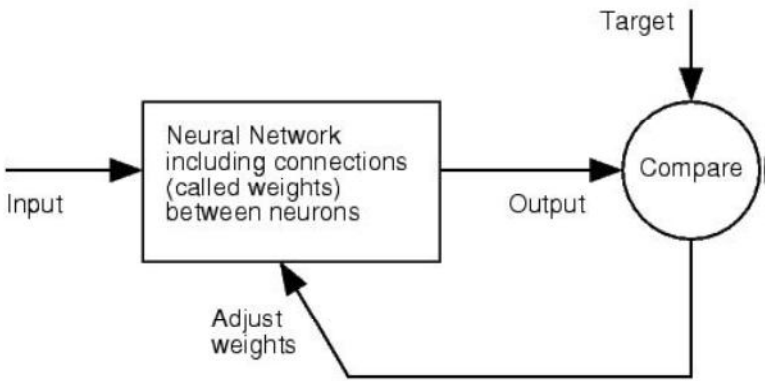

Figure 3.11: Neural Network adjust system

In practice, neural network have been trained to perform complex function in various fields of application. They are especially useful for signal classification. If there are enough training examples and enough computing resources it is possible to train a feed-forward neural network to perform almost any mapping to an arbitrary level of precision.

3.6.1 The neuron

The simplest Neural Network is the single layer perceptron. It is a simple net that can decide whether an input belongs to one of two possible classes. Output of a perceptron usually passed through nonlinearity called a transfer function. This transfer function is of different types; the most popular is a sigmoidal function.

A simple description of the operation of a neuron is that it processes the electric currents, which arrive on its dendrites, and transmits the resulting electric currents to other connected neurons using its axon. The classical biological explanation of this processing is that the cell carries out a summation of the incoming signals on its dendrites. If this summation exceeds a certain threshold, the neuron responds by issuing a new pulse, which is propagated along its axon. If the summation is less than the threshold the neuron remains in active.

$$\mathrm{u_i} = \sum_{i-1}^{N} \mathrm{w_{ji}x_i} \tag{3.22}$$

$$o_j = f\left(u_j - \theta_j\right) \tag{3.23}$$

In these two equations, each set of synapses is characterized by a weight or strength of its own. A signal X, at the input of synapse *i* connected to neuron *j* is multiplied by synaptic weight w_{ji}. It is important to make a note of the manner in which these subscripts of the synaptic weight w_{ji} are written. The first subscript refers to the neuron in question and the other subscript refers to the input end of the synapse to which the weight refers. The weight w_{ji} is positive if the associated synapse is excitatory, it is negative if the synapse is inhibitory. An adder sums the input signals, weighted by the respective synapses of the neuron.

The amplitude of the output of a neuron limits an activation function. The activation function is also referred to as a squashing function in that it squashes the permissible amplitude range of the output signal to some finite value.

3.6.2 Transfer function

Many transfer functions have been included in Matlab neural network toolbox. The most commonly used functions are log-sigmoid, tan-sigmoid and linear transfer functions.

Multi-layer networks often use the log-sigmoid transfer function as shown in Figure 3.12

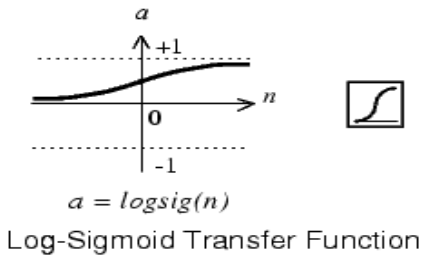

Figure 3.12: Log-Sigmoid Transfer Function (Demuth H. and Beale M., 2001)

Alternatively, multi-layer network may use the tan-sigmoid transfer function as shown in Figure 3.13

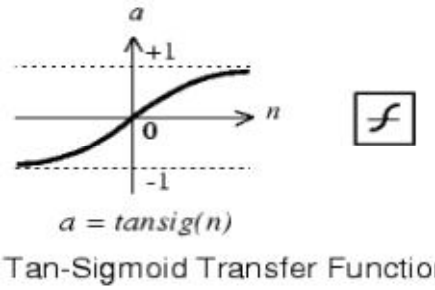

Figure 3.13: Tan-Sigmoid Transfer Function (Demuth H. and Beale M., 2001)

Occasionally, the linear transfer function purelin is used as shown in Figure 3.14

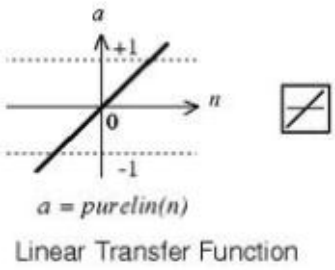

Figure 3.14: Linear Transfer Function (Demuth H. and Beale M., 2001)

The sigmoid transfer function squashes the input, which may have any value between plus and minus infinity into the range of 0 to 1. This transfer function is commonly used in backpropagation networks, in part because it is differentiable.

3.6.3 Single-layer feed-forward network

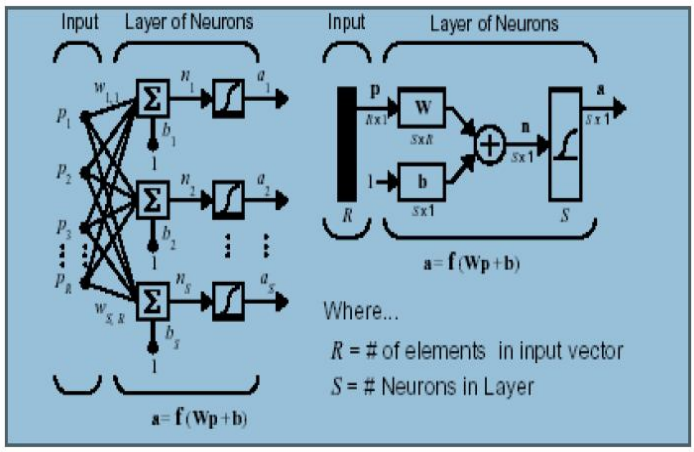

Figure 3.15 Single-layer feed-forward network (Demuth H. and Beale M., 2001)

A layered neural network is a network of neurons organized in the form of layers. Figure 3.15 shows the simplest form of a layered network, which has an input layer of source nodes that projects onto an output layer of neurons but not vice versa.

In other words, this network is strictly of a feed forward type. The input layer of source nodes does not count, because no computation is performed there.

A one-layer network with *R* input elements and *S* neurons are shown in Figure 3.15. In this network each element of the input vector *p* is connected to each neuron input through the weight matrix *Wp*. The *ith* neuron has a summer that gathers its weighted inputs and bias to form its own scalar output *n(i)*. The various n(i) taken together form an *S*-element net input vector *n*. Finally, the neuron layer outputs form a column vector *a*. It is shown the expression for *a* at the bottom of the Figure.

It is common for the number of inputs to a layer to be different from the number of neurons.

A layer is not constrained to have the number of its inputs equal to the number of its neurons.

3.6.4 Matrix-vector input

A neuron with a single R-element input vector, p1,p2……..pR, is shown in Figure 3.15. The individual element inputs are multiplied by weights, w1,1, w1,2,……..w1,R as shown in equation 3.24.

The weighted values are fed to the summing junction. Their sum is simply *Wp*, the dot product of the (single row) matrix *W* and the vector *p*.

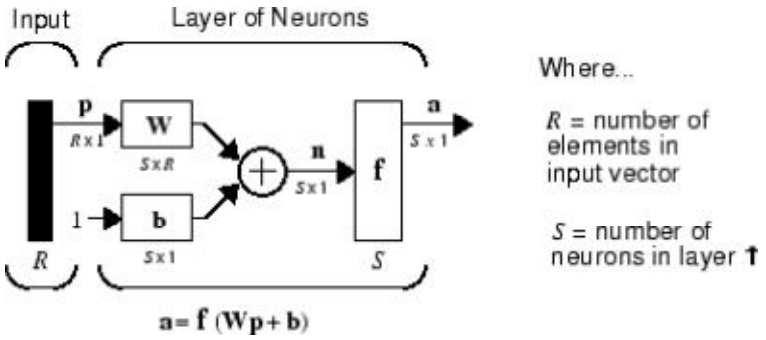

Figure 3.16: A neuron with a single R-element input vector (Howard Demuth, 2001)

The neuron has a bias b, which is summed with the weighted inputs to form the net input n.

This sum, n, is the argument of the transfer function f.

$$n = w_{1,1}\, p_1 + w_{1,2}\, p_2 \; + \cdots + w_{1,R}\, p_R + b \qquad (3.24)$$

A layer of a network is defined in Figure 3.16 shown above. A layer includes the combination of the weights, the multiplication and summing operation (here realized as a vector product Wp), the bias b, and the transfer function f. The array of inputs, vector **p**, will not be included in or called a layer.

The input vector elements enter the network through the weight matrix $\boldsymbol{W}$.

$$\mathbf{W} = \begin{bmatrix} w_{1,1} & w_{1,2} & \cdots & w_{1,R} \\ w_{2,1} & w_{2,2} & \cdots & w_{2,R} \\ & & & \\ w_{S,1} & w_{S,2} & \cdots & w_{S,R} \end{bmatrix} \qquad (3.25)$$

The row indices on the elements of matrix **W** indicate the destination neuron of the weight and the column indices indicate which source is the input for that weight. Thus, the indices in W_{12} say that the strength of the signal from the second source to the first (and only) neuron is W_{12} (Martin, 2002).

3.6.5 Multi-layer feed-forward network

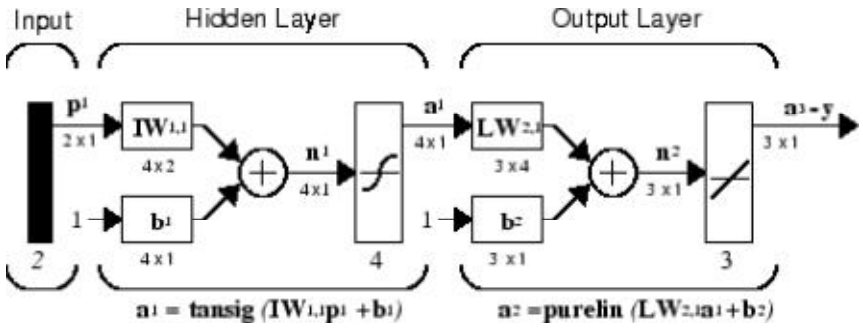

Figure 3.17: Multi-layer feed-forward network (Demuth H. and Beale M., 2001)

The second class of feed forward neural networks is multi-layer, shown in Figure 3.17. It may distinguish itself by the presence of one or more hidden layers, whose computation nodes are correspondingly called hidden neurons or hidden units. The function of the hidden neurons is to intervene between the external input and the network output. By adding one or more hidden layers, the network is enabled to extract higher-order statistics and is particularly valuable when the size of the input layer is large.

Each neuron in the hidden layer is connected to a local set of source nodes that lie in its immediate neighborhood. Likewise, each neuron in the output layer is connected to a local set of hidden neurons. Thus, each hidden neurons responds essentially to local variations of the source signal.

A network can have several layers. Each layer has a weight matrix W, a bias vector b, and an output vector a. To distinguish between the weight matrices, output vectors and so on, for each of these, we will append the number of the layer to the names for each of these variables.

For instance, the weight matrix and output vector for the first layer are denoted as W_1 and A_1, for the second layer these variables are designated W_2, A_2 and so on.

The network shown above has R_1 inputs, S_1 neurons in the first layer, S_2 neurons in the second layer, etc. It is common for the different layers to have different numbers of neurons.

A constant input 1 is fed to the biases for each neuron.

The outputs of each intermediate layer are the inputs to the following layer. Thus layer 2 can be analysed as a one-layer network with S_1 inputs, S_2 neurons, and an $S_1 x S_2$ weight matrix W_2. The input to layer 2 is a1, the output is a2. Now that we have identified all the vectors and matrices of layer 2 we can treat it as a single layer network on its own. This approach can be taken with any layer of the network. The layers of a multi-layer network play different roles. A layer that produces the

network output is called an output layer. All other layers are called hidden layers. (Demuth H. and Beale M., 2001)

Multiple layer networks are quite powerful. For instance, a network of two layers, where the first layer is sigmoid and the second layer is linear, can be trained to approximate any function (with a finite number of discontinuities) arbitrarily well. This kind of two-layer network is used extensively in backpropagation neural network.

3.6.6 Nodes, inputs and layers required

The number of nodes must be large enough to form a decision region, which is as complex as required by the given problem. However, it cannot be so large that the many weights required cannot be reliably estimated from the available training data. No more than three layers are required in perceptron like feed-forward networks, because a three-layer network can generate complex decision regions.

The number of nodes in the second layer must be greater than one when decision regions are disconnected or meshed and cannot be formed from one convex area. The number of second layer nodes required in the worst case is equal to the number of disconnected regions in input distributions. The number of nodes in the first layer must typically be sufficient to provide three or more edges for each convex area generated by every second layer-node. Typically there should be more than three times as many nodes in the second as in the first layer.

3.6.7 Training Algorithm

3.6.7.1 Backpropagation

Generalising the Widrow-Hoff learning rule to multiple-layer networks and nonlinear differentiable transfer function created backpropagation. Input vectors and the corresponding output vectors are used to train a network until it can approximate a function, associate input vectors with specific output vectors, or classify input vectors in an appropriate way as defined.

Standard backpropagation is a gradient decent algorithm, as is the Widrow-Hoff learning rule. The term backpropagation refers to the manner in which the gradient is computed for nonlinear multiplayer networks. There are numbers of variations on the basic algorithm which are based on other standard optimization techniques, such as conjugate gradient and Newton methods.

The backpropagation neural network is a feed-forward network that usually has hidden layers, as shown in Figure 3.17. The activation function for this type of network is generally the sigmoid function. Since the activation function for these nodes is the sigmoid function above, the output from each node is given by (Hessian S.K.U. and Asim., 1999)

$$\sigma_i^k = F\left(a_i^k\right) \tag{3.26}$$

Where a_i is the total input to node *i,* which is given by:

$$\sigma_i^k = \sum_{j=1}^{n} w_{ij}\, a_j^k + \theta_i \tag{3.27}$$

Note how the weights are indexed. Weight w_{ij} is the weight of the connection from node *j* to node *i*. Now, as for the perceptron, we will minimize the error in the network by using the gradient descent algorithm to adjust the weights. So the change in the weight from node *j* to *i* is given by

$$\Delta_k W_{ij} = -a\frac{\partial E^k}{\partial W_{ij}} \tag{3.28}$$

Where E^k is the mean square error for the Kth pattern. The error for a hidden node *i* is calculated from the errors of the nodes in the next layer to which node *i* is connected. This is how the error of the network is backpropagated.

So, putting it all together, the change for weight, where node *i* is in a hidden layer, is given by:

$$\Delta_k W_{ij} = a\delta_i^k \sigma_j^k = a\left[F(a_k^k)\sum_{n=1}^{Np+1}\delta_n^k\, w_{ni}\right]\sigma_j^k = a\left[\sigma_i^k(1-\sigma_i^k)\sum_{n=1}^{Np+1}\delta_n^k\, w_{ni}\right]\sigma_j^k \tag{3.29}$$

The changes in the weights of the network, which allow the network to learn, are now totally defined. This generalized delta rule for backpropagation neural networks defines how the weights between the outputs layer and the hidden layer change, and how the weights between other layers change also. This network is called backpropagation because the errors in the network are fed backward, or backpropagated, through the network.

Generalization is perhaps the most useful feature of a backpropagation network. Since the network uses supervised training, a set of input patterns can be organized into groups and fed to the network. The network will "observe" the patterns in each group, and will learn to identify the characteristics that separate the groups. Often, these characteristics are such that a trained network will be able to correct groups, even if the patterns are noisy. The network learns to ignore the irrelevant data in the input patterns.

3.6.7.2 Conjugate Gradient Algorithm

The basic backpropagation algorithm adjusts the weights in the steepest descent direction (negative of the gradient). This is the direction in which the performance function is decreasing most rapidly. Although the function decreases most rapidly along the negative of the gradient, this does not necessarily produce the fastest convergence. In the conjugate gradient algorithms a search is performed along conjugate directions, which produces generally faster convergence than steepest descent directions.

In most of the conjugate gradient algorithms the step size is adjusted at each iteration. A search is made along the conjugate gradient direction to determine the step size which will minimize the performance function along that line (Demuth H. and Beale M., 2001). There are different search functions that are included in the toolbox.

3.6.7.3 Levenberg-Marquardt (TrainLM)

The Levenberg-Marquardt algorithm appears to be the fastest method for training moderatesized feed-forward neural network. The Levenberg-Marquardt algorithm was designed to approach second order training speed without having to compute the Hassian matrix. When the performance function has the form of a sum of squares (as is typical in training feedforward networks), then the Hessian matrix can be approximated by Newton's method.

Newton's method is faster and more accurate near an error minimum, so the aim is to shift towards Newton's method as quickly as possible.

CHAPTER FOUR

EXPERIMENTS AND SYSTEM DESIGN

4.0 Overview

In this chapter, the methods used for this research will be discussed. All of the proposed methods are implemented in MATlab 2013a on a personal computer. The methods for the system developed (Automatic ECG beats classification system) in this thesis involve data acquisition, noise removal, QRS detection, morphological feature extraction, DWT AND SWT decomposition of extracted features, calculating statistical features, feature enhancement using PCA, output vector formation and artificial neural network (ANN) design for signal classification for each of the above methods. The output can be used for ECG signal classification or making a report of the patient's heart condition as well as comparative study of different methods.

The development procedure is as follows (Figure 3.1):

1. ECG Data acquisition from a web database

2. Separating data into training and testing sub-data sets

3. Loading training and testing data

4. Pre-processing of training and testing data

5. QRS detection of training and testing data

6. Efficient feature extraction for applying to the neural network

7. Output vector formation

8. Designing the neural network structure

9. Evaluating of performance parameters

Below is the flow chart which depicts the general development procedures for Automatic computerized ECG beat detection system.

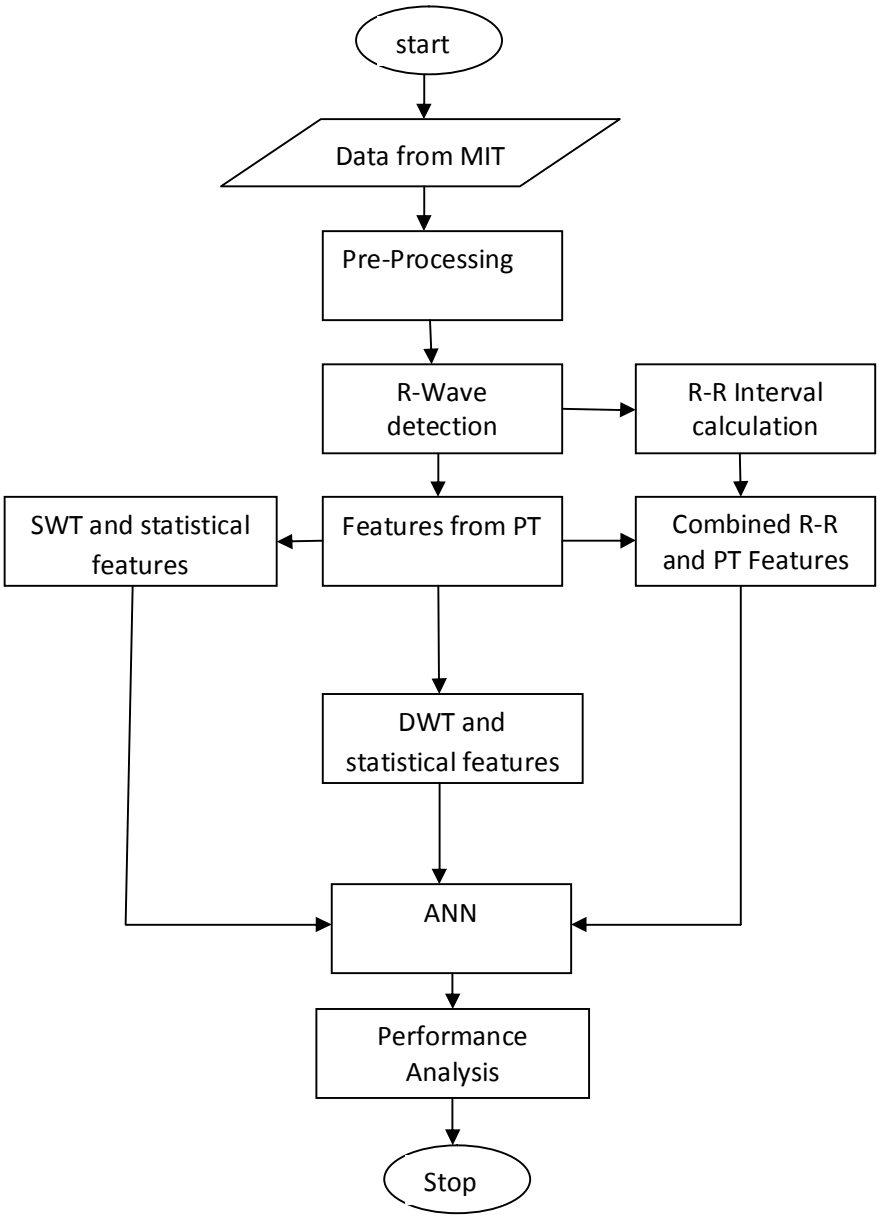

Figure4.1: Automatic ECG Beat Classification System Development Flow Chart

4.1 Experimental Tools: The Matlab Environment

Matlab is a powerful, comprehensive, and easy to use environment for technical computations. It provides engineers, scientists, and other technical professionals with a single interactive system that integrates numeric computation, visualization, and programming. Matlab includes a family of application specific solutions called toolboxes.

One of its greatest strengths is that Matlab allows building its own reusable tools. Customized special functions and programs can be easily created in Matlab code. Biomedical engineers use Matlab in research, design and manufacturing of medical devices and to develop embedded algorithms and systems for medical instrumentation. Matlab has several advantages over other traditional means of numerical computing.

- It allows quick and easy coding in a very high level language.
- Data structures require minimal attention, in particular, arrays need not be declared before first use.
- An interactive interface allows rapid experimentation and easy debugging.
- High-quality graphic and visualization facilities are available.
- Matlab M-files are completely portable across a wide range of platforms.
- Toolboxes can be added to extend the system, giving, for example, specialized signal processing facilities.

Furthermore, Matlab is a modern programming language and problem-solving environment: it has sophisticated data structures, contains built in debugging and profiling tools, and supports object oriented programming. These factors make Matlab to be an excellent language for teaching and a powerful tool for research and practical problem solving.

4.1.1 Signal processing toolbox

The signal processing toolbox is a collection of Matlab functions that provides a rich, customizable framework for analog and digital signal processing (DSP). Graphical user interfaces (GUIs) support interactive designs and analyses, while command-line functions support advanced algorithm development. The Signal Processing Toolbox is the ideal environment for signal analysis and DSP algorithm development. It uses industry-tested signal processing algorithms that have been carefully chosen and implemented for maximum efficiency and numeric reliability. Functions are mostly implemented as M-file routines written in the Matlab language, giving access to the source code and algorithms. The open system philosophy of

Matlab and the toolboxes enables making changes to existing functions or adding own experiments.

The main features of the signal processing toolbox are as follows (Little J.N. and Shure L.,2001):

- A comprehensive set of signal and linear system models
- Tools for analog filter design
- Tools for finite impulse response (FIR) and infinite impulse response (IIR) digital filter design, analysis and implementation.
- The most widely used transforms, such as Fast Fourier transform (FFT) and discrete cosine transform (DCT)
- Methods for spectrum estimation and statistical signal processing.

4.1.2 Wavelet Toolbox

The Wavelet Toolbox is a collection of functions built on the MATLAB® Technical Computing Environment. It provides tools for the analysis and synthesis of signals and images using wavelets and wavelet packets within the framework of MATLAB.

The toolbox provides two categories of tools:

- Command line functions
- Graphical interactive tools

The first category of tools is made up of functions that you can call directly from the command line or from your own applications. Most of these functions are M-files, series of statements that implement specialized wavelet analysis or synthesis algorithms. The second category of tools is a collection of graphical interface tools that afford access to extensive functionality.

The key features of wavelet toolbox are as follow (Michel et al., 1996):

- Standard wavelet families, including Daubechies wavelet filters, complex Morlet and Gaussian, real reverse biorthogonal, and discrete Meyer

- Wavelet and signal processing utilities, including a function to convert scale to frequency
- Methods for adding wavelet families
- Lifting methods for constructing wavelets
- Customizable presentation and visualization of data
- Wavelet Design and Analysis for continuous and discrete wavelet analysis
- Wavelet packets, implemented as MATLAB objects
- One-dimensional multisignal analysis, compression, and denoising
- Multiscale principal component analysis

4.1.3 Neural Network Toolbox

The Neural Network Toolbox extends the Matlab computing environment to provide tools for the design, implementation, visualization and simulation of neural networks. Neural networks are very powerful tools that are used in applications where formal analysis would be difficult or impossible, such as pattern recognition and non-linear system identification and control. The Neural Network Toolbox provides a comprehensive support for many proven network paradigms, as well as a graphical user interface that enables the experiment to design and manage networks. The toolbox's modular, open and extensible design simplifies the creation of customized functions and networks.

The main features of Neural Network Toolbox are as follows (Demuth H. and Beale M., 2001):

- Support for the most commonly used supervised and unsupervised network architectures
- A comprehensive set of training and learning functions
- Modular network representation, allowing an unlimited number of input setting layers, and network interconnections
- Pre and post-processing functions for improving network training and assessing network performance.

4.2 ECG Data Acquisition

In this thesis the source of the ECG data is MIT-BIH Arrhythmia database from Physionet website (**http: // www . physionet . org / physiobank / database / html / mitdbdir /mitdbdir .htm**). MIT-BIH Arrhythmia database is a set of over 4000 long-term Holter recordings. Approximately 60% of these recordings were obtained from in-patients. The database contains 23 records (numbered from 100 to 124, some numbers missing) chosen at random from this set, and 25 records (numbered from 200 to 234, again some numbers missing) selected from the same set to include a variety of rare but clinically important phenomena. Each of the 48 records is slightly over 30 minutes long (Goldberger et al., 2000).

The first group of records is intended to serve as a representative sample of the variety of waveforms and artifacts that an arrhythmia classifier might encounter in routine clinical use.

Records in the second group were chosen to include complex arrhythmia and conduction abnormalities. Some recordings from this group were selected for this thesis because the rhythm, QRS morphology variation or signal quality might be expected to present significant difficulty to arrhythmia classifier.

All the waveforms present in these recordings are studied and classified by expert cardiologist and presented as annotations in the website. Table 4.1 and 4.2 lists the ECG records .mat files that were used for training and testing the neural network in this thesis respectively.

Table 4.1: ECG .mat files used for training in this thesis

	Training		
s/n	File Name(.mat)	Number of R-peak detected	Number of features
1	Normal1_100m	74	73
2	Normal2_100m	75	74
3	Normal1_101m	63	62
4	Normal2_101m	60	59
5	Normal5_106m	59	58
6	Normal6_108m	57	56
7	Normal7_112m	87	86
8	Rbbb1_118m	73	72
9	Rbbb2_118m	71	70
10	Rbbb1_124m	50	49
11	Rbbb2_124m	49	48
12	Rbbb1_212m	90	89
13	Rbbb2_212m	92	91
14	Rbbb1_231m	64	63
15	Paced1_102m	73	72
16	Paced2_102m	73	72
17	Paced1_104m	51	50
18	Paced2_104m	56	55
19	Paced1_107m	71	70
20	Paced2_107m	70	69
21	Paced1_217m	72	71
22	Lbbb1_109m	91	90
23	Lbbb2_109m	85	84
24	Lbbb1_111m	68	67
25	Lbbb2_111m	66	65
26	Lbbb1_207m	79	78
27	Lbbb2_207m	77	76
28	Lbbb1_214m	69	68
Total		**1965**	**1937**

Table 4.2: ECG .mat files used for testing in this thesis

	Testing		
s/n	File Name(.mat)	Number of R-peak detected	Number of features
1	Normal3_100m	80	79
2	Normal3_101m	67	66
3	Normal10_116m	78	77
4	Rbbb3_118m	72	71
5	Rbbb3_124m	50	49
6	Rbbb2_231m	63	62
7	Paced3_102m	72	71
8	Paced3_104m	45	44
9	Paced2_217m	71	70
10	Lbbb3_109m	86	85
11	Lbbb3_111m	62	61
12	Lbbb3_214m	73	72
Total		**819**	**807**

Each of these records is slightly over 30 minutes long, has a sample frequency of 360Hz and contains 2 channels (2 signals recorded from different angles on chest). By using Physionet's built-in web tool only 1 minute long sections of each record is extracted as .mat files that can be readily used in Matlab. As a result 40 recordings (28 for training and 12 for testing amounting to 70-30% training-testing standard) each containing 21600 samples and approximately 60-90 waveforms depending on heart rate and class(normal, rbbb, paced or lbbb) is obtained and loaded into Matlab environment. After loading the data into Matlab one of the channels is removed and only one channel for each recording is used for the rest of the program (channel MLII).

At the end of the Data acquisition part a total of 1937 waveforms (as 7 separate recordings each representing a normal, rbbb, paced and lbbb waveform class) for training and 807 waveforms for testing are prepared ready for next step which is signal pre-processing.

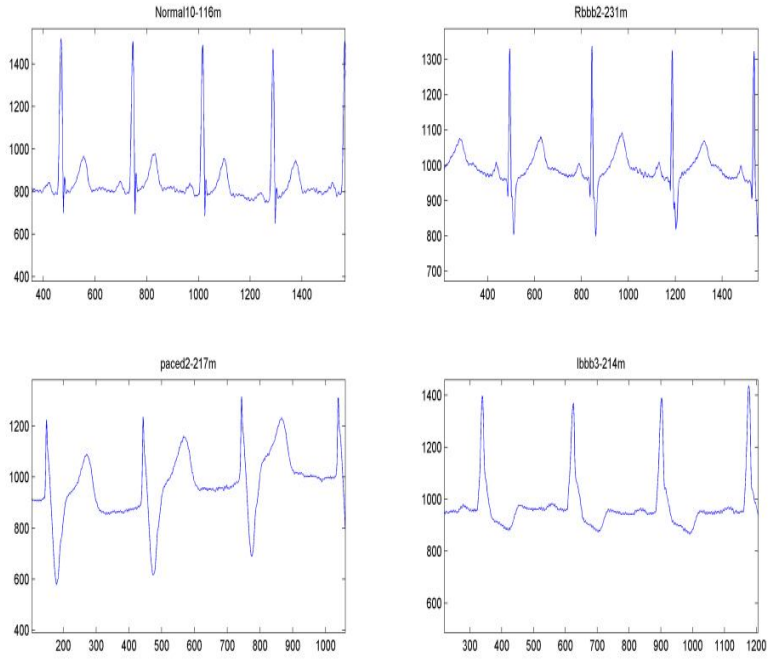

(a)

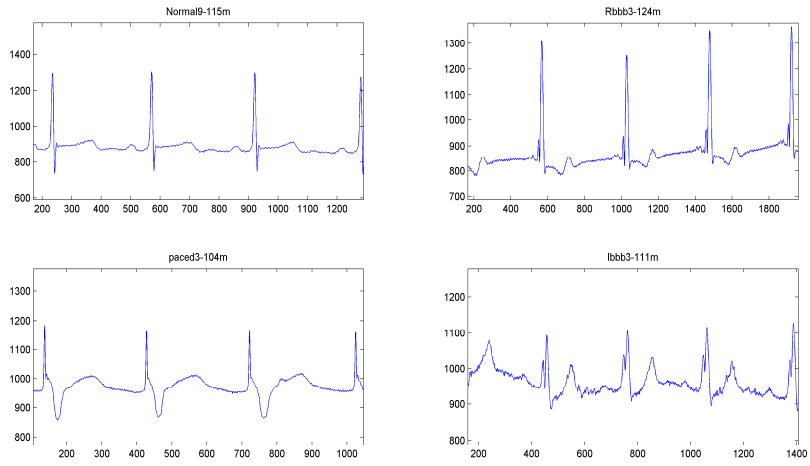

Figure 4.2(a) and (b): Raw ECG signal Obtained from MIT-BIH Database

(b)

4.3 Signal Pre-processing

Signal processing can be defined as the manipulation of a signal for the purpose of extracting information from the signal or producing an alternative representation of the signal. There are numerous specific motivations for signal processing, but many fall into following three categories. First is to remove unwanted signal components that are corrupting the signal of interest. Second is to extract information by rendering it in a more obvious or more useful form and third is to predict future values of the signal in order to anticipate the behavior of its source.

This thesis, at signal pre-processing step is focused on noise removal and after this step processing of the signal will continue with QRS detection and Feature extraction steps. ECG beat detection systems have to be designed in a way that they are capable of working in a noisy hospital environment. ECG signal is normally corrupted with different types of noise.

To obtain useful information from raw signals you have to first process them and remove the noise. Although our system will not be working on real time patient recorded signals, the ECG data that we get from MIT-BIH database may also contain some noise (Figure 3.4) so we also have to pre-process the signal and remove the noise.

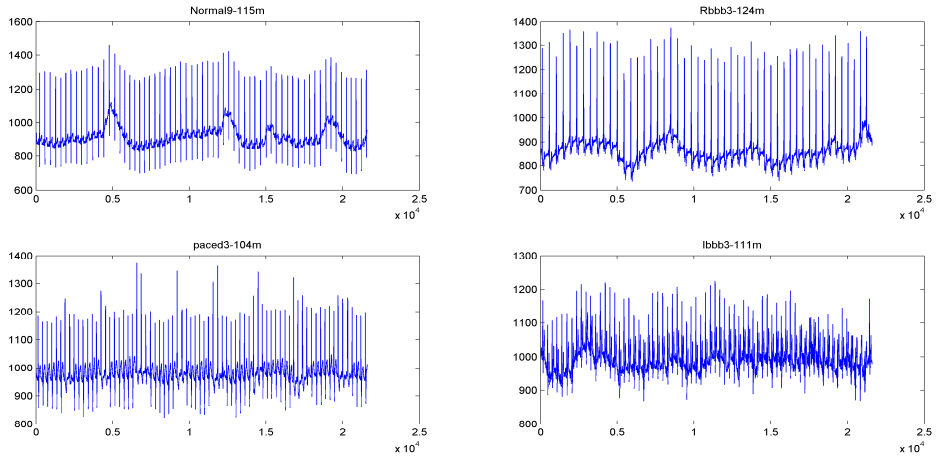

Figure 4.3: A Section of noisy ECG Records Obtained from MIT-BIH Database

To remove unwanted noise from raw ECG signals four levels of filtering is applied to ECG records; DC component removing, 10 point moving average (low pass) filter, derivative based (high pass) filter and a comb filter.

4.3.1 Removing DC Components of the ECG Signal

As it can be clearly seen from Figure 4.2, ECG signals taken from MIT-BIH database contain baseline (sections of ECG where there is no electrical activity of heart) amplitudes higher than zero. In this step by subtracting the mean of the signal from itself, the unwanted dc component is removed and the signal baseline amplitude is pulled back to level zero.

$$ECGSignal = ECGSignal - mean(ECGSignal) \quad (4.1)$$

4.3.2 Removing Low Frequency and High Frequency Noise

ECG data used for the system contains low and high frequency noise components that may be caused by the sources explained in the previous chapter. Before the design of the software both frequency domain and time domain filters were tested for noise removal. It is observed that time domain filters provide better noise removal on the signals obtained from MIT-BIH database than frequency domain filters (butterworth filters in our case). Because of this and since most of the

noise present in the database are random noise, time domain filters were chosen to filter unwanted high and low frequency noise.

To remove high frequency random noise, mostly caused by patients muscle contractions during recording, from the ECG signals a 10 point moving average (low pass) filter (Figure 4.3) which passes low frequencies but attenuates high frequencies chosen and the signals are filtered by using Matlab's filter function.

$$B=(1/10)*ones(1,10);$$

$$A=1;$$

$$ECGSignal=filter(B,A,ECGSignal) \qquad (4.2)$$

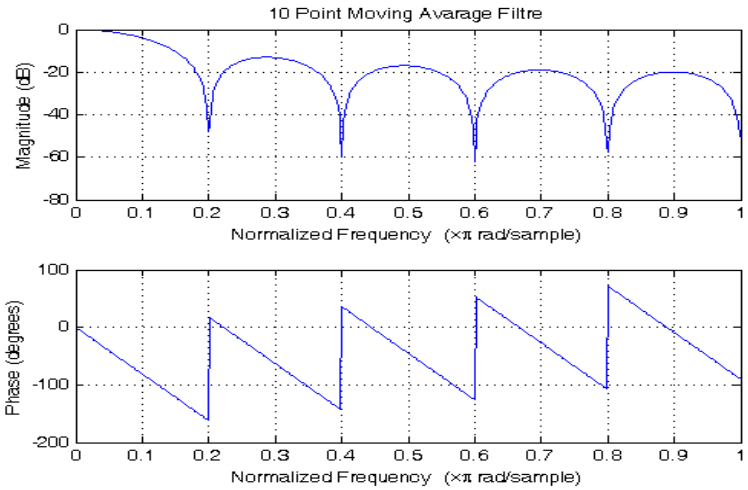

Figure 4.4: Low Pass Filter

After the removal of high frequency noise from the signal next step is to remove low frequency noise components. This low frequency noise shows itself as baseline wandering that is caused mostly by the respiration of the patient. To remove this low frequency noise, a derivative based (high pass) filter (Figure 3.6) that passes high frequencies but attenuates low frequencies used.

$$B=(1/1.0025)*[1\ -1];$$

$$A=[1\ -0.995];$$

ECGSignal=filter(B,A,ECGSignal) (4.3)

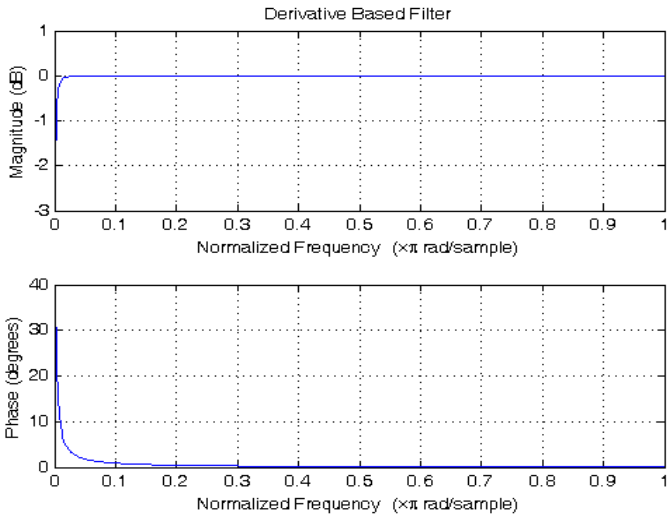

Figure4.5: High Pass Filter

4.3.3 Removing 60Hz Powerline Interference

Powerline interference is a noise caused by the electrical current flowing in wires and power lines. Powerline interference that is present in our ECG signals consists of 60Hz pickup and harmonics. Since frequency of 60Hz overlaps with our ECG signal frequency range we have to suppress only 60Hz frequency components and its harmonics without disturbing the frequencies around. To achieve this, comb filter (Figure 4.5) is used and 60Hz powerline interference with its harmonics is removed from the ECG signals. Comb filter is a band-stop filter which attenuates a certain band of frequencies and their harmonics.

B=conv([1 1],[0.6310 -0.2149 0.1512 -0.1288 0.1227 -0.1288 0.1512 -0.2149 0.6310]);

A=1;

ECGSignal=filter(B,A,ECGSignal) (4.4)

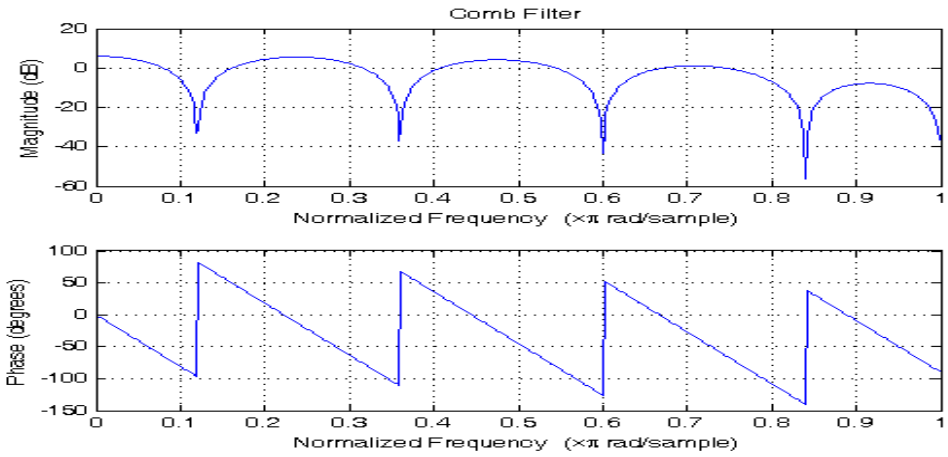

Figure 4.6: Comb Filter

All of the above steps are applied to all training and testing ECG records and filtered ECG signals (Figure 4.6) are obtained ready for the next QRS detection step.

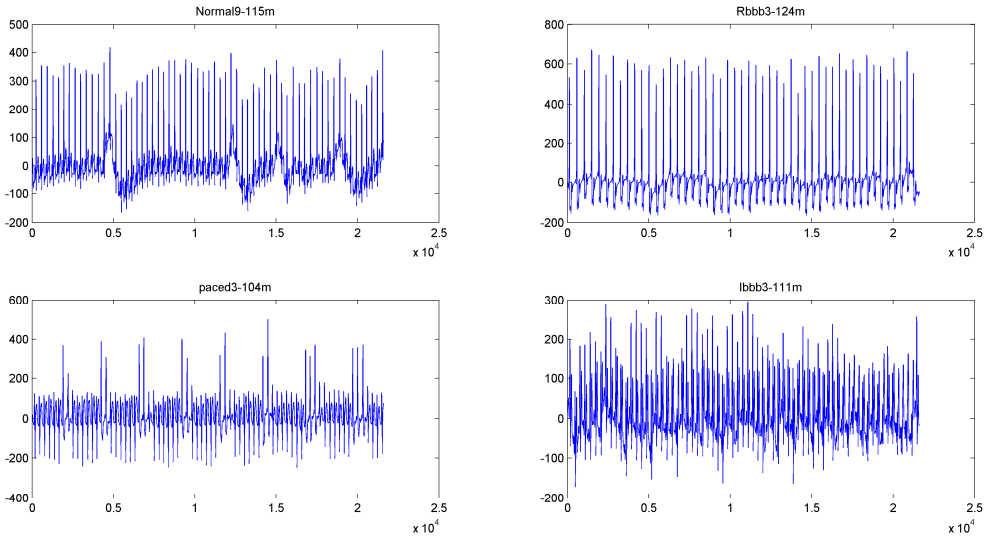

Figure 4.7: Sample filtered ECG signal after preprocessing

4.4 QRS Detection

As mentioned before in previous chapter, the QRS complex is the most striking waveform within the ECG. Since it reflects the electrical activity within the heart during the ventricular contraction, the time of its occurrence as well as its shape

provide much information about the current state of the heart. Due to its characteristic shape it serves as an entry point for classification scheme of cardiac cycle. In that sense, QRS detection provides the fundamentals for almost all automated ECG analysis algorithms. Supporting this, previous researches (Ozbay Y. And Karlik B., 1996) proved that taking samples as feature values in the intervals of R-R are very effective in representing the class of those ECG waves (one cardiac cycle) cardiac condition. Apart from this, since the 4 ECG class records, each representing a different cardiac condition, used for training and testing in this thesis are 1 minute long (each containing 60-90 ECG waveform), in order to separate each waveform (we need to do this because cardiologist classify cardiac conditions by looking at single ECG waveforms (cardiac cycles), not by looking at whole record) and find how many waveforms each record contain, therefore, we also need to detect the QRS complexes.

There are many different QRS detection techniques but this thesis is focused on well known and acceptable QRS detection using Pan-Tompkins algorithm (Pan J and Tompkins WJ., 1985). Pan and Tompkins proposed a real-time QRS detection algorithm based on analysis of the slope, amplitude and width of QRS complexes. The algorithm includes a series of methods that perform derivative, squaring, integration, adaptive thresholding and search procedures.

4.4.1 Derivative Operator

The derivative procedure suppresses the low-frequency components of the P and T waves, and provides a large gain to the high-frequency components arising from the high slopes of the QRS complex. Derivative operation is implemented in Matlab by using *diff* function which finds the differences between the adjacent values in the signal.

Derivative=diff(ECGSignal) (4.5)

4.4.2 Squaring Operation

The squaring operation makes the result positive and emphasizes large differences resulting from QRS complexes; the small differences arising from P and T waves are suppressed. QRS complex is further enhanced. Squaring operation is implemented simply by multiplying the signal by itself in Matlab.

*Squaring=derivative.*derivative* (4.6)

4.4.3 Integration

The output of a derivative based operation may contain multiple peaks within the duration of a single QRS complex. A moving window integrator is applied to perform smoothing of the output of the preceding operations so that multiple peaks are avoided. This step is performed in Matlab by using medfilt1 function and a window width of 54 is found to be suitable for sampling frequency 360Hz.

window=ones[1,54];

Integration=medfilt1(filter(window,1,squaring),10); (4.7)

4.4.4 Thresholding

Maximum value of the signal that had passed from above steps is taken and multiplied by a threshold percentage value. This is done because the output of preceding operations may contain noise peaks. These noise peaks do not have as large amplitude as R peaks but if we take all the peaks present in the output of above steps as R peaks then noise peaks will also be classified as R peaks (QRS complexes). So by taking a certain percentage of the highest peak amplitude as a threshold we avoid this. Different values for threshold percentage were tested and value 0.2 found to be suitable for removing noise peaks in our signals. This threshold value is used for searching R peak in search procedures.

maxvalue=max(integration)

*threshold=maxvalue*0.2* (4.8)

4.4.5 Search Procedures for QRS (Location of R Peaks)

In the last step of QRS detection, regions of the output signal, of the preceding steps, that is above the threshold value is found. Starting and ending locations of each region is recorded.

Then each specific region is again searched on the original ECG signal for a maximum value which represents the exact R peak of that wave. Locations of all R peaks are then recorded and the QRS searching algorithm is finalized (Figure 4.7).

position_region=integration>threshold

left=find(diff([0 position_region])==1)

right=find(diff([position_region 0])==-1)

for i=1:length(left)

[maxvalue(i) maxlocation(i)]=max(ECGSignal(left(i):right(i)))

end (4.9)

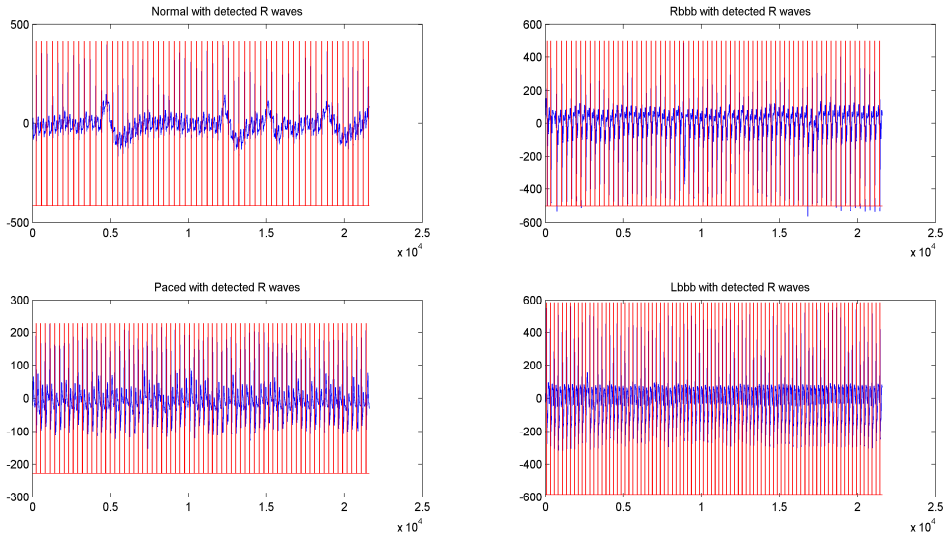

Figure 4.8: ECG signal with R peaks detected

4.5 Feature Extraction using Pan Tompkins Algorithm

Feature extraction is extracting and converting the input data information into a set of features which called feature vector, by reducing the data representation pattern. The features set will extract the relevant information from the input data in order to perform the classification task.

As we mentioned before, previous research suggested that taking samples between R-R intervals of ECG waves as feature values enables a good representation of the cardiac condition of those ECG waves. As we investigate our ECG signals used in this thesis we can easily see that the features that clearly distinguishes each class (normal, rbbb, paced and lbbb) lies between the R-T intervals (Discrimination). Also it can be easily observed that each member of a class shows same form of pattern in this interval (Reliability). So we took 200 samples between R-R intervals (Figure 4.8) (approximately this amount of samples corresponds to R-T interval with sampling frequency of 360Hz) starting from R peaks as our feature values excluding (deleting) all other parts of the ECG waveforms (Optimality).

```
for i=1:length(maxlocation)-1

for j=1:200

feature_vector(I,j)=ECGSignal(maxlocation(I)+j);

end

end
```
(4.10)

When this method is applied to all training ECG records we obtained 1937x200 feature vector (Figure 4.8) which will fed inputs to our neural network. While for testing is 807x200, the features were sorted in this order; normal, normal,…normal, rbbb, rbbb,…rbbb, paced, paced,…paced, lbbb, lbbb,…lbbb.

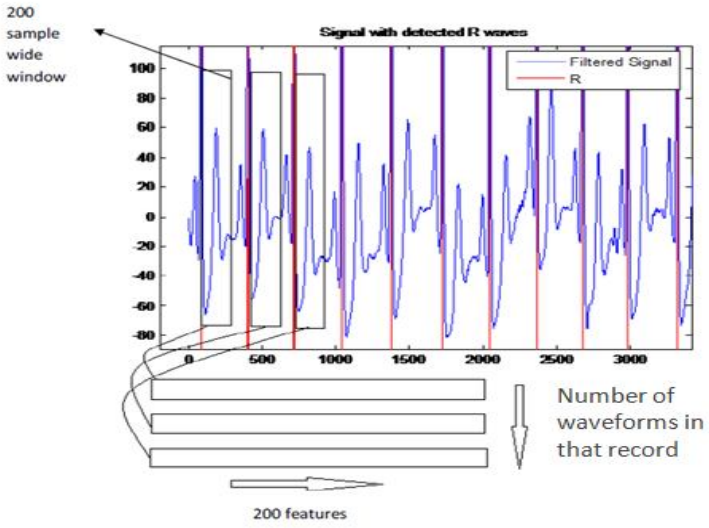

` Figure 4.9: Method of R-T intervals Feature Extraction

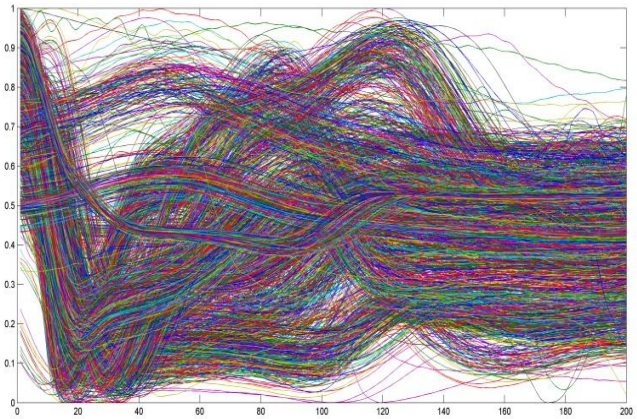

Figure 4.10: R-T Intervals Features (200*1937) for Training

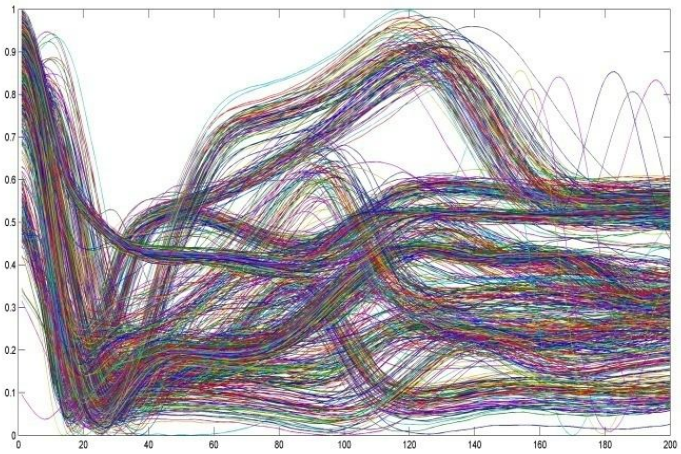

Figure 4.11: R-T Intervals Features (200*807) for Testing

4.5.1 R-R Time intervals Combined with R-T intervals

R-R time interval and amplitude of each R peak in the ECG waveform were calculated using the same algorithm, and then it was combined with R-T interval already obtained. The size of the feature is now 202x1937 and 202x807 for training and testing respectively.

4.5.2 Feature Extraction using Discrete Wavelet Transform

In the scope of this thesis, the morphological features extracted from Pan Tompkins algorithm which represents an R-T interval and another feature representing R-R time interval and R-peak amplitude were decomposed using wavelet decomposition analysis, thus increasing ECG characteristic point detection capabilities in which features from time domain were decomposed again into time-frequency domain. Since most recently published detectors are based on standard database libraries and limited wave detection, this application is an attempt to expand the horizons of current research efforts.

The input selection of feature extraction methods applied in this thesis has to select well to make sure which components of an inputs best represent the given pattern of ECG signals. Since the details and approximations wavelet coefficients contain a significant amount of information about the signal, the wavelet coefficients

of ECG signal of each subject were computed. The procedures of DWT implementation is describe as follows in figure 4.12.

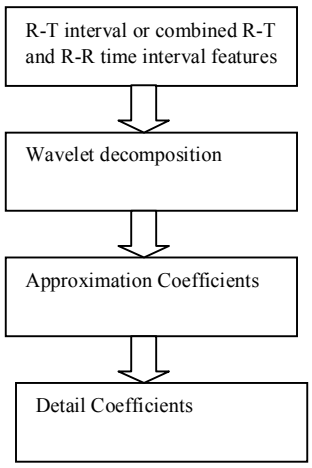

Figure 4.12: Feature extraction technique using DWT

4.5.2.1 Features Extraction Procedures

Selection of appropriate wavelet and the number of decomposition level is very important in DWT. The levels are chosen such that those parts of the signal that correlate well with the frequencies required for classification of the signal are retained in the wavelet coefficients.

The general wavelet decomposition of DWT procedure involves three steps. The result of decomposed signal will shows the important details and approximation coefficients which represent the original signal. The basic version of the procedure follows the steps described below.

- Choose a wavelet types
- Choose a wavelet name
- Choose a level N which will compute the wavelet decomposition of the signal s at level N

The discrete wavelet types have been chosen in this features extraction method and the ECG signals were decomposed into time-frequency representations using single-level one dimensional wavelet decomposition. Different wavelet names

which has wavelet filter with scaling function more closely similar to the shape of the ECG signal to achieved better detection have been choosing and the number of decomposition levels was chosen to be 12. Thus, the ECG signals were decomposed into the details coefficients D_1-D_{12} and one final approximation coefficient, A_{12}.

4.6 Statistical feature Extraction

The computed wavelet coefficients provide a compact representation that shows the energy distribution of the signal in time and frequency. Therefore, the computed details and approximation wavelet coefficients of the ECG signal were used as the features vector representing the signals.

In this study, from the original intervals of ECG signal, seven standard measures parameters are used. In order to reduce the dimensionality of feature vectors and to determine a precise and robust ECG features, statistics over the set of the wavelet coefficients were used. The following statistical features were used to represent the time-frequency distribution of the ECG signals: the flows of the calculated wavelet transform coefficients and statistical features are shown in figure 4.12 below.

1. mean of the wavelet coefficients of each ECG signals sample
2. median of the wavelet coefficients of each ECG signals sample
3. Maximum of the wavelet coefficients of each ECG signals sample
4. Minimum of the wavelet coefficients of each ECG signals sample
5. Standard deviation of the wavelet coefficients of each ECG signals sample
6. Energy deviation of the wavelet coefficients of each ECG signals sample
7. Entropy of the wavelet coefficients of each ECG signals sample

The feature vector of subband 1-10, D1-D10 of details coefficients and Approximation coefficient A12 from the wavelet decomposition structures has been extracted. These vectors are extracted at each scale without scale 11 and 12 for details coefficients. It is ignoring the higher levels of decomposition because it contains high frequency details and noise. These details are insignificant information that will not affect the classification accuracy and signal quality (Daubechies, 1990).

4.6.1 Feature extraction using Stationary Wavelet Transform

The procedure for calculating stationary wavelet transform and feature extraction is the same as in discrete wavelet transform only that in SWT the level of decomposition is eight because the length of the signal must be in form of 2^n.

Where *n* is the level of decomposition

Therefore, the R-T interval samples from PT algorithm are 256 instead of 200 for DWT and the level should be eight.

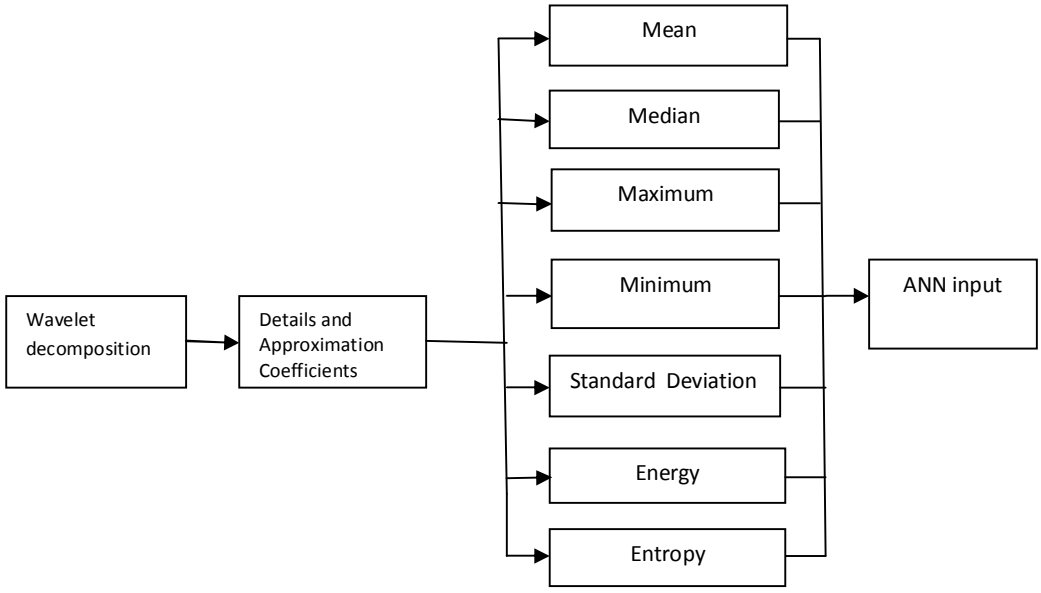

Figure 4.13: Wavelet and Statistical Analysis

4.7 Wavelet Time-Frequency Entropy

The concept of entropy has been widely used as a measure of disorder of a system. In this study, the wavelet entropy was calculated from the vector magnitude of SWT after decomposing with different wavelet name at level eight. Therefore the length of SWT detail and approximation coefficients is 8x256 each. wavelet transform feature vector for calculating entropy was constructed from eight level detail coefficients and one approximation coefficient which constitute 9x256. Energy

(E_{ij}) of this ECG signal in the time-scale domain was calculated for each time *i* and scale *j as follows*.

$$E_{ij} = |SWT_{ij}| \quad (4.11)$$

The total energy is calculated as

$$E_{total} = \sum_i \sum_j E_{ij} \quad (4.12)$$

Next, the probability distribution of energy for each scale was obtained as in Equation 3.

$$P_{ij} = \frac{E_{ij}}{E_{total}} \quad (4.13)$$

Where *Pij* is the probability distribution at time *i* and scale *j*

Eij is the energy at time *i* and scale *j*

E_{total} is the total energy

The wavelet time-frequency entropy (*WTFE*) is defined as in Equation 4

$$WTFE_{ij} = -P_{ij} \log P_{ij} \quad (4.14)$$

4.8 Output Target Vector Formation

Accompanying each record in the MIT-BIH database there is an annotations file in which each heartbeat has been identified by expert cardiologist annotators. This annotated information can be employed for designing the target vector and evaluating the classifier performance. This thesis is focused on classifying four different cardiac condition namely normal beats, right bundle branch block, paced beats and left bundle branch block. These cardiac conditions are defined as follows Table 3.1

Table 4.3: Target Vector Formation

ECG Class beat	Target Vector
Normal	[1 0 0 0]
Lbbb	[0 1 0 0]
Paced	[0 0 1 0]
Lbbb	[0 0 0 1]

Table4.4: Output Target Vector

Normal	1	0	0	0
Normal	1	0	0	0
Normal	1	0	0	0
. . .				
Normal	1	0	0	0
Rbbb	0	1	0	0
Rbbb	0	1	0	0
Rbbb	0	1	0	0
. . .				
Rbbb	0	1	0	0
Paced	0	0	1	0
Paced	0	0	1	0
Paced	0	0	1	0
. . .				
Paced	0	0	1	0
lbbb	0	0	0	1
lbbb	0	0	0	1
lbbb	0	0	0	1
. . .				
lbbb	0	0	0	1

When these representations are applied to the whole records and the output vectors are sorted in the order same as the feature vector, the 1937x4 output target vector is formed as in table 4.4 above.

This output target vector will be used by neural network during training stage. Network will compare these desired outputs with its actual results and hence calculate errors and adapt its weights to learn the patterns. After the training completed this vector will be used in calculating correct training recognition rate by comparing it to networks actual output.

4.9 Designing the Neural Network

Developing a classifier based on neural network involves choosing an appropriate classifier model and then using the training algorithm to train and then test the input signal to classify them into different categories. Backpropagation algorithm will be used in this thesis as a training function to train feed forward neural networks to solve our ECG signal classification problem.

A two-layer feed-forward network, with sigmoid hidden and output neurons (*patternnet*), can classify vectors arbitrarily well, given enough neurons in its hidden layer. Four different structures of neural networks are designed and will be tested for best performance. Each of them has same number of input (200), (202) and (77) for R-T intervals, combined R-R and R-T intervals and Statistical features respectively, output (4) neurons but differ in their number of hidden neurons (7, 10, 15, 20).

Maximum epochs are set to 1000 and error limit is set to 0.001. '*Trainsgc*' scale conjugate back propagation is used as backpropagation learning algorithm with momentum value. Learning rate and momentum coefficients are remained as defaults of the Matlab's function and log sigmoid '*Logsig*' functions are used for neuron transfer functions.

4.9.1 Training the Neural Network

Feature vectors that contains feature values obtained from training data set, along with its corresponding 1937x4 output target vector is fed into the networks designed in previous step for training with backpropagation algorithm. Training is continued until error goal is achieved or maximum epoch is reached. After the training finished, networks outputs are compared with output target vector and

correct training recognition rates and accuracies are recorded. Correct recognition is counted when the same output neuron shows the maximum value both for actual output and desired output. Accuracy is found by subtracting networks actual output of the neuron that should show the maximum value (that should be classified) from the desired output which is always 1. The example of the feature data for training is shown in Figure 3.13. Matlab's train function is used for training the network designed in previous step.

```
hiddenLayerSize = 15;

net = patternnet(hiddenLayerSize);

[net,tr,train_out] = train(net,inputs,targets);
```
(4.12)

4.10 Testing the Neural Network

While testing the trained networks testing feature vector was fed into the network for only one forward pass through the network and the classification outputs that the network produced is compared with desired testing output target vector (807x4) to calculate the networks correct testing recognition rates and accuracies. Testing was done in Matlab with function *sim*. Already trained network is fed into the function along with testing feature vector and the function returns the classifications (outputs) that the network produces.

```
outputs = sim(net,feature_vector_tst);

errors = gsubtract(NTargets3in,outputs);
```
(4.13)

After training and testing completed performance analysis was conducted based on the error performance and confusion matrix generated by neural network.

CHAPTER FIVE

RESULTS AND DISCUSSION

5.0 Overview

This chapter contains the results and discussion from the Automatic ECG beat detection system model developed in this thesis. It includes features extracted from QRS detection using Pan Tompkins algorithm that represents R-T intervals, R-R time interval features, discrete wavelet transform decomposition and statistical parameters features, stationary wavelet decomposition and time and frequency entropy features. The chapter begins with an introduction to the analysis that has been investigated. Next it covers the result of the features extraction methods mentioned above. Some conclusions concerning the rational of features on classification ECG signals that were obtained through ANN. The performance of ANN model was evaluated in terms of testing performance and classification sensitivity, specificity, Positive Predictive Value (PPV), Negative Predictive Value (NPV) and accuracy in classifying Normal, RBBB, Paced beat and LBBB. The results confirmed that the proposed method has a potential in classifying the ECG signals.

The training samples were randomly divided into three processes, Training process with 70% of the sample, Validation process with 15% of the sample and testing process with 15% of the sample. Training's samples are presented to the network during training, and the network is adjusted according to its error. Validation's samples are used to measure network generalization when the network stops improving. While Testing's sample have no effect on training and so provide an independent measure of network performance during and after training. After training the actual testing samples were loaded and tested using created training network.

5.1 Performance Parameters Measure

5.1.1 Sensitivity

Sensitivity (also called the *true positive rate*) measures the proportion of actual positives which are correctly identified as such (e.g. the percentage of sick people who are correctly identified as having the condition).Sensitivity can be calculated using the Formula 5.1 below.

$$Sensitivity = \frac{TruePositive(TP)}{TruePositive(TP)+FalseNegative(TN)} \quad (5.1)$$

Where

In general, Positive = identified and negative = rejected. Therefore:

- True positive: Sick people correctly diagnosed as sick (correctly identified)
- False positive: Healthy people incorrectly identified as sick (incorrectly identified)
- True negative: Healthy people correctly identified as healthy (correctly rejected)
- False negative: Sick people incorrectly identified as healthy (incorrectly rejected)

5.1.2 Specificity

Specificity (sometimes called the *true negative rate*) measures the proportion of negatives which are correctly identified as such (e.g. the percentage of healthy people who are correctly identified as not having the condition). Specificity can be calculated using the Formula 5.2 below (Adam and Witold, 2012).

$$Specificity = \frac{TrueNegative(TN)}{TrueNegative(TN)+FalsePositive(FP)} \quad (5.2)$$

5.1.3 Positive Predictive Value

It is the percentage of patients with a positive test who actually have the disease (Raul et al., 2008). How likely is someone with a positive test result to

actually have the characteristic? Positive predictive value can be calculated using the Formula 5.3 below.

$$Positive\ predictive\ value = \frac{TruePositive(TP)}{TruePositive(TP)+FalsePositive(FP)} \quad (5.3)$$

5.1.4 Negative Predictive Value

It is the percentage of patients with a negative test who do not have the disease (Raul et al., 2008). How likely is someone with a negative test result to actually not have the characteristics? Negative predictive value can be calculated using the Formula 5.4 below.

$$Negative\ predictive\ value = \frac{TrueNegative(TN)}{TrueNegative(TN)+FalseNegative(FN)} \quad (5.4)$$

5.1.5 Accuracy

Accuracy or efficiency is the percentage of test results correctly identified by the test. Accuracy can be calculated using the formula 5.5 below.

$$Accuracy = \frac{True\ Positive(TP)+True\ Negative(TN)}{TP+TN+FP+FN} \quad (5.5)$$

Note that, the PPV and NPV are not intrinsic to the test, they depends on the prevalence of the characteristic in a given population (Wikipedia and Wikihow, 2014).

5.2 Performance Analysis of Equivalent R-T Interval Features

ECG Data obtained from MIT-BIH database were pre-processed, QRS complexes were detected and 200 samples between R-R intervals which is equivalent R-T interval were extracted as feature values representing ECG classes. After all these steps four different network structures are trained with training data, training performances were recorded and finally they were all tested with testing data and testing performances were recorded for result analysis and discussions.

5.2.1 Performance with reduced number of ECG beats samples

Below are the results for the algorithms developed to detect and classify 3 types of ECG signal beats including normal beats (N), right bundle branch block beats (R), and paced beats (P) using Pan Tompkins algorithm for QRS detection and

features extraction. Six and two ECG record samples were used for each beat resulting in 1189 and 413 features for training and testing respectively.

Table 5.1: Performance of R-T interval features with reduced samples (413 patterns)

Hidden layer	Correct recognized patterns	Recognition rate (%)
7	400	96.85
10	401	97.09
15	402	**97.34**
20	397	96.13

From the table above, four different networks were designed with different number of hidden layer and the result for testing samples were depicted based on recognition rates while as we can see from the results and figure 5.1 below, a network which has the architecture 200:15:3 showed the best results during its best training and testing run with testing recognition rate of 97.54%.

These results can change with each run of the program because with each new run program starts training the networks again with different random weights and the testing rates may change due to different final training weights obtained in each training. So the training and testing recognition rates may vary from run to run. However, in this result and the subsequent ones, confusion matrix of test network at its best run can be used in evaluating performance measures of the system as it's shown below for the above network.

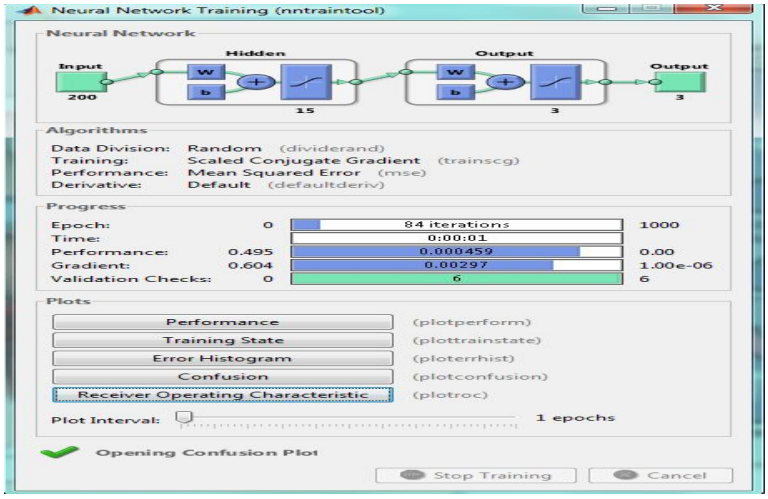

Figure 5.1: Best Run Network for reduced R-T interval samples

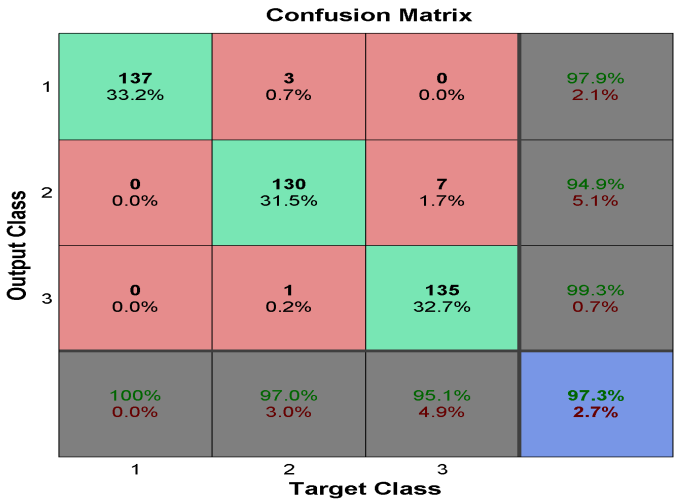

Figure 5.2: Test Data Confusion Matrix for reduced R-T interval samples

Table 5.2 shows the parameters after extraction from the Figure 5.2. Column 1 is set for Normal samples; Column 2 is set for Rbbb samples, while Column 3 for Paced beat samples respectively. Green box in each column shows the True Positive value. The other two red boxes in each column indicate the False Negative value while the other two red boxes in each row will give the False Positive value. True Negative value is the other 4 box that are not included in all those criteria at certain time. Final blue box gives a recognition rate of the system.

Table 5.2: Extracted parameters from figure 5.2

ECG Class beat	TP	FN	FP	TN
Normal	137	0	3	273
Rbbb	130	4	7	272
Paced	135	7	1	270

Table 5.3: Performance measures for reduced R-T interval samples

ECG Class Beat	Sensitivity (%)	Specificity (%)	Positive Predictive value	Negative Predictive value	Accuracy (Efficiency)
Normal	100	98.91	97.85	100	99.27
Rbbb	97.01	97.49	94.89	98.55	97.34
Paced	95.07	99.63	99.26	97.47	98.06
Average	**97.36**	**98.68**	**97.33**	**98.67**	**98.22**

From the above tables and figures, the average sensitivity and specificity, PPV, NPV and accuracy of the system is 97.36%, 98.86%, 97.33, 98.67 and 98.22 respectively. While network performance parameters at its best run were shown in figure 5.1 and 5.2.

5.2.2 Performance of DWT with reduced number of ECG beats

In order to increase the classification accuracy of the system, the equivalent R-T interval features were decomposed using DWT and statistical features were extracted and used for classification. The performance of discrete wavelet decomposition and statistical features for reduce number of ECG beats is shown below. Different wavelet families were chosen for the decomposition in order to find the most effective among the families.

Table 5.4: DWT features performance for reduced number of samples

Hidden Layer=15		
Wavelet Name	Correct recognized patterns	Recognition rates (%)
Db2	347	84.02
Db4	411	**99.76**
Db7	409	99.03
Db10	411	99.52
Bior1.5	351	84.99

Bior2.6	392	94.92
Bior3.7	412	99.52
Bior6.8	408	98.79
Coif2	409	99.03
Coif5	411	**99.76**
Sym5	410	99.27
Sym8	410	99.27

From the results above, it is clearly shown that there is an improvement when using a hybrid system that is combining time domain, time-frequency domain and statistical features. The feature vector includes 200 samples extracted between R-R interval as equivalent R-T interval, they were decomposed using DWT and statistical parameters such as mean, median, maximum etc were calculated from 12-level decomposition. The final size of the feature vector is 77x1189 and 77x413 for training and testing respectively. Among DWT families family Db4 and coif5 shows better performance with a recognition rate of 99.76%. The best run network performance is shown below.

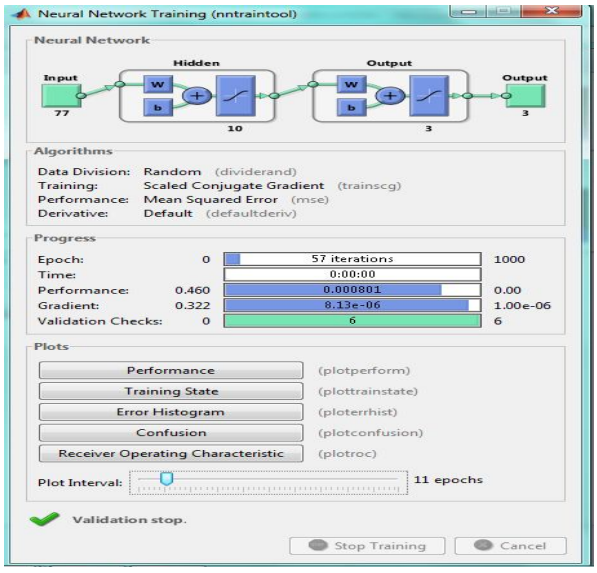

Figure 5.3: Best Run Network for DWT features with reduced samples

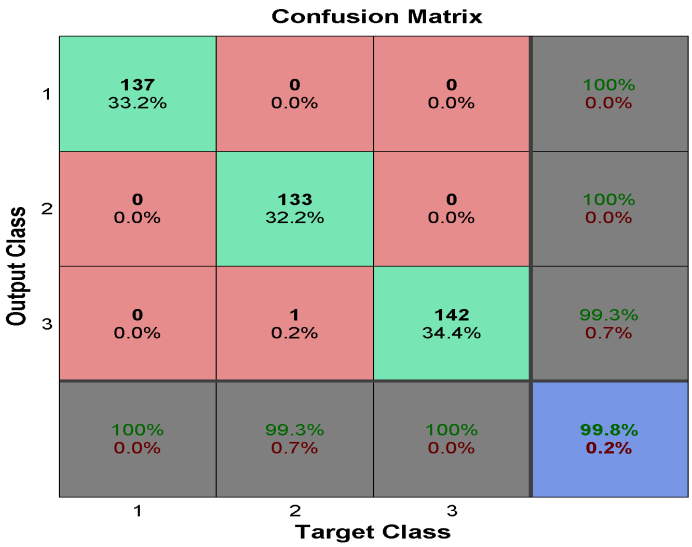

Figure 5.4: Test Data Confusion Matrix for DWT with reduced samples

The performance of the system in terms of performance measures was calculated and tabulated as shown below.

Table 5.5: Extracted parameters from figure 5.4

ECG Class beat	TP	FN	FP	TN
Normal	137	0	0	276
Rbbb	133	1	0	279
Paced	142	0	1	270

Table 5.6: Performance measures for DWT with reduced samples

ECG Class Beat	Sensitivity (%)	Specificity (%)	Positive Predictive value (%)	Negative Predictive Value (%)	Accuracy (%)
Normal	100	100	100	100	100
Rbbb	99.25	100	100	99.64	99.76
Paced	100	99.63	99.30	100	99.76
Average	**99.75**	**99.88**	**99.77**	**99.88**	**99.84**

Based on the results obtained from the above table, all the performance measures of the proposed system are approximately 100% which shows how well and good the system performed in classifying ECG beats from normal to arrhythmias.

5.3. Performance Analysis of Larger Number of Samples and ECG Beats

Since the performance of a system for reduced number of samples and ECG class beats is almost 100%, therefore, we increased the number of samples from 1188 to 1937 and 413 to 807 for training and testing respectively. Also the number of ECG class beats was increased from three to four, which are Normal, Rbbb, Paced and Lbbb. Therefore, it is believed that expanding the overall data set would be more realistic and introduces a more challenging problem due to significant variation in ECG morphology among different patients.

5.3.1 Performance analysis of equivalent R-T interval features

The performance of each R-T interval features with increased number of samples for different network is shown in table 5.7 below. The feature vector size is 200x1937 for training and 200x807 for testing.

Table 5.7: Performance of R-T interval features with large samples

Hidden layer	Correct recognized patterns	Recognition rate (%)

7	698	86.49
10	700	86.74
15	713	88.35
20	699	86.62

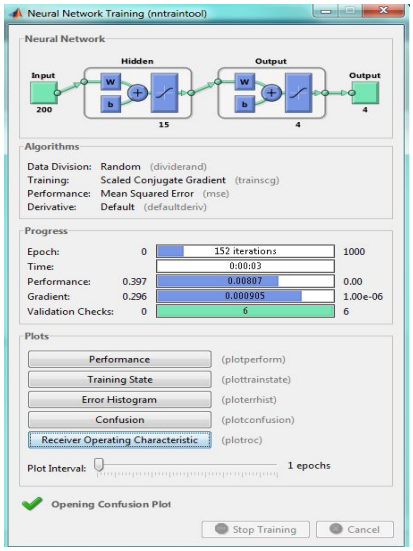

Figure 5.5: Best Run Network for R-T interval features with large samples

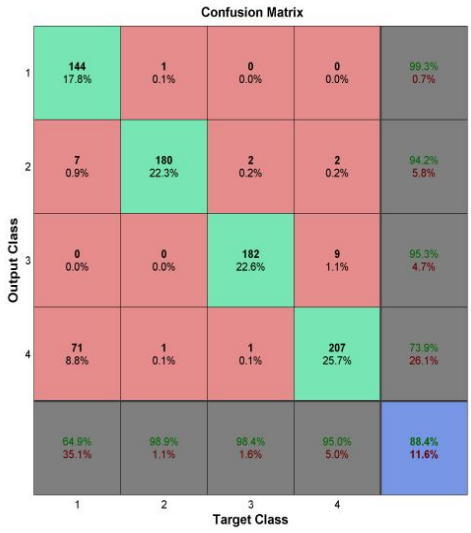

Figure 5.6: Test Data Confusion Matrix for R-T interval with large samples

Table 5.8: Extracted parameters from figure 5.6

ECG Class beat	TP	FN	FP	TN
Normal	144	78	1	584
Rbbb	180	2	11	614
Paced	182	3	9	613
Lbbb	207	11	73	516

Table 5.9: Performance measures for R-T interval with large samples

ECG Class Beat	Sensitivity (%)	Specificity (%)	Positive Predictive Value (%)	Negative Predictive Value (%)	Accuracy (%)
Normal	64.86	99.83	99.31	88.22	90.21
Rbbb	98.90	98.24	94.24	99.68	98.39
Paced	98.38	98.55	95.29	99.51	98.51
Lbbb	94.95	87.61	73.93	97.91	89.59
Average	**89.27**	**96.06**	**90.69**	**96.33**	**94.18**

The results above shows the decrease in performance of the system when the number of samples and ECG class beat was increased, the result shows 89.61% sensitivity, 96.06% specificity and 94.18% accuracy which indicates low percentage in classifying correct ECG class beat as seen from sensitivity of normal class beat which is 64.86%. Therefore, we need to develop and investigate other methods and system for robust and efficient feature extraction and classification.

5.3.2 Performance of DWT with Large Number of Samples and ECG Beats

In order to improve the classification accuracy we need to search for a reliable and efficient ECG features extraction technique, therefore the R-T interval features were decomposed using DWT decomposition as explained before. After the decomposition statistical features were extracted and used as features for ECG classification which result in a hybrid method of future extraction and classification.

Below is the performance of DWT decomposition of equivalent R-T interval extracted after Pan-Tompkins algorithm. The statistical parameters were calculated after the decomposition and features extracted.

Table 5.10: DWT features performance for large number of samples

Hidden Layer=15		
Wavelet Name	Correct recognized patterns	Recognition rates (%)
Db2	714	88.48
Db4	768	**95.17**
Db7	683	84.63
Db10	718	88.97
Bior1.5	703	87.11
Bior2.6	743	92.07
Bior3.7	760	94.18
Bior6.8	708	87.73
Coif2	706	87.48
Coif5	762	94.42
Sym5	747	92.57
Sym8	724	89.71

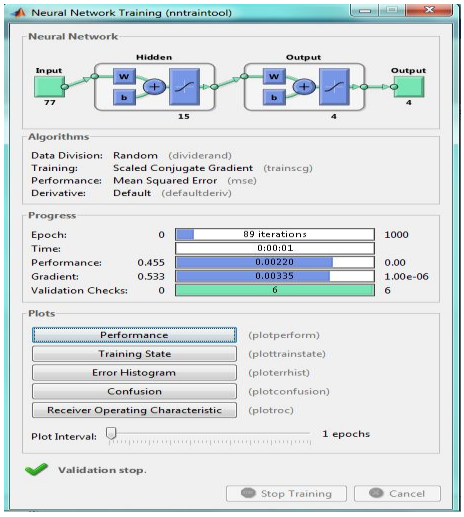

Figure 5.7: Best Run Network for DWT features with large samples

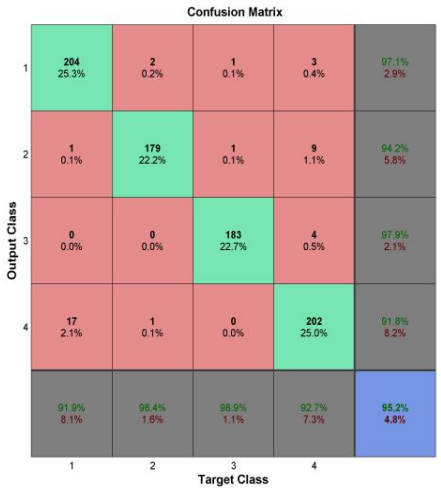

Figure 5.8: Test Data Confusion Matrix for DWT with large samples

Table 5.11: Extracted parameters from figure 5.8

ECG Class beat	TP	FN	FP	TN
Normal	204	18	6	579
Rbbb	179	3	11	614
Paced	183	2	4	618
Lbbb	202	16	18	571

Table 5.12: Performance measures for DWT with large samples

ECG Class Beat	Sensitivity (%)	Specificity (%)	Positive Predictive value (%)	Negative Predictive Value (%)	Accuracy (%)
Normal	91.89	98.97	97.14	96.98	97.03
Rbbb	98.35	98.24	94.21	99.51	98.27
Paced	98.92	99.36	97.86	99.68	99.27
Lbbb	92.66	96.94	91.82	97.27	95.79
Average	**95.46**	**98.38**	**95.26**	**98.36**	**97.59**

From the above results it is clearly seen an improvement when compared with classification using R-T interval features alone as the average sensitivity is now around 95.46% while average specificity around 98.80%. This improvement can be traced due to high sensitivity for normal ECG class which is 91.89% against 64.86% when using R-T interval features only. However, though there is an improvement when using DWT and statistical features there is still need to address the challenges of classifying ECG classes accurately due to a minutes morphological parameter values, significant variation in ECG morphological information and presence of noise. Therefore, another method was developed based on Stationary wavelet transform for extracting another set of time-frequency and a statistical feature for better and successful classification and diagnostic of ECG beats.

5.4 Performance of SWT with Large Number of Samples

Below is the performance of SWT decomposition of equivalent R-T interval extracted after Pan-Tompkins algorithm. The statistical parameters were calculated after the decomposition using different wavelets, features extracted for classification using ANN and db4 was used in evaluating system performance indices.

Table 5.13: SWT features performance for large number of samples

Hidden Layer=15		
Wavelet Name	Correct recognized patterns	Recognition rates (%)
Db2	728	90.21
Db4	780	**96.65**
Db7	743	92.07
Db10	765	94.79
Bior1.5	724	89.71
Bior2.6	764	94.67
Bior3.7	721	89.31
Bior6.8	743	92.07
Coif2	759	94.05
Coif5	735	91.08
Sym5	769	95.29
Sym8	778	96.41

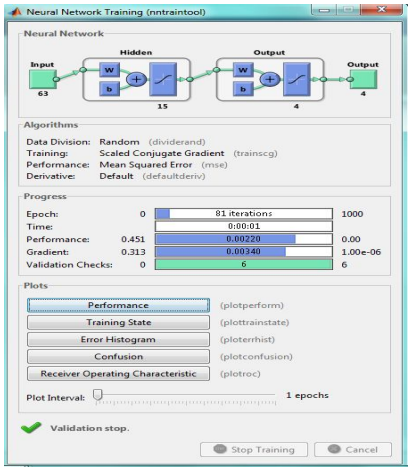

Figure 5.9: Best Run Network for SWT features with large samples

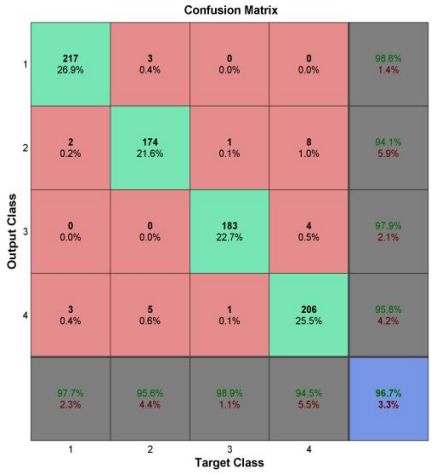

Figure 5.10: Test Data Confusion Matrix for SWT with large samples

Table 5.14: Extracted parameters from figure 5.10

ECG Class beat	TP	FN	FP	TN
Normal	217	5	3	582
Rbbb	174	8	11	614
Paced	183	2	4	618
Lbbb	206	12	9	580

Table 5.15: Performance measures for SWT with large samples

ECG Class Beat	Sensitivity (%)	Specificity (%)	Positive Predictive Value (%)	Negative Predictive Value (%)	Accuracy (%)
Normal	97.75	99.49	98.64	99.15	99.01
Rbbb	95.60	98.24	94.05	98.71	97.65
Paced	98.92	99.36	97.86	99.68	99.26
Lbbb	94.50	98.47	95.81	97.97	97.40
Average	**96.69**	**98.89**	**96.59**	**98.88**	**98.33**

By using SWT to decompose the R-T interval features and extracting a new set of features based on statistical parameters the performance of this proposed system was successful in terms of classifying ECG class beats. The average sensitivity of the system is 96.44% while average specificity is 98.89% against 95.86% and 98.80 for DWT. Also, the most interesting point to note in using SWT features is that while in DWT features few of the wavelet families like Db4, coif5 and sym5 shows higher number of recognition rates, in SWT many of the wavelet families indicates a great improvement with higher values of recognition greater than 90%, for example, Db2, bior6.8, coif2 and sym8 has a recognition rate of 88.48%, 87.73, 87.48 and 89.71% respectively. While for SWT features the classification recognition rate for the above wavelet families is 90.21%, 92.07%, 94.05% and 96.41% respectively.

5.5 Performance of Combined R-R-time Interval and R-T Interval

Another feature comprises of R-R time interval and R peak amplitudes were extracted from QRS detection using Pan-Tompkins algorithm and then combined with equivalent R-T interval of 200 samples extracted also from the same algorithm. After calculating the difference between R-peak time interval and R-peak amplitude and then combined with already 200 samples of R-T interval, the size of feature vector becomes 202x1937 and 202x 807 for training and testing respectively. The performance of the combined features was shown below:

Table 5.16: Performance of combined R-R time and R-T features with large samples

Hidden layer	Correct recognized patterns	Recognition rate (%)
7	691	85.63
10	698	86.49
15	704	**87.24**
20	697	86.37

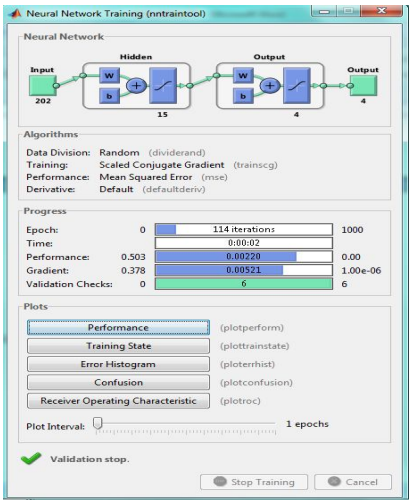

Figure 5.11: Best Run Network for combined R-R time and R-T features with large samples

Figure 5.12: Test Data Confusion Matrix for combined R-R time and R-T interval with large samples

Table 5.17: Extracted parameters from figure 5.12

ECG Class beat	TP	FN	FP	TN
Normal	144	78	6	579
Rbbb	179	3	62	563
Paced	183	2	15	607
Lbbb	198	20	20	569

Table 5.18: Performance measures for combine R-R time and R-T interval with large samples

ECG Class Beat	Sensitivity (%)	Specificity (%)	Positive Predictive Value (%)	Negative Predictive Value (%)	Accuracy (%)
Normal	64.87	98.97	96.00	88.13	89.59
Rbbb	98.35	90.08	74.27	99.47	91.95
Paced	98.92	97.59	92.42	99.67	97.89
Lbbb	90.83	96.60	90.83	96.60	95.04
Average	**88.24**	**95.81**	**88.74**	**95.97**	**93.62**

After calculating R-R time intervals and R-peak amplitudes they were combined with R-T intervals samples as a new feature for classification, from the results above in tables and figures the performance of this system is low when compares with all other systems developed in this thesis.

5.5.1 Performance of Combined R-R Time and R-T Intervals with DWT

As done previously, the combined features from R-R time intervals and R-T intervals were decomposed using DWT and statistical features were calculated and extracted. The size of feature vector after calculating mean, median, standard deviation etc is 77x1937 for training and 77x807 for testing. The performance of this system is shown in table 5.19 below.

Table 5.19: R-R time and R-T with DWT features performance for large number of samples

Hidden Layer=15		
Wavelet Name	Correct recognized patterns	Recognition rates (%)
Db2	578	71.62
Db4	481	59.60

Db7	577	71.49
Db10	692	**85.5**
Bior1.5	576	71.38
Bior2.6	627	77.69
Bior3.7	584	72.37
Bior6.8	381	47.21
Coif2	412	51.05
Coif5	640	79.31
Sym5	549	68.03
Sym8	495	61.34

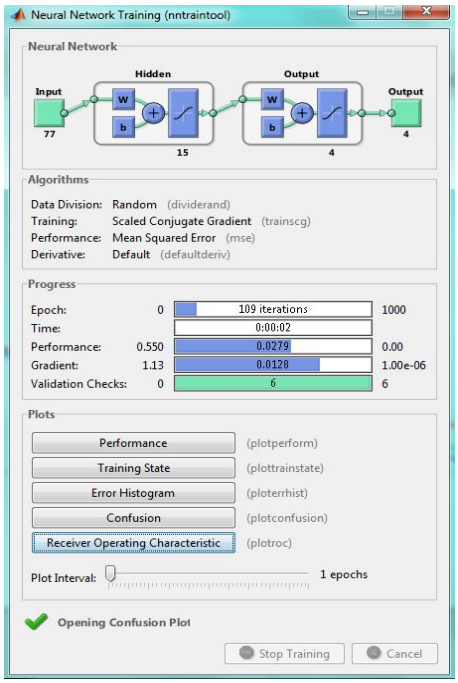

Figure 5.13: Best Run Network for combined R-R time and R-T features with DWT

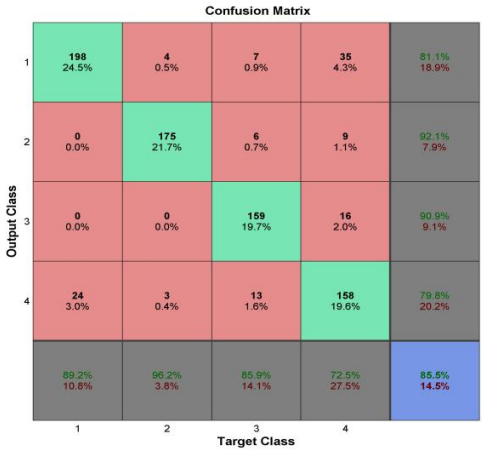

Figure 5.14: Test Data Confusion Matrix for combined R-R time and R-T interval with DWT

Table 5.20: Extracted parameters from figure 5.14

ECG Class beat	TP	FN	FP	TN
Normal	198	24	46	539
Rbbb	175	7	15	610
Paced	159	26	16	606
Lbbb	158	60	40	549

Table 5.21: Performance measures for combine R-R time and R-T interval with DWT

ECG Class Beat	Sensitivity (%)	Specificity (%)	Positive Predictive Value (%)	Negative Predictive Value (%)	Accuracy (%)
Normal	89.19	92.14	81.15	95.74	91.33
Rbbb	96.15	97.60	72.11	98.87	97.27
Paced	85.95	97.43	90.86	95.89	94.80
Lbbb	72.48	93.21	79.80	90.15	87.61
Average	**85.94**	**95.10**	**85.98**	**95.16**	**92.75**

5.6 Performance of SWT Entropy

In this case, equivalent R-T interval features extracted from between R-R interval after QRS detection using Pan-Tompkins algorithm as 256x1937 were decomposed using SWT and then statistical parameters were calculated as before. The difference in this case is we have calculated separately time and frequency entropy with statistical mean, median, standard deviation etc and formed a feature vector of 63x1937 and 63x807 for training and testing respectively.

Table 5.22: Frequency Entropy features performance for large number of samples

Hidden Layer=15		
Wavelet Name	Correct recognized patterns	Recognition rates (%)
Db2	746	92.44
Db4	750	92.94
Db7	762	94.42
Db10	738	91.45
Bior1.5	695	86.12
Bior2.6	741	91.82
Bior3.7	682	84.51
Bior6.8	747	92.57
Coif2	764	94.67
Coif5	734	90.95
Sym5	756	93.68
Sym8	771	**95.54**

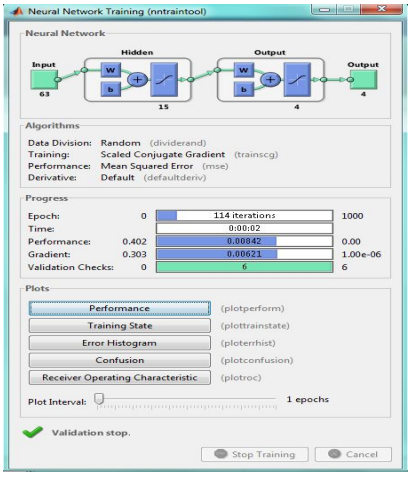

Figure 5.15: Best Run Network for Frequency Entropy using SWT

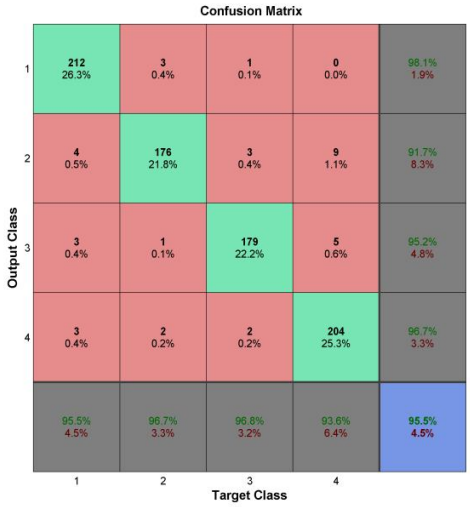

Figure 5.16: Test Data Confusion matrix for Frequency Entropy

Table 5.23: Extracted parameters from figure 5.16

ECG Class beat	TP	FN	FP	TN
Normal	212	10	4	581
Rbbb	176	6	16	609
Paced	179	6	9	613
Lbbb	204	14	7	582

Table 5.24: Performance measures of frequency Entropy with large number of samples

ECG Class Beat	Sensitivity (%)	Specificity (%)	Positive Predictive Value (%)	Negative Predictive Value (%)	Accuracy (%)
Normal	95.50	99.32	98.15	98.31	98.27
Rbbb	96.70	97.44	91.67	99.02	97.27
Paced	96.76	98.55	95.21	99.03	98.14
Lbbb	93.58	98.81	96.68	97.65	97.40
Average	**95.64**	**98.53**	**95.43**	**98.50**	**97.77**

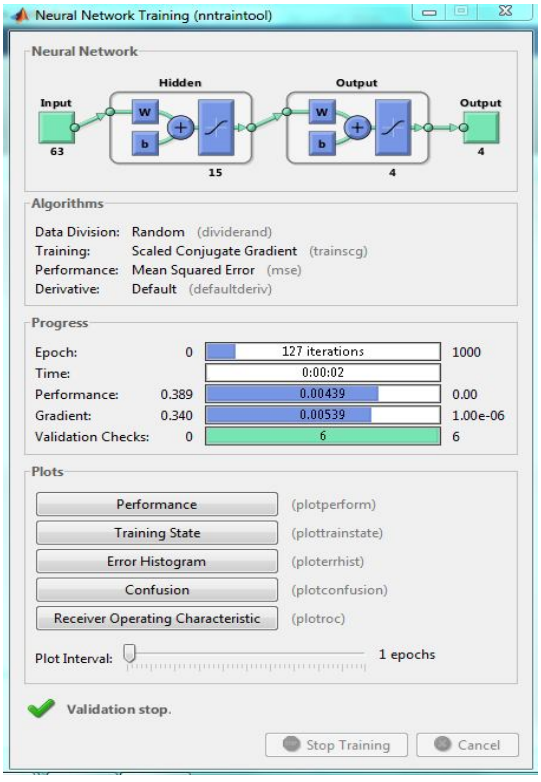

Figure 5.17: Best Run Network for Time Entropy using SWT

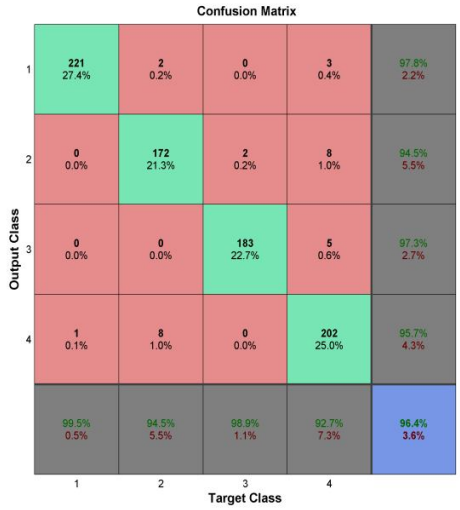

Figure 5.18: Test Data Confusion matrix for Time Entropy

Table 5.26: Extracted parameters from figure 5.18

ECG Class beat	TP	FN	FP	TN
Normal	221	1	5	580
Rbbb	172	10	10	615
Paced	183	2	5	617
Lbbb	202	16	9	580

Table 5.27: Performance measures of Time Entropy features with large number of samples

ECG Class Beat	Sensitivity (%)	Specificity (%)	Positive Predictive Value (%)	Negative Predictive Value (%)	Accuracy (%)
Normal	95.55	99.15	97.79	99.83	99.26
Rbbb	94.51	98.40	94.51	98.40	97.52
Paced	98.92	99.20	97.34	99.68	99.13
Lbbb	92.67	98.47	95.73	97.32	96.90
Average	**96.41**	**98.81**	**96.34**	**98.81**	**98.21**

5.7 Comparative Performance Analysis

Different methods and techniques of ECG feature extraction developed in this thesis for the purpose of ECG beats detection and recognition automatically using ANN classification was presented below, the result indicates different effects of features on the classification.

Tables below indicate comparative performance analysis of different feature extraction and classification techniques developed in this thesis.

Table 5.28 Comparison between reduced sample and large sample set

Performance Measures	Reduced Sample Set		Large Sample Set		
	R-T intervals	DWT	R-T intervals	DWT	SWT
Sensitivity	97.36	99.75	89.27	95.46	96.69
Specificity	99.68	99.88	96.06	98.38	98.89
PPV	97.33	99.77	90.69	95.26	96.59
NPV	98.67	99.88	96.33	98.36	98.88
Accuracy	98.22	**99.84**	94.18	**97.59**	**98.33**

Table 5.29 Comparison of different methods

Methods	Sensitivity	Specificity	PPV	NPV	Accuracy
R-T intervals	89.27	96.06	90.69	96.33	94.18
DWT	95.46	98.38	95.26	98.36	97.59
SWT	**96.69**	**98.89**	**96.59**	**98.88**	**98.33**
R-T and R-R	88.24	95.81	88.74	95.97	93.62
DWT with R-R and R-T	85.94	95.10	85.98	95.16	92.75

Table 5.30: Comparison between wavelet families

Wavelet Name	**DWT**	**SWT**
	Recognition rate (%)	Recognition rate (%)
Db4	95.17	**96.65**
Db10	88.97	94.79
Bior6.8	87.73	92.07
Coif5	94.42	91.08
Sym8	89.71	96.41

Generally, the performance of the proposed automatic ECG beat detection system developed in this thesis was successful and efficient in classifying ECG class

beats using a hybrid technique of extracting time domain features, time-frequency domain features and statistical features. Based on the results obtained when designing different network, the network with 15 numbers of neurons in its hidden layer prove to be effective. The performance parameters for best run network in each system was depicted on the figures which shows mean square error, gradient and best validation as well as number of epoch reached by that particular network.

Moreover, by decomposition using different wavelet families for both discrete wavelet decomposition and its counterpart stationary wavelet decomposition, db4 and coif5 shows higher number of recognition rates when compared to other families. Also, based on different systems developed in this thesis, SWT with statistical features gives higher number of accuracy as shown in the above table. Also, feature extraction technique using combined R-R time interval, R-peak amplitude and R-T interval with DWT decomposition shows less effective in accurate classification of ECG beats. Furthermore, it has been shown that selection of a suitable wavelet is critical to the success of classification.

5.7.1 Comparison between Time and Frequency Wavelet Entropy

Wavelet time and frequency entropy was calculated using SWT decomposition and the comparison between the two was tabulated in table below.

Table 5.31: Comparison between these two Entropies

Performance measures	Time Entropy	Frequency Entropy
Sensitivity	96.41	95.64
Specificity	98.81	98.53
PPV	96.34	95.43
NPV	98.81	98.50
Accuracy	**98.21**	97.77

Based on the results obtained after classification with time and frequency entropy algorithm developed in this work, it was shown that time SWT entropy performed better with accuracy of 98.21% which states that the shape of the ECG wave contains more information than the frequency bands.

CHAPTER SIX

WIRELESS ECG ACQUISITION DEVICE

6.0 Overview

Heart disease is one of leading cause of death worldwide, even in developed countries like USA the disease claims a lot of lives every year as shown in the previous chapter. In developing and under developed country where there is no sophisticated equipment like that of United States and western countries the number is much higher. A need of portable equipment for monitoring and processing of heart rhythms as well as to detect ECG arrhythmias would never be over emphasized. My experiences of been growing up in a developing country where the rules of the healthcare system are very different from that of the western world, most places have little to no infrastructure, and there is a lack of basic amenities such as water, food, electricity, hospital, reliable source of constant power supply, lack of medical equipments and personnel encourages me to focus on the design of a portable, low power, and low cost alternative to the sophisticated cardiac monitoring systems that are found in most hospitals in the western world which when developed and incorporated with automatic beat detection system developed in this thesis would be easy to operate, easy to transport and would be used to monitor admitted patients in these areas; patients who unfortunately can't afford the luxury of accommodation in the few well equipped hospitals that exist in their locale as well as ease clinicians and doctors work.

This chapter discusses the design of wireless ECG acquisition device using a low cost ECG analog front end with low power msp430 microcontroller set from Texas Instrument by exploiting the features of ez430-rf2500 development tool that has CC2500 low-power wireless RF transceivers which are suitable for low-power, low-cost wireless applications.

6.1 ECG Hardware Acquisition Module

ECG signal has some basic and essential electrical characteristics that need to be considered in design and development of its hardware acquisition module for its collection from a patient. ECG is a non-stationary signal with amplitude of ±3mV maximum and Most of the clinically significant information in ECG is found in the spectral band 0–100 Hz (Rajarshi et al., 2014).

During ECG recording, there are other unwanted signals that are collectively called 'artifacts' which contaminated the desired ECG signal, some of these are generated within the human body (Physiological of origin) while others are external to the body (non-physiological). Below are some of these artifacts and their sources.

1. Electromyography (EMG) noise: these are noise due to muscular activity like coughing, breathing, or squirming of the patient. The amplitude and frequency band of this signal is 0.1–1 mV and 5 Hz–1 kHz respectively, are partly overlapping with ECG signal. EMG noise and it may completely destroy the signal based analysis if proper care was not taken.

2. Power Line interference (PLI): A 50/60 ± 0.2 Hz current flows through the lead wires can get mixed with our signal of interest from the lead wires of neighboring cables as a result of capacitive coupling of ECG lead wires.

3. Electrode pop or contact noise: Sometimes when there is loss of contact between the patient body and ECG electrodes the output of amplifier may be temporarily saturated for a certain period of time.

4. Baseline wander: The respiration of the patient during ECG recording causes the ECG to oscillate at a very low frequency of 0.15 and 0.3HZ by changing the impedance between heart muscle and electrode.

5. Motion Artifacts: A patient movement or improper preparation of the skin can cause an overlap with ECG signal spectrum in the range of 1-10Hz.

6. Electrosurgical noise: In a clinical setup, there are number of neighboring medical equipments that generate noise at frequencies between 100 kHz and 1 MHz.

7. Amplifier noise: Amplifier generates two types of unwanted signals; that is Noise and drift which contaminate ECG signal during measurement. Noise has a spectral component above 0.1Hz while drifts generally refer to slow changes in the baseline frequencies below 0.1Hz.

We can minimize those artifacts by suitable clinical setup and design; however, using hardware to eliminate them altogether is almost impossible. Therefore, many software computational techniques for denoising digitized ECG are available now a day.

Generally, ECG wireless acquisition device consist of ECG electrode sensor, analog front end circuit which comprise of Instrumentation amplifier and filters for amplification and denoising respectively, low power microcontroller for timing, sampling, conversion and processing of the signal for transmission, CC2500 for wireless transmission. At the receiver part, CC2500 used to receive the incoming RF signal, low power microcontroller process the signal and send it to personal computer for visualization and further processing.

Below is the general block diagram of wireless ECG acquisition module

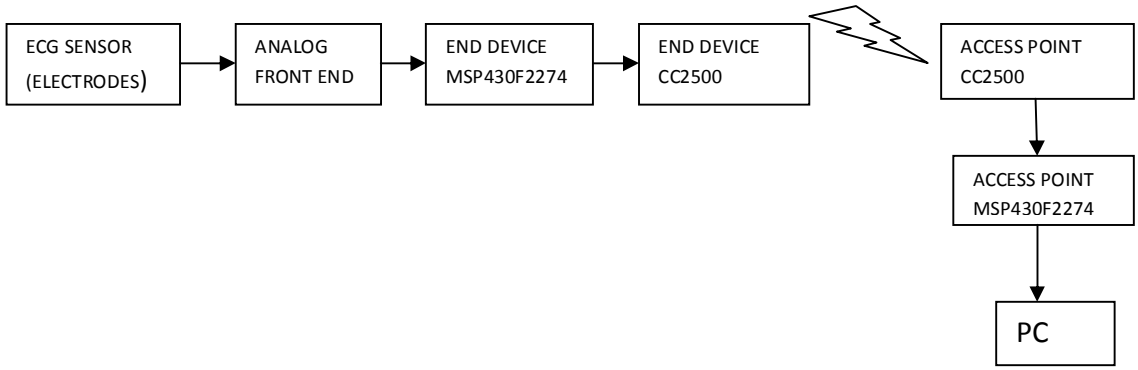

Figure 6.1: General block diagram of wireless ECG acquisition module

6.2 Analog Front End Design

ECG Analog front end consist of instrumentation amplifier, operational amplifier, low pass and high pass filters.

6.2.1 Instrumentation amplifier

ECG signal has an amplitude of approximately 1mV peak-peak, detecting this low frequency low magnitude signal is a serious problem because of the noise signals picked up by human body as described above. Therefore, a device with low cutoff frequency and high gain is required for signal conditioning, conversion and processing. The instrumentation amplifier used in this system is AD620 it is low cost device with high accuracy that requires only one external resistor to set gains of 1-10,000. It has a common mode rejection ratio (CMRR) specification of 100dB at G=10 up to 100 kHz at G=100, quiescent current of 490 μ A, and shutdown current levels less than 1 μ A. It can operate to a minimum supply voltage of 2.3V. Furthermore, the AD620 features 8-lead SOIC and DIP packaging that is smaller than discrete designs and offers lower power (only 1.3 mA max supply current), making it a good fit for battery-powered, portable (or remote) applications as well as suitable for medical application like ECG which cancel out the common mode signal from a conductive pad and amplifies the input differential ECG signal(AD620, 2011).

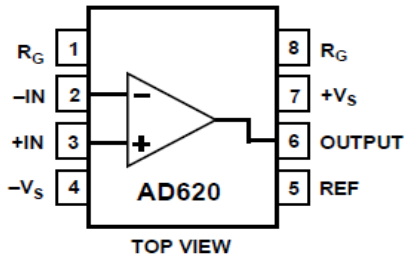

Figure 6.2: AD620 pinsout(AD620, 2011)

AD620 is the resistor gain programmable by R_G

Where R_G is the gain resistor

From the data sheet, $R_G = \frac{49.4k\Omega}{G-1}$ (6.1)

Where G is the gain

R_G Was calculated as 2.2kΩ

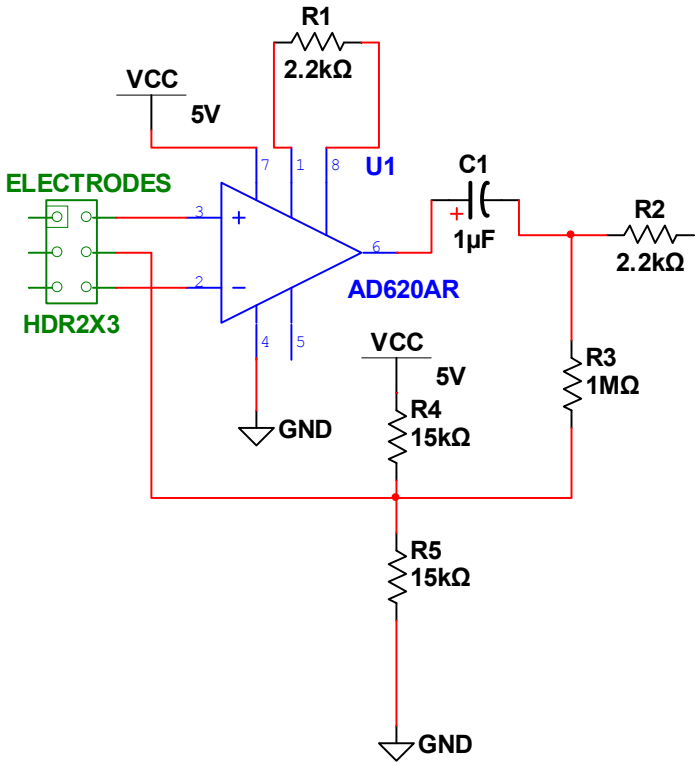

Figure 6.3: AD620 Instrumentation amplifier

The gain for the second amplifier which is op-amp amplifier CA3140 is calculated as

$$Gain = \frac{R_2}{R_1} \quad (6.2)$$

$$Gain = \frac{1M\Omega}{2.2k\Omega} = 454 \quad (6.3)$$

Also in-between amplification steps Low and high pass filtering are performed and during the second amplification step, and then after amplification a bank of three low-pass filters follows to remove additional 60 Hz noise.

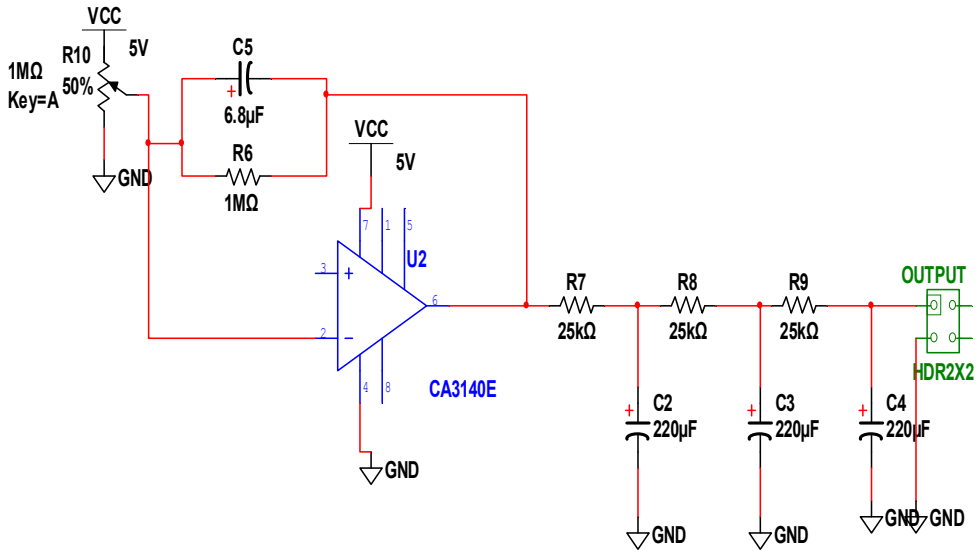

Figure6.4: CA3140 Op-Amp and filters connection

6.3 eZ430-RF2500 Wireless Development Module

The eZ430-RF2500 is one of the excellent product from Texas Instrument which provides all the hardware and software required for a complete MSP430 wireless development tool by combining MSP430F2274 microcontroller and CC2500 2.4-GHz wireless transceiver with their features. There are two target boards included in the kit, end device and access point. End device transmits wirelessly the information collected from sensor like ECG electrodes to the access point, while a gateway that is connected via USB to the computer is called access point.

EZ430-RF2500 has a unique feature of using USB debugging interface which allow users to conveniently debug each target board. Also it may be used as a standalone device with or without external sensors, or may be incorporated into an existing design. For development purposes, each end and access point has 18 available development pins that can be technically altered to suit different development purposes as shown in table 6.1 and 6.2 below.

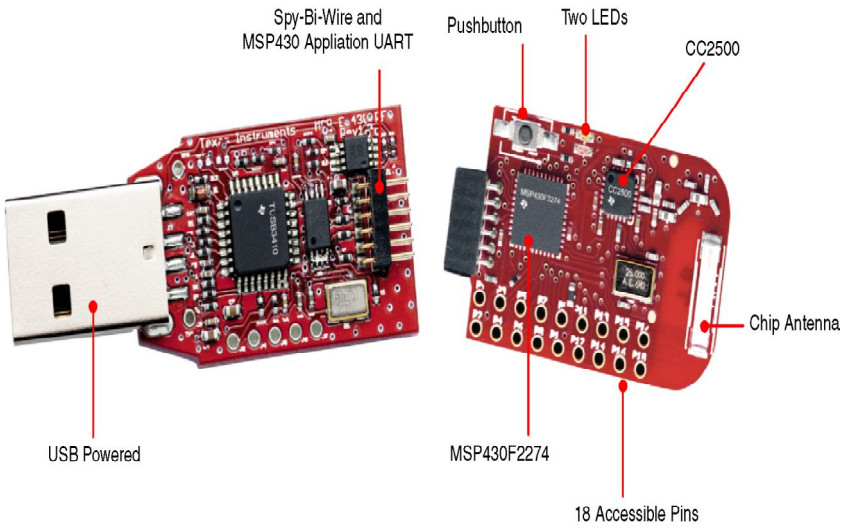

Figure 6.5: eZ430-RF2500 Access point and USB debugging interface(Slauu227e, 2009)

Figure 6.6: eZ430-RF2500 End device Battery Board (Slauu227e, 2009)

6.4 SimpliciTI Network Protocol

In this thesis eZ430-RF2500 is using SimpliciTI wireless network protocol developed by Texas Instrument targeting simple and small radio frequency (RF) networks for easy implementation with minimal microcontroller resource requirement. This feature makes it suitable for low cost and low power RF networks.

Table 6.1: eZ430-RF2500T Target Board Pinouts (SLAU227E, 2009)

Pin	Function	Description
1	GND	Ground reference
2	VCC	Supply voltage
3	P2.0 / ACLK / A0 / OA0I0	General-purpose digital I/O pin / ACLK output / ADC10, analog input A0
4	P2.1 / TAINCLK / SMCLK / A1 / A0O	General-purpose digital I/O pin / ADC10, analog input A1 Timer_A, clock signal at INCLK, SMCLK signal output
5	P2.2 / TA0 / A2 / OA0I1	General-purpose digital I/O pin / ADC10, analog input A2 Timer_A, capture: CCI0B input/BSL receive, compare: OUT0 output
6	P2.3 / TA1 / A3 / VREF– / VeREF– / OA1I1 / OA1O	General-purpose digital I/O pin / Timer_A, capture: CCI1B input, compare: OUT1 output / ADC10, analog input A3 / negative reference voltage output/input
7	P2.4 / TA2 / A4 / VREF+ / VeREF+ / OA1I0	General-purpose digital I/O pin / Timer_A, compare: OUT2 output / ADC10, analog input A4 / positive reference voltage output/input
8	P4.3 / TB0 / A12 / OA0O	General-purpose digital I/O pin / ADC10 analog input A12 / Timer_B, capture: CCI0B input, compare: OUT0 output
9	P4.4 / TB1 / A13 / OA1O	General-purpose digital I/O pin / ADC10 analog input A13 / Timer_B, capture: CCI1B input, compare: OUT1 output
10	P4.5 / TB2 / A14 / OA0I3	General-purpose digital I/O pin / ADC10 analog input A14 / Timer_B, compare: OUT2 output
11	P4.6 / TBOUTH / A15 / OA1I3	General-purpose digital I/O pin / ADC10 analog input A15 / Timer_B, switch all TB0 to TB3 outputs to high impedance
12	GND	Ground reference
13	P2.6 / XIN (GDO0)	General-purpose digital I/O pin / Input terminal of crystal oscillator
14	P2.7 / XOUT (GDO2)	General-purpose digital I/O pin / Output terminal of crystal oscillator
15	P3.2 / UCB0SOMI / UCB0SCL	General-purpose digital I/O pin USCI_B0 slave out/master in when in SPI mode, SCL I2C clock in I2C mode
16	P3.3 / UCB0CLK / UCA0STE	General-purpose digital I/O pin USCI_B0 clock input/output / USCI_A0 slave transmit enable
17	P3.0 / UCB0STE / UCA0CLK / A5	General-purpose digital I/O pin / USCI_B0 slave transmit enable / USCI_A0 clock input/output / ADC10, analog input A5
18	P3.1 / UCB0SIMO / UCB0SDA	General-purpose digital I/O pin / USCI_B0 slave in/master out in SPI mode, SDA I2C data in I2C mode

Table 6.2: Battery Board Pinouts (SLAU227E, 2009)

Pin	Function	Description
1	P3.4 / UCA0TXD / UCA0SIMO	General-purpose digital I/O pin / USCI_A0 transmit data output in UART mode (UART communication from 2274 to PC), slave in/master out in SPI mode
2	GND	Ground reference
3	$\overline{\text{RST}}$ / SBWTDIO	Reset or nonmaskable interrupt input Spy-Bi-Wire test data input/output during programming and test
4	TEST / SBWTCK	Selects test mode for JTAG pins on Port1. The device protection fuse is connected to TEST. Spy-Bi-Wire test clock input during programming and test
5	VCC (3.6V)	Supply voltage
6	P3.5 / UCA0RXD / UCA0SOMI	General-purpose digital I/O pin / USCI_A0 receive data input in UART mode (UART communication from 2274 to PC), slave out/master in when in SPI mode

6.5 Software Design

When ECG signal was received from ECG analog front end by end device target board, MSP430F2274 will sample the signal using ADC10 analog to digital converter implemented in the microcontroller after initializing the board, timers and oscillator. The device starts searching for access point to connect, during searching green and red leds toggle on/off. When it discovers the access point the red led flash

to indicate the link attempt, once connected all leds are turned off and sampled ECG signal will be send to the access point. End device default is low power mode 3 (LPM3) and wakes up once to sample ECG signal and send it to access point as shown in Figure 6.7 below.

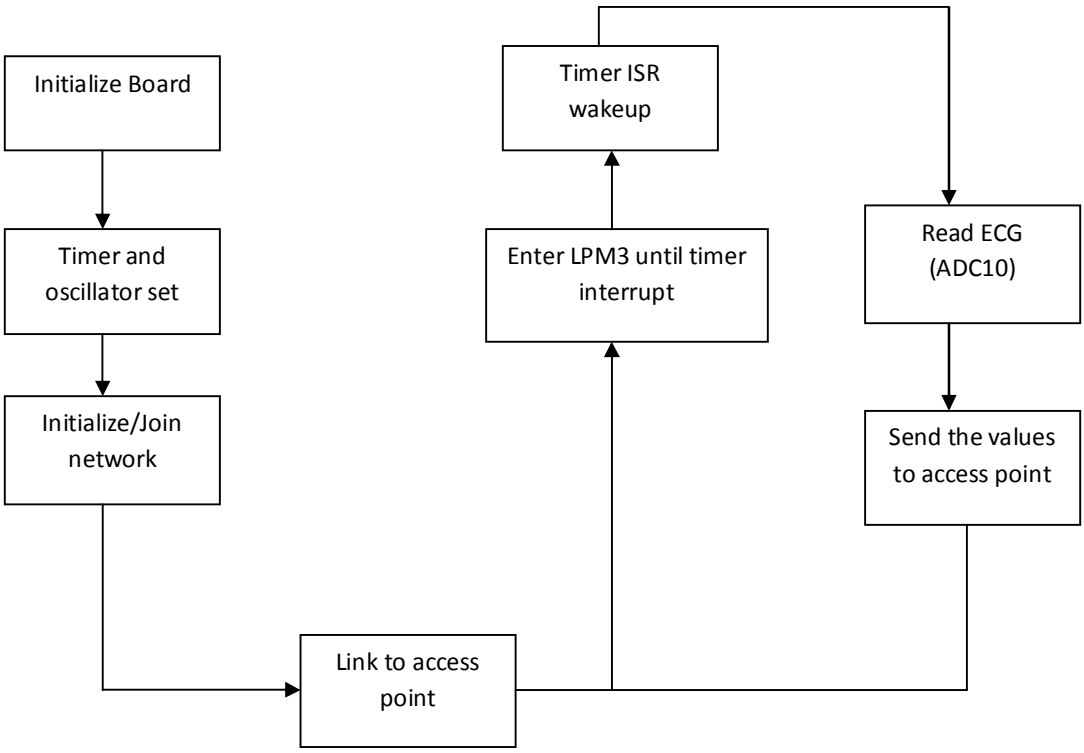

Figure 6.7: End device software flowchart

From the access point side as shown in Figure 6.8 below, after initializing the board, timers and oscillator it listen for end device to join and for packages that have already joined from end device. There are two leds that notifies transaction between two boards in the network; green led indicates packet received from end device while red led indicates transmission to the computer. Access point sends ECG signal through application of Universal Asynchronous Receiver Transmitter (UART) to a computer com port for visualization using a Matlab environment or graphical user interface.

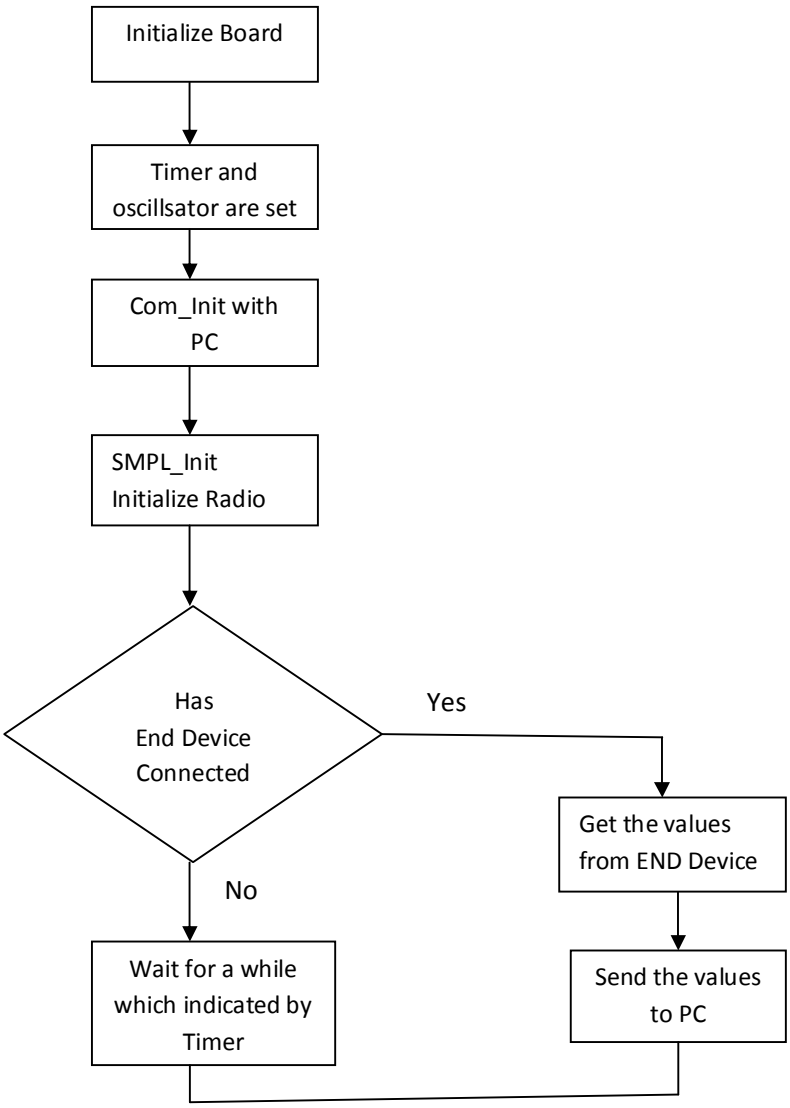

Figure 6.8: Access point program flowchart

In this thesis IAR Embedded Workbench Integrated Development Environment (IDE) was used by eZ430-RF2500 to write, download, and debug the application. The debugger is unobtrusive, allowing the user to run an application at full speed

with both hardware breakpoints and single stepping available while consuming no extra hardware resources (SLAU227E, 2009).

6.6 Result

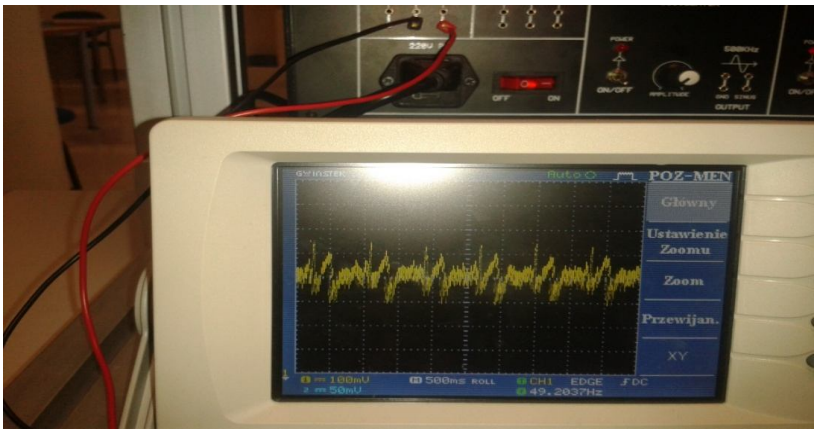

Figure 6.9: First ECG result via an oscilloscope

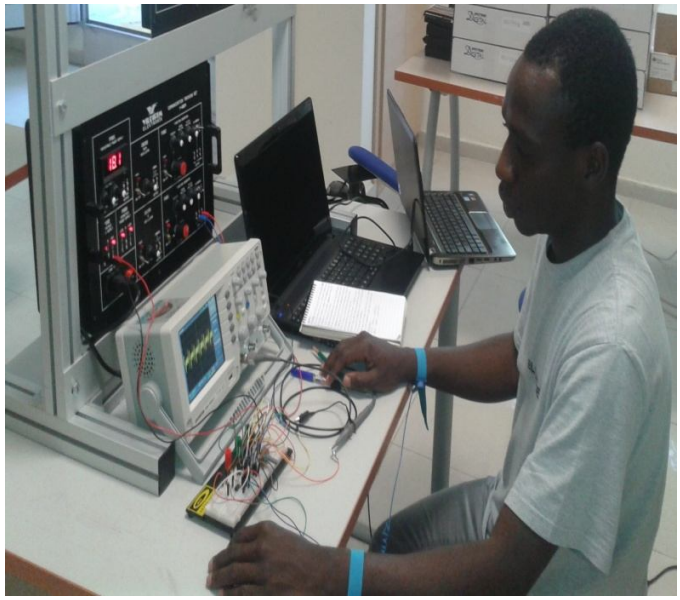

Figure 6.10: complete setup of ECG analog front end

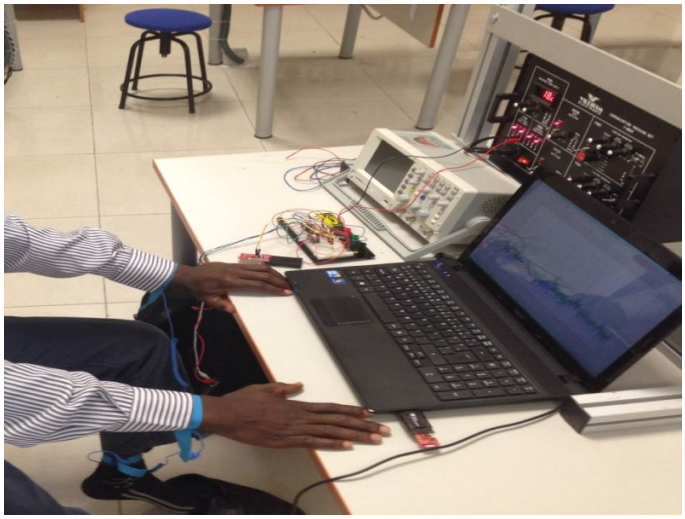

Figure 6.11: Full set up with eZ430-RF2500 wireless development tool

Matlab environment was used in this work for visualizing the ECG signal through one of the PC com.

CHAPTER SEVEN

CONCLUSIONS

6.1 Summary

This thesis is an endeavor to address and gives solutions to various challenges associated with ECG acquisition and automatic beat classification system. The system includes both hardware and software in order to reduce an existing gap in health care environment by proposing low cost, easy to use and simpler method of wireless acquisition system and automatic ECG beat classification using a hybrid technique which is capable of classifying four ECG beats with higher number of samples successfully.

One of the most important steps in ECG analysis is denoising and QRS detection; that is removing unwanted signal or artifacts that contaminate the signal during recording. In this thesis work a well known and acceptable algorithm developed by Pan and Tompkins was used to remove noise and detect QRS complex correctly. After detecting R-peaks, different methods were proposed for feature extraction and classification. Equivalent R-T interval was extracted as 200 samples between two successive R-peaks and then decomposed using DWT and SWT with statistical parameters calculated in each case as a new features. It was concluded that the method proposed in this thesis as hybrid technique proved to be effective by extracting time domain, time frequency domain and statistical features in which while equivalent R-T interval features gives average sensitivity of 97.36% and 89.27% with average accuracy of 98.22% and 94.18%, the DWT with statistical features gives average sensitivity of 99.75% and 95.46% with average accuracy of 99.84 and 97.59% for reduced and large number of samples respectively. However, an improvement was recorded when employing SWT for wavelet decomposition using large number of samples with average sensitivity and average accuracy of 96.69% and 98.33% respectively.

Moreover, classification was carried out using neural network back propagation algorithm where among different network design in this thesis a network

of 15 numbers of hidden neurons found to yields more effective than 7, 10, and 20. Another comparative performance was carried out between wavelet time and frequency entropy using SWT in which time entropy shows a slight improvement of average accuracy of 98.21% against frequency entropy of 97.77% which indicates that the shape of ECG wave contains more information than the frequency bands. Also, among different wavelet families tested in this work, it was concluded that selection a wavelet type is an important factor in determining the success of classification with db4, coif5 and sym8 shows a better performance.

This thesis also explore the features of Texas Instrument low power and low cost development tool by designing ECG analog front end with eZ430-RF2500 for simple solution of wireless ECG acquisition and transmission which when implemented will provide a greater solution of low cost, easy to use and simple wireless sensor network.

Finally, among different methods developed in this thesis, SWT with statistical features shows better result and R-R time interval with amplitude shows less performance.

6.2 Future Works

With rapid development in technological advancement and computer intelligence, automatic ECG beats detection system is an important tool used in health care community however, based on some observations made throughout this thesis; recommendations can be made for further improvement and implementation.

1. A possible research investigation into other hybrid techniques is recommended for finding more robust feature extraction technique.
2. Investigate other classifiers apart from neural network and also different types of neural network algorithms.
3. Wavelet selection is critical on the performance of classifiers; therefore there is a need for further research and analysis in selecting a suitable wavelet.
4. Real time patient data acquisition, preprocessing and classification need to be studied further by implementing and incorporating low cost wireless acquisition system with

automatic ECG beat detection system in hardware format and other programming language like C code.

BIBLIOGRAPHY

Acharya, R., Suri, T.S., Span, A.E., Krishnan, S.M., 2012, Advances in cardiac signal processing, Springer.

AD620 Datasheet, 2011, "Analog Devices", www.analog.com

Anton, K., 2007, Automatic ECG analysis using principal component analysis and wavelet transformation-Universitats verlag Karlsruhe.

Adam G., Witold P., 2012, ECG signal processing, Classification and Interpretation, A computational frame work of computational Intellihence. Springer-Verlag London Limited.

Akansu, A.N., Liu, Y., 1991, On Signal Decomposition Techniques, Optical Engineering, pp. 912-920.

Blanco, S., Figliola, A., Quian Quiroga R, Rosso O.A., Serrano E., 1998, Time–frequency analysis of electroencephalogram series (III): wavelet packets and information cost function. Phys Rev E.

Bruce, R.A., Yarnall, S.R., 1966, Computer-aided diagnosis of cardiovascular disor-ders, J.ChronicDis.19, pp473–484.

Chatterjee, H.K., Gupta, R., Mitra, M., 2011, A statistical approach for determination of time plane features from digitized ECG. Comput Biol Med. 41(5):278–84.

Christian, C., 2011, Applications of digital signal processing-In Tech Education and Publishing.

Chawla, M.P.S., 2011, PCA and ICA processing methods for removal of artifacts and noise in electrocardiograms: a survey and comparison. Appl Soft Comput. 11(2):2216–2226.

Chazal, P., O'Dwyer, M., Reilly, R.B., 2004, Automatic classification of heart beats using ECG morphology and heart beat interval features. IEEE Tran Biomed Eng. 51(7):1196–206.

Chazal, P., Reilly, R.B., 2006, A patient- adapting heart beat classifier using ECG morphology and heartbeat interval features. IEEE Tran Biomed Eng. 53(12):2535–43.

Chazal, D.P., 1998, Automatic classification of the Frank lead ECG, Unpublished PHD Thesis, University of South Wales.

Daubechies, I., 1990, The wavelet transform, time-frequency location and signal analysis". IEEE Trans, IT, 36(5), pp. 961-1005.

Demuth, H., Beale, M., 2001, Neural Network Toolbox for use with Matlab: The Mathworks, Inc.

Dubowik, K., 1999, Automated Arrhythmia Analysis-An Expert System for an Intensive Care Unit. Lund University, Sweeden, Lund.

EMEDU, 2012, Emergency Electrocardiograpy: Online training module http://www.emedu.org/ecg/lbbb.htm

EMEDU, 2012, Emergency Electrocardiograpy: Online training module http://www.emedu.org/ecg/rbbb.htm

Frank, G., Yanowitz, M.D., 2014, Characteristics of the Normal ECG Professor of Medicine University of Utah School of Medicine Medical Director, ECG Services Intermountain Healthcare, http://ecg.utah.edu/

Farahabadi, E., Farahabadi, A., Rabbani, H, Mahjoob, M.P., Dehnavi, A.M., 2009, Noise removal from electrocardiogram signal employing an artificial neural network in wavelet domain. In: Proceedings of the 9th international conference on information technology and applications in biomedicine (ITAB), pp. 1–4.

Fook, J., 2012, A real time data mining technique applied for critical ECG rhythm on hand held device, RMIT University, Melbourn Australia.

Gari D., Francisco A., Patric, M,. 2006, Advanced methods and Tools for ECG data Analysis-Artech House Publishers.

Germann, W.J., Standield, C.C., 2002, Principles of Human Physiology, Benjamin Cummings, San Farancisco.

Goldberger, A.L., Amaral, L.A.N., Glass, L., Hausdorff, J.M., Ivanov, P.Ch., Mark, R.G., Mietus, J.E., Moody, G.B., Peng, C.K., Stanley, H.E., 2000, PhysioBank, PhysioToolkit, and PhysioNet: Components of a New Research Resource for Complex Physiologic Signals. *Circulation* **101**(23):e215-e220 [Circulation Electronic Pages; http: // circ.ahajournals. org / cgi / content / full / 101 / 23 / e215];

Guyton, A. C.; Hall, J. E., 2006, Textbook of Medical Physiology (11th ed.). Philadelphia: Elsevier Saunder.

Hasnain, S.K., Asim S.M., 1999, Artificial Neural Network in Cardiology-ECG wave Analysis and Diagnosis using Back propagation Neural Network .

Ifeachor, E.C., Jervis, B.W., 1993, Digital Signal Processing- A Practical Approach: Addison Wesley Publishers Ltd.

James, Fowler, E., 2014, The Redundant Discrete Wavelet Transform and Additive Noise, contains an overview of different names for this transform, http://en.wikipedia.org/wiki/Stationary_wavelet_transform

Hamilton, P.S., 1996, A Comparison of Adaptive and Non-adaptive Filters for Reduction of Power line Interference in the ECG. IEEE Tran on Biomed Eng. 43(1):105–9.

Hannu, O., 2011, Discrete wavelet transform, Biomedical applications, In-Tech Inc.

Hessian, S.K.U., Asim, S.M.. 1999, *Artificial Neural network in Cardiology-ECG Wave Analysis and Diagnosis Using Backpropogation Neural network.*

Hirano, K., Nishimura, S., Mitra SK., 1974, Design of digital notch filters. IEEE Tran on Comm COM-22. 7:964–974.

Inan, O.T. L., Giovangrandi, G.T.A., Kovacs, 2006, Robust neural-network-based classification of premature ventricular contractions using wavelet transform and timing interval features, IEEE Trans. Biomed. Eng.53, pp2507–2515

Holschneider, M., Kronland-Martinet, R., Morlet, , Tchamitchian, P., 1989, A real-time algorithm for signal analysis with the help of the wavelet transform. In *Wavelets, Time-Frequency Methods and Phase Space*, pp. 289–297. Springer-Verlag.

Klabunde R.E., 2008, Electrocardiogram Standard Limb Leads (bipolar), in Cardiovascular Physiology concepts.

KCUMB, 2006, "Conduction Blocks "
http://en.wikipedia.org/wiki/left_bundle_branch_block

KCUMB, 2006, "Conduction Blocks "
http://en.wikipedia.org/wiki/Right_bundle_branch_block

Krummen D.E., Patel M., Nguyen H., Ho G., Kazi D.S., Clopton P., Holland M.C., Greenberg S.L., Feld G.K., Faddis M.N., 2010, Accurate ECG diagnosis of atrial tachyarrhythmias using quantitative analysis: a prospective diagnostic and cost-effectivenessstudy,J.Cardiovasc.Electrophysiol.21, pp1251–1259.

Lagerholm, M., Peterson C., Braccini, G., Edenbrandt, L., Sornmo, L., 2000, Clustering ECG complexes using Hermite functions and self-organizing maps, IEEE Trans.Biomed.Eng.47, pp838–848

Li, C., Zheng, C., Tai, C., 1995, Detection of ECG characteristic points using wavelet transform. IEEE Tran Biomed Eng. 42(1):21–8.

Little, J.N., Shure, L., 2001, Signal Processing Toolbox for use with Matlab: The Mathworks Inc.

Mahmoodabadi,S.Z., Ahmadian, A., Abolhasani, D., Eslami, M. and Bidgoli, J.H., 2005. ECG Feature Extraction Using Daubechies Wavelets. Proceedings of the Fifth IASTED International Conference ,Benidorm, Spain.

Mahmoodabadi,S.Z., Ahmadian, A., Abolhasani, D., Eslami, M. and Bidgoli, J.H., 2005, ECG Feature Extraction based on multiresolution wavelet transform, in proceedings of the IEEE engineering in medicine and biology 27th annual conference, Shangai china,

Mahesh, A.N., 2010, ECG feature extraction using Time-Frequency analysis, Innovation in computing sciences and software engineering.

Mallat, S., 1989, A theory for multiresolution signal decomposition: The wavelet representation". IEEE Trans. PAMI. 11(7), pp. 674-693.

Martin, T., Howard, B,. Mark, B., 2002, Neural network design, PWS Publishing Company USA.

Martis, R.J., Acharya, U.R.K., Mandana, M., Ray, A.K., Chakraborty, C., 2012, Application of principal component analysis to ECG signals for automated diagnosis of cardiac health, Expert Syst. Appl.39, pp11792–11800.

Martis, R.J., Acharya, U.R., Lim, C.M., 2013, ECG beat classification using PCA, LDA, ICA and discrete wavelet transform, Biomed. Signal Process. Control8(5), pp437–448.

Mazomenos, E.B., Chen, T., Acharyya, A., Bhattacharya, A., Rosengarten, J., Maharatna, K., 2012, A timedomain morphology and gradient based

algorithm for ECG feature extraction. In: Proceedings of IEEE international conference on industrial technology (ICIT), pp. 117–122.

Marlar, C., Aung, S.K., 2014, Implementation of ECG beat classification, International journal of Societal Applications of Computer Science.

Martinez, J.P., Almeida, R., Olmos, S., Rocha, A.P., Laguna, P., 2004, A wavelet-based ECG delineation: evaluation of standard databases. IEEE Tran Biomed Eng. 51(4):570–81.

Michel, M. et al., 1996, Wavelet Toolbox for use with Matlab: The Mathworks, Inc.

Milliken, J.A., Wartak, J., Skoulikidis, A.P., Lywood, D.W., 1969, Use of computers in the interpretations of electrocardiograms. Can Med Assoc J. 01(7):39–43.

Mneimneh, M.A., Yaz, E.E., Johnson, M.T., Povinelli, R.J., 2006, An adaptive kalman filter for removing baseline wandering in ECG signals. In: Proceeding of Computers in cardiology, pp 253–256

Molly, C., 2000, Advanced Nursing Skills: Principles and practice, Cambridge University Press.

Moss A.J., Stern, S., 1996, Non-invasive Electrocardiography, Clinical aspect of Holter, London, Philadelphia.

Murray, T.H., 1982, The design, development, and implementation of a microprocessor-based ECG analysis system. Behav Res Methods Instrum. 14(2):281–9.

Murugavel, R., 2005, Heart-Rate and EKG Monitor Using the MSP430FG439, Application Report SLAA280A, pp.1-12.

Natwong, B., Sooraksa, P., Pintavirooj, C., Bunluechokchai, S., Ussawwongaraya, W., 2006, Wavelet entopy analysis of the high resolution ECG, IEEE Explore.

Nor, H. Binti K., 2010,Feature extraction and classification of ECG signal to detect Arrhythmia and Ischemia disease, University of Malaya.

Osowski, S., Linh, T.H., 2001, ECG beat recognition using fuzzy hybrid neural network, IEEETrans. Biomed. Eng.48, pp1265–1271.

Ozbey, Y., Karlik, B., 1996 A New Approach for Arrhythmias Classification, Proc. Of Annual International Conference of IEEE of Medicine and Biology Society.

Pal, S., Mitra, M., 2010, Detection of ECG characteristic points using multiresolution wavelet analysis based selective coefficient method. 43(2):255–61.

Papaloukas, C., Fotiads, D.I., Likas, A., Michalis, L.K., (2003), Automated method for Ischemia detection in long duration ECGs, Cardiovascular reviews and reports, vol. 24, no. 6, pp313-319

Raul, P., Annie, M., et al. 2008, http: // en. Wikipedia . org / wiki / Positive_and_negative_predictive_values (Date accessed: May, 2014)

Rajarshi G., Madhuchhanda M., Jitendranath B., 2014, ECG Acquisition and Automated Remote Processing, Springer New Delhi

Robi, P., 2006, The wavelet tutorial, Rowan University college of Engineering.

Saxena, S.C., Kumar, V., Hamde, S.T., 2003, Feature extraction from ECG signals using wavelet transforms for disease diagnosis. Int J Syst Sci. 33(13):1073–85.

Shannon, C.E., 1948, A mathematical theory of communication. Bell Syst Technol J 27:379–23, 623–56

Slau227e, 2009, eZ430-RF2500 Development Tool User's Guide http://focus.ti.com/lit/ug/slau227e/slau227e.pdf

Stevenson, W.G., Hernaddez, A.F., Carson, P.E., et al., 2012, Indications for cardiac resynchronization therapy: 2011 update from the Heart Failure Society of America guideline committee. J Card Fail , pp94-106.

Tazebay, M.V., Akansu, A.N., 1994, Progressive Optimality in Hierarchical Filter Banks, Proc. IEEE International Conference on Image Processing (ICIP), Vol 1, pp. 825-829.

Tazebay, M.V., Akansu, A.N., 1995, Adaptive Subband Transforms in Time-Frequency Excisers for DSSS Communications Systems , IEEE Transaction on Signal Processing, Vol 43, No 11, pp. 2776-2782.

Texas, H.I., 2014, "Conduction system" in health information centre, http://www.texasheartinstitute.org/HIC/Anatomy/

Texas, H.I., 2012, "Heart Anatomy" in health information centre, http://www.texasheartinstitute.org/HIC/Anatomy/

Tompkins, W., 2008, 12-lead ECG Configurations, in 12-lead ECG Trainer A. Schuler.

Tompkins, W.J., Ahlstrom, M.L., 1985, Digital filters for real-time ECG signal processing using microprocessors. IEEE Tran on Biomed Eng BME-32. pp708–713.

Wartak, J., 1978, Electrocardiogram Interpretation, http: //www . ncbi . nlm . nih . gov / pubmed /?term=wartak+j

Wolter K., 2011, ECG Interpretation made incredibly easy. 5th edition-Lippincott Williams and wilkins.

Yuksel, C., "Heart Failure Working Group of the Turkish Society of Cardiology (TDK)" http://www.todayszaman.com/news (2014) (Date accessed: May 10, 2014)

.

Zheng-You, H.E., chen X., Luo G., 2006, Wavelet Entropy Measure Definition and ItsApplication for Transmission Line FaultDetection and Identification' International Conference on Power System Technology

APPENDICES

APPENDIX A: Matlab and C Codes

The detailed Matlab and C codes used in this thesis work are in the attached DVD.

Appendix B: Data Sheet Samples

SPECIFICATIONS

Typical @ 25°C, V_S = ±15 V, and R_L = 2 kΩ, unless otherwise noted.

Table 2.

Parameter	Conditions	AD620A Min	AD620A Typ	AD620A Max	AD620B Min	AD620B Typ	AD620B Max	AD620S[1] Min	AD620S[1] Typ	AD620S[1] Max	Unit
GAIN	G = 1 + (49.4 kΩ/R_G)										
Gain Range		1		10,000	1		10,000	1		10,000	
Gain Error[2]	V_{OUT} = ±10 V										
G = 1			0.03	0.10		0.01	0.02		0.03	0.10	%
G = 10			0.15	0.30		0.10	0.15		0.15	0.30	%
G = 100			0.15	0.30		0.10	0.15		0.15	0.30	%
G = 1000			0.40	0.70		0.35	0.50		0.40	0.70	%
Nonlinearity	V_{OUT} = −10 V to +10 V										
G = 1–1000	R_L = 10 kΩ		10	40		10	40		10	40	ppm
G = 1–100	R_L = 2 kΩ		10	95		10	95		10	95	ppm
Gain vs. Temperature											
	G = 1			10			10			10	ppm/°C
	Gain > 1[2]			−50			−50			−50	ppm/°C
VOLTAGE OFFSET	(Total RTI Error = V_{OSI} + V_{OSO}/G)										
Input Offset, V_{OSI}	V_S = ±5 V to ± 15 V		30	125		15	50		30	125	μV
Overtemperature	V_S = ±5 V to ± 15 V			185			85			225	μV
Average TC	V_S = ±5 V to ± 15 V		0.3	1.0		0.1	0.6		0.3	1.0	μV/°C
Output Offset, V_{OSO}	V_S = ±15 V		400	1000		200	500		400	1000	μV
	V_S = ± 5 V			1500			750			1500	μV
Overtemperature	V_S = ±5 V to ± 15 V			2000			1000			2000	μV
Average TC	V_S = ±5 V to ± 15 V		5.0	15		2.5	7.0		5.0	15	μV/°C
Offset Referred to the Input vs. Supply (PSR)	V_S = ±2.3 V to ±18 V										
G = 1		80	100		80	100		80	100		dB
G = 10		95	120		100	120		95	120		dB
G = 100		110	140		120	140		110	140		dB
G = 1000		110	140		120	140		110	140		dB
INPUT CURRENT											
Input Bias Current			0.5	2.0		0.5	1.0		0.5	2	nA
Overtemperature				2.5			1.5			4	nA
Average TC			3.0			3.0			8.0		pA/°C
Input Offset Current			0.3	1.0		0.3	0.5		0.3	1.0	nA
Overtemperature				1.5			0.75			2.0	nA
Average TC			1.5			1.5			8.0		pA/°C
INPUT											
Input Impedance											
Differential			10||2			10||2			10||2		GΩ||pF
Common-Mode			10||2			10||2			10||2		GΩ||pF
Input Voltage Range[3]	V_S = ±2.3 V to ±5 V	−V_S + 1.9		+V_S − 1.2	−V_S + 1.9		+V_S − 1.2	−V_S + 1.9		+V_S − 1.2	V
Overtemperature		−V_S + 2.1		+V_S − 1.3	−V_S + 2.1		+V_S − 1.3	−V_S + 2.1		+V_S − 1.3	V
	V_S = ± 5 V to ±18 V	−V_S + 1.9		+V_S − 1.4	−V_S + 1.9		+V_S − 1.4	−V_S + 1.9		+V_S − 1.4	V
Overtemperature		−V_S + 2.1		+V_S − 1.4	−V_S + 2.1		+V_S + 2.1	−V_S + 2.3		+V_S − 1.4	V

AD620

Parameter	Conditions	AD620A Min	AD620A Typ	AD620A Max	AD620B Min	AD620B Typ	AD620B Max	AD620S[1] Min	AD620S[1] Typ	AD620S[1] Max	Unit
Common-Mode Rejection											
Ratio DC to 60 Hz with											
1 kΩ Source Imbalance	V_{CM} = 0 V to ± 10 V										
G = 1		73	90		80	90		73	90		dB
G = 10		93	110		100	110		93	110		dB
G = 100		110	130		120	130		110	130		dB
G = 1000		110	130		120	130		110	130		dB
OUTPUT											
Output Swing	R_L = 10 kΩ										
	V_S = ±2.3 V to ± 5 V	$-V_S$ + 1.1		$+V_S$ – 1.2	$-V_S$ + 1.1		$+V_S$ – 1.2	$-V_S$ + 1.1		$+V_S$ – 1.2	V
Overtemperature		$-V_S$ + 1.4		$+V_S$ – 1.3	$-V_S$ + 1.4		$+V_S$ – 1.3	$-V_S$ + 1.6		$+V_S$ – 1.3	V
	V_S = ±5 V to ± 18 V	$-V_S$ + 1.2		$+V_S$ – 1.4	$-V_S$ + 1.2		$+V_S$ – 1.4	$-V_S$ + 1.2		$+V_S$ – 1.4	V
Overtemperature		$-V_S$ + 1.6		$+V_S$ – 1.5	$-V_S$ + 1.6		$+V_S$ – 1.5	$-V_S$ + 2.3		$+V_S$ – 1.5	V
Short Circuit Current			±18			±18			±18		mA
DYNAMIC RESPONSE											
Small Signal –3 dB Bandwidth											
G = 1			1000			1000			1000		kHz
G = 10			800			800			800		kHz
G = 100			120			120			120		kHz
G = 1000			12			12			12		kHz
Slew Rate		0.75	1.2		0.75	1.2		0.75	1.2		V/µs
Settling Time to 0.01%	10 V Step										
G = 1–100			15			15			15		µs
G = 1000			150			150			150		µs
NOISE											
Voltage Noise, 1 kHz	Total RTI Noise = $\sqrt{(e_{ni}^2) + (e_{no}/G)^2}$										
Input, Voltage Noise, e_{ni}			9	13		9	13		9	13	nV/√Hz
Output, Voltage Noise, e_{no}			72	100		72	100		72	100	nV/√Hz
RTI, 0.1 Hz to 10 Hz											
G = 1			3.0			3.0	6.0		3.0	6.0	µV p-p
G = 10			0.55			0.55	0.8		0.55	0.8	µV p-p
G = 100–1000			0.28			0.28	0.4		0.28	0.4	µV p-p
Current Noise	f = 1 kHz		100			100			100		fA/√Hz
0.1 Hz to 10 Hz			10			10			10		pA p-p
REFERENCE INPUT											
R_{IN}			20			20			20		kΩ
I_{IN}	V_{IN+}, V_{REF} = 0		50	60		50	60		50	60	µA
Voltage Range		$-V_S$ + 1.6		$+V_S$ – 1.6	$-V_S$ + 1.6		$+V_S$ – 1.6	$-V_S$ + 1.6		$+V_S$ – 1.6	V
Gain to Output		1 ± 0.0001			1 ± 0.0001			1 ± 0.0001			
POWER SUPPLY											
Operating Range[4]		±2.3		±18	±2.3		±18	±2.3		±18	V
Quiescent Current	V_S = ±2.3 V to ±18 V		0.9	1.3		0.9	1.3		0.9	1.3	mA
Overtemperature			1.1	1.6		1.1	1.6		1.1	1.6	mA
TEMPERATURE RANGE											
For Specified Performance		–40 to +85			–40 to +85			–55 to +125			°C

[1] See Analog Devices military data sheet for 883B tested specifications.
[2] Does not include effects of external resistor R_G.
[3] One input grounded. G = 1.
[4] This is defined as the same supply range that is used to specify PSR.

Absolute Maximum Ratings

DC Supply Voltage (Between V+ and V- Terminals) 36V
Differential Mode Input Voltage 8V
DC Input Voltage . . . . . (V+ +8V) To (V- -0.5V)
Input Terminal Current 1mA
Output Short Circuit Duration (Note 2) . . . . . Indefinite

Operating Conditions
Temperature Range . . . . . -55°C to 125°C

Thermal Information

Thermal Resistance (Typical, Note 1)	θ_{JA} (°C/W)	θ_{JC} (°C/W)
PDIP Package*	115	N/A
SOIC Package	165	N/A

Maximum Junction Temperature (Plastic Package) . . . . . 150°C
Maximum Storage Temperature Range . . . . . -65°C to 150°C
Maximum Lead Temperature (Soldering 10s) . . . . . 300°C
(SOIC - Lead Tips Only)

*Pb-free PDIPs can be used for through hole wave solder processing only. They are not intended for use in Reflow solder processing applications.

CAUTION: Stresses above those listed in "Absolute Maximum Ratings" may cause permanent damage to the device. This is a stress only rating and operation of the device at these or any other conditions above those indicated in the operational sections of this specification is not implied.

NOTES:

1. θ_{JA} is measured with the component mounted on a low effective thermal conductivity test board in free air. See Tech Brief TB379 for details.
2. Short circuit may be applied to ground or to either supply.

Electrical Specifications $V_{SUPPLY} = \pm15V$, $T_A = 25°C$

PARAMETER	SYMBOL	TEST CONDITIONS		TYPICAL VALUES CA3140	TYPICAL VALUES CA3140A	UNITS
Input Offset Voltage Adjustment Resistor		Typical Value of Resistor Between Terminals 4 and 5 or 4 and 1 to Adjust Max V_{IO}		4.7	18	kΩ
Input Resistance	R_I			1.5	1.5	TΩ
Input Capacitance	C_I			4	4	pF
Output Resistance	R_O			60	60	Ω
Equivalent Wideband Input Noise Voltage (See Figure 27)	e_N	BW = 140kHz, R_S = 1MΩ		48	48	µV
Equivalent Input Noise Voltage (See Figure 35)	e_N	R_S = 100Ω	f = 1kHz	40	40	nV/√Hz
			f = 10kHz	12	12	nV/√Hz
Short Circuit Current to Opposite Supply	I_{OM^+}		Source	40	40	mA
	I_{OM^-}		Sink	18	18	mA
Gain-Bandwidth Product, (See Figures 6, 30)	f_T			4.5	4.5	MHz
Slew Rate, (See Figure 31)	SR			9	9	V/µs
Sink Current From Terminal 8 To Terminal 4 to Swing Output Low				220	220	µA
Transient Response (See Figure 28)	t_r	R_L = 2kΩ, C_L = 100pF	Rise Time	0.08	0.08	µs
	OS		Overshoot	10	10	%
Settling Time at $10V_{P-P}$, (See Figure 5)	t_S	R_L = 2kΩ, C_L = 100pF, Voltage Follower	To 1mV	4.5	4.5	µs
			To 10mV	1.4	1.4	µs

Electrical Specifications For Equipment Design, at $V_{SUPPLY} = \pm15V$, $T_A = 25°C$, Unless Otherwise Specified

PARAMETER	SYMBOL	CA3140 MIN	CA3140 TYP	CA3140 MAX	CA3140A MIN	CA3140A TYP	CA3140A MAX	UNITS
Input Offset Voltage	$\|V_{IO}\|$	-	5	15	-	2	5	mV
Input Offset Current	$\|I_{IO}\|$	-	0.5	30	-	0.5	20	pA
Input Current	$\|I_I\|$	-	10	50	-	10	40	pA

Specifications

MSP430F2274

- 16-MIPS performance
- 200-ksps 10-bit SAR ADC
- Two built-in operational amplifiers
- Watchdog timer, 16-bit Timer_A3 and Timer_B3
- USCI module supporting UART/LIN, (2) SPI, I2C, or IrDA
- Five low-power modes drawing as little as 700 nA in standby

PARAMETER	MIN	TYP	MAX	UNIT
OPERATING CONDITIONS				
Operating supply voltage	1.8		3.6	V
Operating free-air temperature range	-40		85	°C
CURRENT CONSUMPTION				
Active mode at 1 MHz, 2.2 V		270	390	µA
Standby mode		0.7	1.4	µA
Off mode with RAM retention		0.1	0.5	µA
OPERATING FREQUENCY				
VCC ≥ 3.3 V			16	MHz

CC2500

- 2.4-GHz radio-frequency (RF) transceiver
- Programmable data rate up to 500 kbps
- Low current consumption

PARAMETER	CONDITION	MIN	TYP	MAX	UNIT
OPERATING CONDITIONS					
Operating supply voltage		1.8		3.6	V
CURRENT CONSUMPTION					
RX input signal at the sensitivity limit, 250 kbps	Optimized current		16.6		mA
	Optimized sensitivity		18.8		mA
RX input signal 30 dB above the sensitivity limit, 250 kbps	Optimized current		13.3		mA
	Optimized sensitivity		15.7		mA
Current consumption TX (0 dBm)			21.2		mA
Current consumption TX (-12 dBm)			11.1		mA
RF CHARACTERISTICS					
Frequency range		2400		2483.5	MHz
Data rate (programmable)		1.2		500	kbps
Output power (programmable)		-30		0	dBm
Sensitivity, 10 kbps	Optimized current, 2-FSK, 230-kHz RX filter bandwidth, 1% PER		-99		dBm
	Optimized sensitivity		-101		dBm
Sensitivity, 250 kbps	Optimized current, 500-kHz RX filter bandwidth, 1% PER		-87		dBm
	Optimized sensitivity		-89		dBm

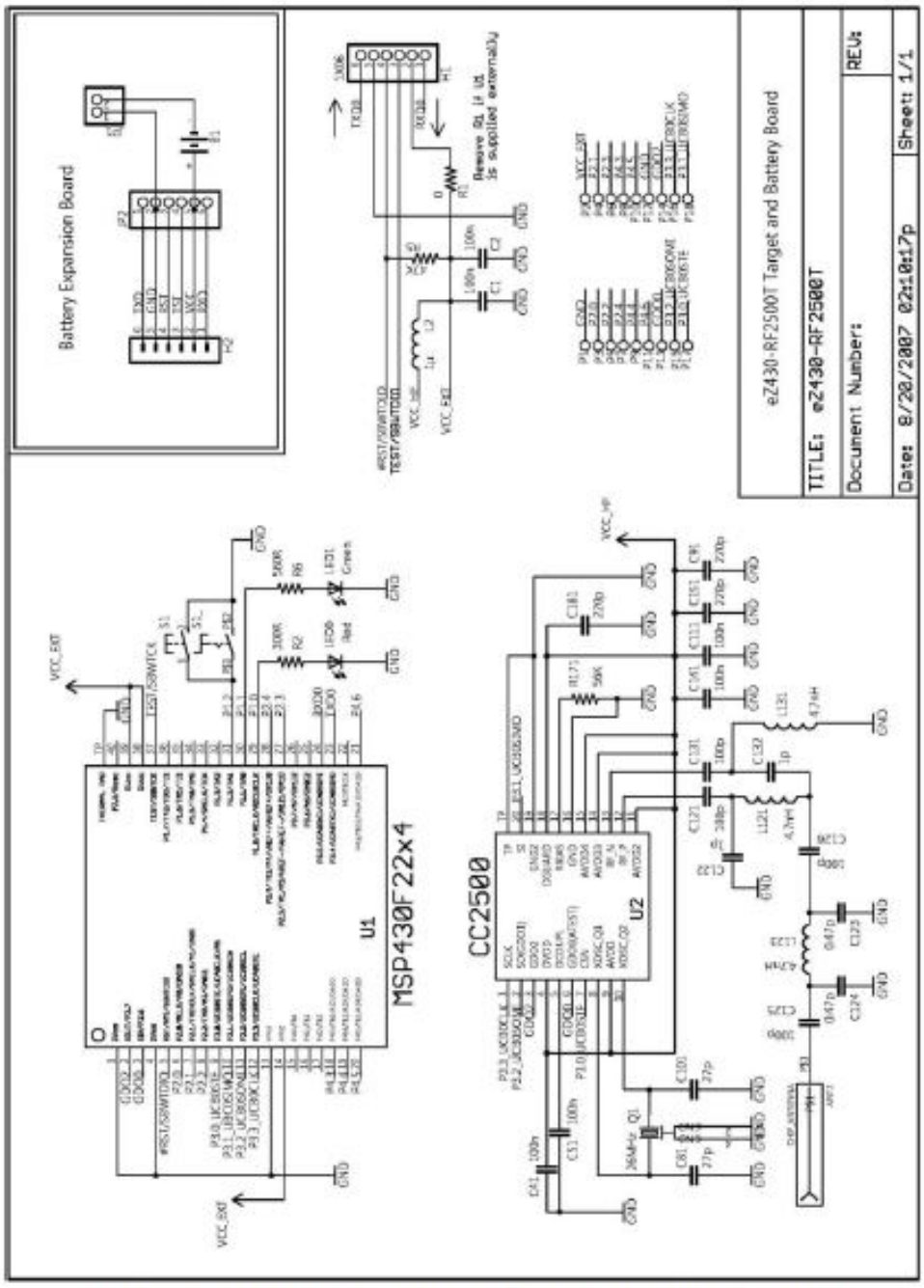

Figure 10. eZ430-RF2500T, Target Board and Battery Board, Schematic

Appendix C: ECG Analog Front End Complete Circuit Diagram